INVESTIGATION OF STRESS DISTRIBUTION IN A DRAGLINE BUCKET USING FINITE ELEMENT ANALYSIS

A THESIS SUBMITTED TO
THE GRADUATE SCHOOL OF APPLIED AND NATURAL SCIENCES
OF
MIDDLE EAST TECHNICAL UNIVERSITY

BY

ONUR GÖLBAŞI

IN PARTIAL FULFILLMENT OF THE REQUIREMENTS
FOR
THE DEGREE OF MASTER OF SCIENCE
IN
MINING ENGINEERING

FEBRUARY 2011

Approval of the thesis:

INVESTIGATION OF STRESS DISTRIBUTION IN A DRAGLINE BUCKET USING FINITE ELEMENT ANALYSIS

submitted by **ONUR GÖLBAŞI** in partial fulfillment of the requirements for the degree of **Master of Science in Mining Engineering Department, Middle East Technical University** by,

Prof. Dr. Canan Özgen _____
Dean, Graduate School of **Natural and Applied Sciences**

Prof. Dr. Ali İhsan Arol _____
Head of Department, **Mining Engineering**

Asst. Prof. Dr. Nuray Demirel
Supervisor, **Mining Engineering Dept., METU** _____

Examining Committee Members:

Prof. Dr. Naci Bölükbaşı _____
Mining Engineering Dept., METU

Asst. Prof. Dr. Nuray Demirel _____
Mining Engineering Dept., METU

Prof. Dr. H. Şebnem Düzgün _____
Mining Engineering Dept., METU

Assoc. Prof. Dr. Serkan Dağ _____
Mechanical Engineering Dept., METU

Ömer Ünver _____
World Energy Council, Turkish National Committee

Date: 11.02.2011

I hereby declare that all information in this document has been obtained and presented in accordance with academic rules and ethical conduct. I also declare that, as required by these rules and conduct, I have fully cited and referenced all material and results that are not original to this work.

Name, Last Name: Onur Gölbaşı

Signature :

ABSTRACT

INVESTIGATION OF STRESS DISTRIBUTION IN A DRAGLINE BUCKET USING FINITE ELEMENT ANALYSIS

Gölbaşı, Onur
M.Sc., Department of Mining Engineering
Supervisor: Asst. Prof. Dr. Nuray Demirel

February 2011, 110 pages

Overburden stripping is one of the essential activities in open-cast mines before starting the ore production. Due to the economic advantages, dragline is a widely utilized machinery in the overburden excavation. These earthmovers carry out the earthmoving process with dragging, hoisting and dumping actions of the bucket. Dragline excavator's efficiency is critically important, since poor performance of a dragline in the mine site directly affects the total efficiency of ore production. Therefore, productivity studies about dragline should be directed to decrease cycle time and increase payload, with avoiding catastrophic failure. In this regard, determination of stress distribution on the front-end components of dragline is meaningful to detect the external factors against dragline operation.

In order to provide insight into the dragline bucket-formation interaction and stress distribution on the bucket, this research studies the simulation of horizontally moving dragline bucket where passive earth forces of the formation create resistance to the movement. Within the scope of simulation, (i) solid models of dragline bucket and the rigging mechanism were created in the Computer-Aided

Drawing (CAD) environment, (ii) the model was transferred to the Finite-Element Analysis (FEA) software, (iii) two different case studies were simulated in the FEA virtual environment. One of the cases handled the stress investigation on the dragline bucket at the first interaction with the formation, while the other focused on the stress formations on a moving dragline bucket. Simulation results showed that overloading conditions occurred on bottom edges of the bucket lip for the first case, and drag hitch part and digging teeth for the second case. Moreover, a sensitivity analysis was carried out to measure the effects of formation specification changes on the stress values on the bucket. The analysis showed that stress values on the bucket elements were most sensitive to internal friction angle and least sensitive to density.

Consequently, this thesis study discusses stress and deformation components on the dragline bucket during the interaction with formation. Since there is not enough number of research studies in the literature about the stress investigation on a moving dragline bucket, this thesis study is expected to provide benefit to understand the basis of dragline bucket actions.

Keywords: Dragline Bucket, Bucket-Formation Interaction, Stress Distribution, Computer-Aided Design, Finite Element Analysis

ÖZ

SONLU ELEMANLAR ANALİZİ İLE ÇEKME KEPÇELİ YERKAZARIN KEPÇESİNDEKİ GERİLME DAĞILIMININ İNCELENMESİ

Gölbaşı, Onur
Yüksek Lisans, Maden Mühendisliği Bölümü
Tez Yöneticisi: Yrd. Doç. Dr. Nuray Demirel

Şubat 2011, 110 sayfa

Örtü kazı faaliyeti, açık kömür ocaklarında üretime geçilmeden önceki en temel madencilik aktivitelerinden biridir. Ekonomik faydaları düşünüldüğü zaman, çekme kepçeli yerkazarlar, örtü kazı işlemlerinde sıklıkla kullanılmaktadır. Bu yerkazarlar pasa harfiyatını, kepçesinin çekme, kaldırma ve boşaltma hareketini kullanarak gerçekleştirmektedir. Çekme kepçenin düşük performansı doğrudan bütün üretim verimliliğini etkileyeceği için, bu yerkazarların kazı esnasındaki verimliliği önem arz etmektedir. Bu nedenden ötürü, çekme kepçeli yerkazar için yapılan verimlilik çalışmaları, yapısal bir zarara neden olmayacak şekilde, devir sayısını azaltmaya ve taşıma yükünü arttırmaya yönelik olmalıdır. Bu bakımdan, çekme kepçe ön-uç elemanları üzerindeki gerilme dağılımının incelenmesi, çekme kepçe faaliyetindeki dışsal etkenlerin belirlenmesi açısından anlam taşımaktadır.

Çekme kepçeli yerkazar kepçesi ve zemin arasındaki etkileşim ve kepçe üzerindeki gerilme dağılımı hakkında bilgi sahibi olunması amacıyla, bu tez çalışmasında, pasif zemin kuvvetlerinin harekete karşı direnç oluşturduğu bir ortam içerisindeki kepçenin yatay hareketi, bir benzetim çalışmasıyla modellenmiştir. Bu çalışma kapsamında, (i) çekme kepçeli yerkazarın kepçe ve zincir-halat kombinasyonlarının katı modelleri oluşturulmuştur, (ii) model, sonlu-elemanlar analizi yapabilen bir

yazılıma aktarılmıştır, (iii) sanal ortam içerisinde iki farklı durum için benzetim çalışması yapılmıştır. Bu çalışmaların birisi, zeminle ilk etkileşim halindeki kepçe üzerinde oluşan gerilme dağılımını incelerken, diğer çalışma hareket halindeki kepçe üzerindeki gerilme oluşumlarına odaklanmıştır. Çalışma sonuçları, birinci durum için kepçe ağzının alt köşelerinde, ikinci durum için ise çekiş zinciri bağlantı yerinde ve de kazıcı dişlerde fazla yüklenme olduğunu göstermiştir. Aynı zamanda, zemin özelliklerindeki değişimlerin kepçe üzerindeki gerilme değerlerine olan etkilerinin ölçülmesi amacıyla bir duyarlılık analizi de yapılmıştır. Bu analiz, kepçe üzerindeki gerilme değerlerinin en fazla içsel sürtünme açısına, en az ise zemin yoğunluğa bağlı olduğunu göstermiştir.

Sonuç olarak, bu tez çalışması, çekme kepçeli yerkazarın zeminle etkileşimi sırasındaki oluşan gerilmeleri ve kepçedeki yapısal bozulmaları tartışmaktadır. Hareket halindeki bir çekme kepçeli yerkazar kepçesi hakkında daha önce yapılmış yeterli sayıda çalışma olmamasından dolayı, bu çalışmanın kepçe hareketinin prensiplerinin anlaşılması açısından faydalı olması beklenmektedir.

Anahtar Kelimeler: Çekme Kepçeli Yerkazar Kepçesi, Kepçe-Zemin Etkileşimi, Gerilme Dağılımı, Bilgisayar-Destekli Tasarım, Sonlu Elemanlar Analizi

To My Parents and Friends

ACKNOWLEDGEMENTS

First of all, I would like to express my sincere appreciation and gratitude to my supervisor dear Asst. Prof. Dr. Nuray Demirel for her invaluable supervision, kind support, endless patience, and continuous guidance in preparation of this thesis. I also present my special thanks to the examining committee members, Prof. Dr. Naci Bölükbaşı, Prof. Dr. Şebnem Düzgün, Assoc. Prof. Dr. Serkan Dağ, and Mr. Ömer Ünver for serving on the M.Sc. thesis committee.

I must express my special thanks to my officemate Mustafa Kemal Emil for his valuable suggestions and comments. I would also like to thank to my brothers and sisters, Ayşe Doğru, Şerif Kaya, Ömer Bayraktar, Halil Sözeri, Mustafa Çırak, Mustafa Erkayaoğlu, Yağmur Duran, Derya Duran, Nazlı Uygun, Şenol Reçber, Erdem Kazaklı, Mervegül Kazaklı, Hüsne Midilli and Ayça Çakır for their infinite motivation.

My other colleagues and friends are gratefully acknowledged for their support during the thesis writing period. Finally, I feel indebted to my family whose encouragement, support and existence helped me to accomplish this study.

TABLE OF CONTENT

LIST OF TABLES

TABLES

LIST OF FIGURES

FIGURES

NOMENCLATURE

Φ	:	Internal Friction Angle
ρ	:	Shear Plane Angle
δ	:	External Friction Angle
γ	:	Specific Weight
β	:	Rake (Cutting) Angle
c	:	Cohesion
C_0	:	Compactness and Cutting Index
C_a	:	Adhesion
d	:	Tool Depth
$d_1,\ldots, d_7$	:	Graphical Distances
F	:	Tangential Excavation Force
$f_1,\ldots, f_6$	:	Excavation Force Vectors
g	:	Gravitational Force
H	:	Horizontal Force
k	:	Pure Cutting Resistance of the Medium
l	:	Tool Length
N_0	:	Normal Load on the Inclined Tool
P	:	Penetration-Cutting Force
q	:	Surcharge
r_0, r_1	:	Curvature Radius
t	:	Depth of Rankine Zone
T	:	Resultant Cutting Force
v	:	Tool Speed
w	:	Tool Width

CHAPTER 1

INTRODUCTION

1.1 General Remarks

Open-cast mining is one of the surface mining practices used for the extraction of layered coal reserves relatively near the surface. Overburden stripping is the essential activity in open-cast mines to remove the overlying formation. Due to the economical advantages, draglines are predominantly utilized in this kind of mines for the removing of overburden, where the operation pit height is less than 35 m (Köse, 1987). A dragline achieves the earthmoving process using with the dragging, hoisting, and dumping actions of the bucket suspending from the boom. Figure 1.1 illustrates a dragline operation in an open-cast mine.

Figure 1.1 Dragline Operation in DemirExport Coal Mine

A dragline machine basically consists of two main sections as upper and lower constructions. Lower part contains walking mechanism and metal chassis while upper part includes drives and operator cabins, excavation and haulage elements such as boom, bucket, chain, and metal rope (Tahir, 1985). Basic components of a dragline are shown in Figure 1.2. Performance of such an earthmover is controlled by the operator. Dragline operator provides the control of independent swing, hoist, and drag mechanisms to excavate and lift pre-blasted or soft rock from a pit, and dumping it onto an adjacent spoil pile (Ridley, 2004). During dragline activity, performance of the stripping is clearly affected by external factors. In general, these factors can be classified in two main categories, mine planning factors and operational factors (Demirel, 2009). Mine planning factors mainly deal with the subjects such as the selection of suitable dragline according to the excavation geometry and expected production amount, and blasting criteria of the site which determines the diggability of a dragline (Demirel, 2009). On the other hand, availability of dragline, fatigue life of working parts and maintenance program, operator skill, cycle time, bucket load are the operational factors acting in dragline performance (Demirel, 2009).

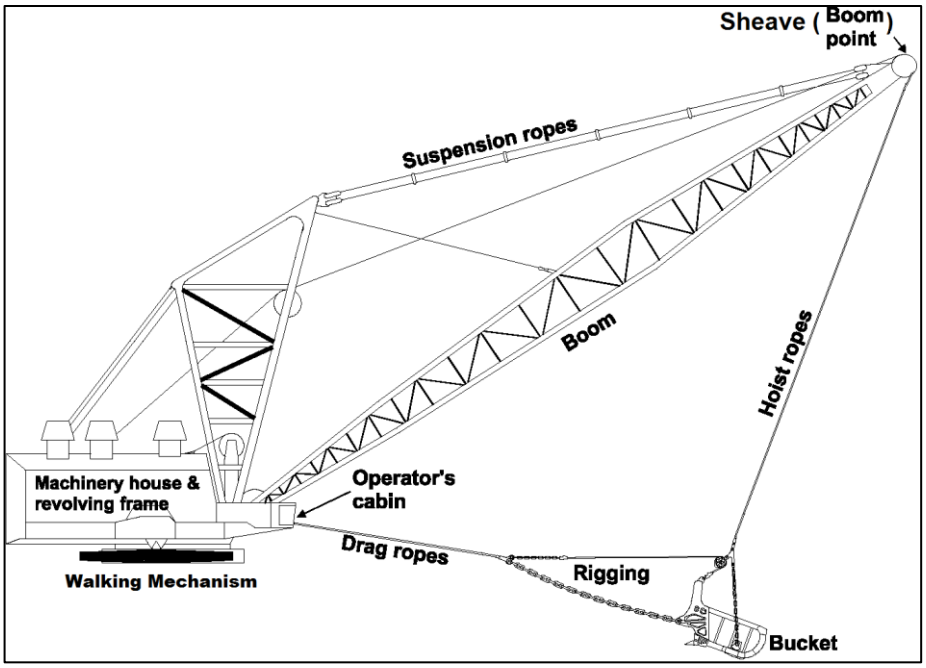

Figure 1.2 Schematic View of a Dragline (Modified after Gurgenci and Guan, 2001)

Dragline utilization is common in various open-cast mines in different countries. Only in America, 101 units of draglines with the bucket capacity ranging from 30 m^3 (40 yd^3) to 108 m^3 (140 yd^3) are utilized in 56 large open-cast mines and 40% of overall overburden removing operations in open-cast mines is achieved by the draglines (Gilewicz, 1999). This percentage is approximately equal to 1.5 billion m^3 (1.9 billion yd^3) removed spoil per year. Following America, Australia (61 units), South Africa (25 units), Canada (22 units) and India (17 units) are the foremost countries in dragline utilization. In Turkey, eight units in Turkish Coal Enterprises and one unit in private sector, a total of nine units of dragline are operated in various open-cast coal mines. Performance of such a common earthmover, dragline, directly affects the production schedules in the mines. Detection of the negative factors during bucket-formation interaction is important for an efficient dragline operation.

In this regard, this research study investigates the mechanical loading simulation of the bucket during formation cutting process. Main focus in this study is the analysis of stress-strain components on the bucket during interaction with the formation.

1.2 Statement of the Problem

Walking draglines are massive earthmoving machines which their weights typically range from 2000 to 7000 tons. They manage the stripping operations with penetrating, dragging, and hoisting actions of the bucket and carry the overburden with their booms with a length up to 128 m. During the execution of the procedure, working elements of dragline are exposed to sudden changes in stress and strain. These variations can cause fractures, wearings, and fatigue failures in the working parts of dragline. Especially, investigation of the interaction between formation and bucket tooth and determination of stress distribution on the bucket and its components during penetration and dragging processes are critical to estimate the diggability of dragline and the failure in bucket components. Therefore, modeling dragline bucket-formation interactions and investigating stress distribution in the bucket are critical for an efficient excavation.

1.3 Objectives and Scope of the Study

The main objective of this study is to investigate the stress and strain distributions in the dragline bucket induced by the tool-formation interaction and loading conditions.

The elements of the main objective are:

i. To create three-dimensional solid models of dragline bucket and rigging mechanism in Computer-Aided Design (CAD) software,

ii. To determine formation resistive forces against the bucket action using earthmoving theories,

iii. To perform a static loading simulation of the three-dimensional model using a Finite Element Analysis (FEA) software, with the selection of suitable materials for the bucket elements and realistic loading and boundary conditions,

iv. To investigate and analyze mechanical effects on the bucket components as stress and strain, and

v. To identify the sensitivity of stress values to various formation properties.

The scope of this thesis is the investigation of stress and strain components in a solid model of dragline bucket during horizontal dragging action, with the help of static analysis in FEA environment. Dynamic finite element analysis of dragline front-end components is not included within the scope of the study due to the insufficient data about dragline front-end components.

1.4 Research Methodology

The thesis study was progressed as a combination of analytical approaches to earthmoving activity, three-dimensional CAD design, and stress-failure analyses in the FEA environment.

The essential components of the research methodology are listed below as:

i. Collection of sketch data to create the solid models of dragline bucket and rigging mechanism: Technical sketches are formed using available data of existing bucket in Kangal Demir Export Coal Mine and technical specifications obtained from dragline spare part catalogues.

ii. Development of solid models for dragline bucket and rigging mechanism: It is accomplished using Solidworks (Solidworks Co., 2009), a CAD software being capable of generating sketches, solid parts, and assemblies.

iii. Transferring of the solid models from CAD environment to FEA environment: Abaqus (Simulia, 6.9-2) is used as the FEA software, which can solve linear or nonlinear problems. Transfer between the CAD and the FEA software is managed with the help of Associative Interface for Solidworks, which is an add-in of Abaqus.

iv. Estimation of the passive earth pressure against the movement of bucket inside the formation: Since the thesis study aims at investigating stress components in the bucket during the dragging action, formation counter resistance is found using the earth cutting theory of Mckyes (1984). Formation specifications in the theory are taken from the study of Mouazen and Nemenyi (1999), by authors' permissions.

v. Simulations of the bucket horizontally cutting the formation: Static simulation is executed with meshing, material assignment, loading and boundary condition steps. Two different case studies are carried out. One of them investigates effect of passive earth pressure on the bucket just before the movement. Another one is about the observation of the stresses on a bucket with constant velocity. The cases are repeated for three different formation specifications.

vi. Visualization of the simulation results: Analysis results are illustrated according to stress and strain components on the model. Yield points are detected during the simulation.

vii. Performing sensitivity analysis to identify the formation properties, which affect the stress values on a dragline bucket element at most.

About the methodology, Figure 1.3 visualizes the flowchart followed in the thesis study.

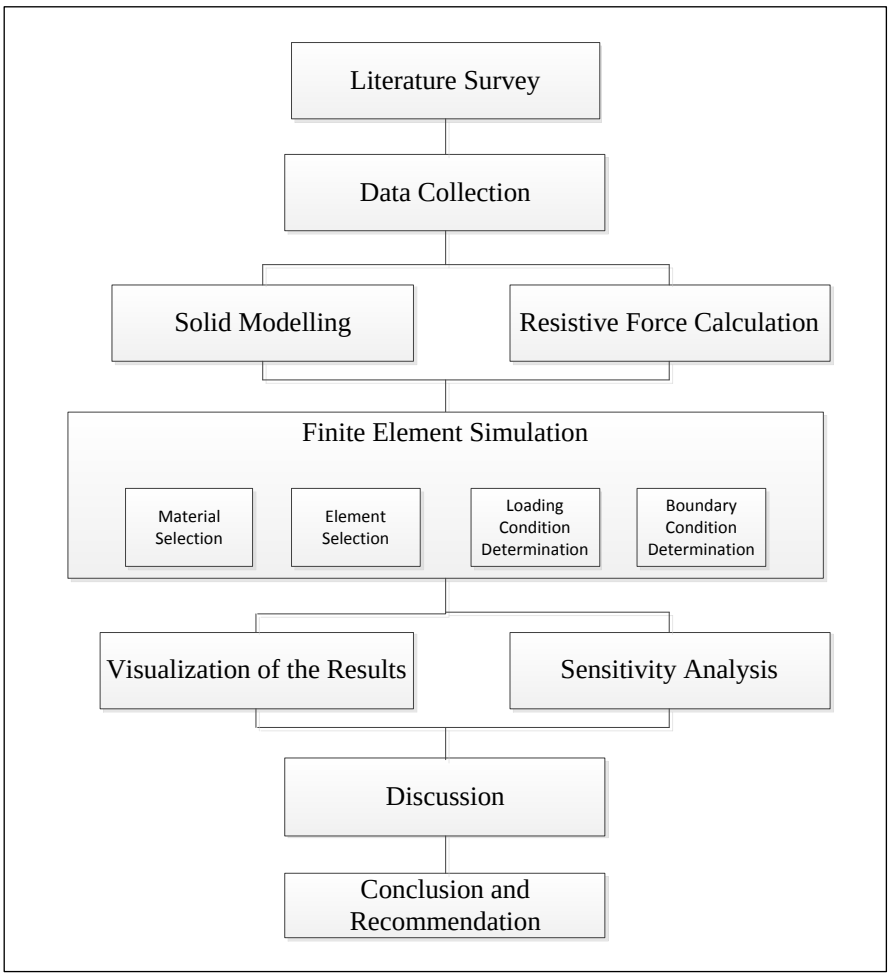

Figure 1.3 Flowchart of the Thesis Study

1.5 Outline of the Thesis

General information about the thesis is provided in the first chapter. Following the introductory chapter, a comprehensive literature review is presented in the second chapter. Literature review basically contains previous studies about dragline productivity, tool-formation interaction studies, earthmoving penetration and cutting theories and finite element analysis. The third chapter discusses preliminary works for the simulation. In the chapter three, the three-dimensional models of dragline

bucket and its rigging system in Solidworks CAD software are described in detail. The fourth chapter mainly focuses on the determination of resistive formation forces and also implementation of the simulation in Abaqus (Simulia, Version 6.9-2) environment. In addition, basis of the sensitivity analysis in the study is also explained in the fourth chapter. Numerical and graphical visualization of simulation results and discussion parts are the subjects of fifth chapter. The thesis study ends with the conclusion and recommendation part in the sixth chapter.

CHAPTER 2

LITERATURE SURVEY

2.1 An Overview of Walking Draglines

Draglines are massive earthmoving machines predominantly been used in open-cast coal mines to strip the overburden covering the coal (Figure 2.1). Draglines have a history in the excavation fields for decades. First dragline was invented by John W. Page in 1904, the founder of Page Company. The company then merged with The Harnischfeger Corporation under single name, P&H, in 1988. Other two companies in dragline market, Marion Steam Shovel Dredge and Bucyrus also merged under the name of Bucyrus. Today, Bucyrus and P&H are only two dragline manufacturer in the world.

Figure 2.1 Dragline Stripping in a Coal Mine (Anonymous, 2008)

Dragline-based stripping systems bring an economical saving up to 40 percent, compared to shovel-truck method (Özdoğan, 1984). Figure 2.2 shows the relative changes of unit cost for different stripping ratios, economical advantage of dragline over shovel-truck system. Considering the production utility of draglines, 142 units of dragline whose bucket capacities are larger than 30 m^3 (40 yd^3) are employed in 69 mines over the world (Gilewicz, 2000). These massive machines have a working capability of more than 10,000 service hours and most of them have a production capacity of 1 million tpy or more (Gilewicz, 2000). Prevalence of dragline utilization in open-cast coal mining according to the countries is indicated in
Table 2.1.

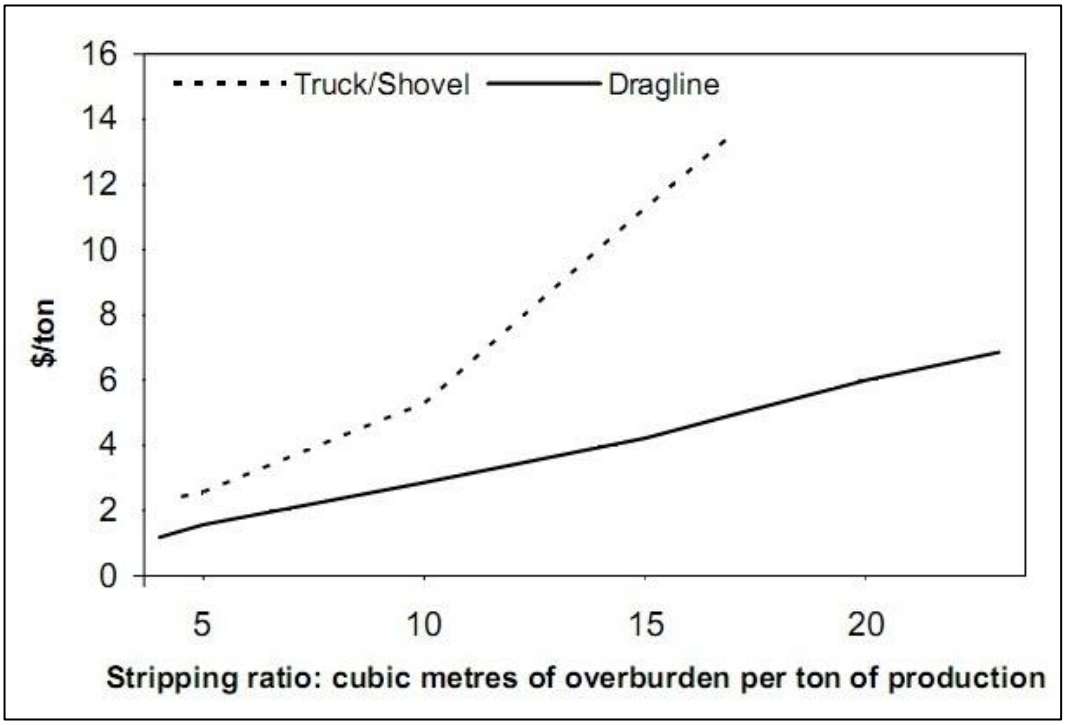

Figure 2.2 Economical Comparison of Shovel and Dragline (Hartman, 2002)

Draglines can be utilized in different configurations according to the mining method applications. There are some effective factors to determine the type of the method such as geology, dragline characteristics and mine production targets, coal and overburden thicknesses, number of coal seams, formation stability of the area,

Table 2.1 International Coal Production by Country and Output from Dragline Mines (Gilewicz, 2000)

Country	1998 Total Production, (million tons)	Number of Mines	Number of Draglines	1998 Dragline Production, (million tons)	% of Country Total
Australia	355	25	61	134	38
South Africa	222	10	25	76	34
Canada	75	12	22	40	53
India	323	9	17	23	23
Others(*)	133	13	17	57	43
Total	1108	69	142	380	34

blasting design, strength of loose material and skill of the dragline operator determines the selection of operation type (Mirabediny and Baafi, 1998). After specifying the method, pit length and pit width are required to be determined for the dragline operation. In dragline mining applications, working pit dimensions ranges from 300 to 3000 m in length, 25 to 60 m in width (Kennedy, 1990). Length of a dragline pit is affected by the factors such as topographical and geological changes and human based handicaps (Hartman, 1992). On the other hand, width of the pit is specified according to formation properties, dragline specifications such as maneuverability, dumping radius, movement rate, and design parameters such as pit height and blasting pattern (Hartman, 1992).

According to the utilization types, there are seven representative dragline mining methods used in Australian stripping mines, where the geology is more complex and much more amount of overburden should be removed, compared to the United States and European stripping mines (Mirabediny and Baafi, 1998). Name of these methods are simple side cast, standard extended bench with an advance bench, split bench (deep stripping), chop cut in-pit bench, extended key cut, single high wall and double

low wall multi-pass, double high wall and single low wall multi-pass (Mirabediny and Baafi, 1998). Unlike Australia, tandem dragline method, which allows two draglines work together, is also applied in European and United States mines. In surface coal mines, simple side casting is a common dragline stripping method (Kennedy, 1990). Operation in simple side casting starts with initial longitudinal excavation, named as box cut. This preliminary excavation is fulfilled to create an initial space for casting overburden. After box cut, the operation progresses in an order of digging and dumping the overburden with 90^0 angles rotational movements. Since the dragline completes side casting operation along the pit, it passes the next parallel pit. Figure 2.3 illustrates simple side casting method.

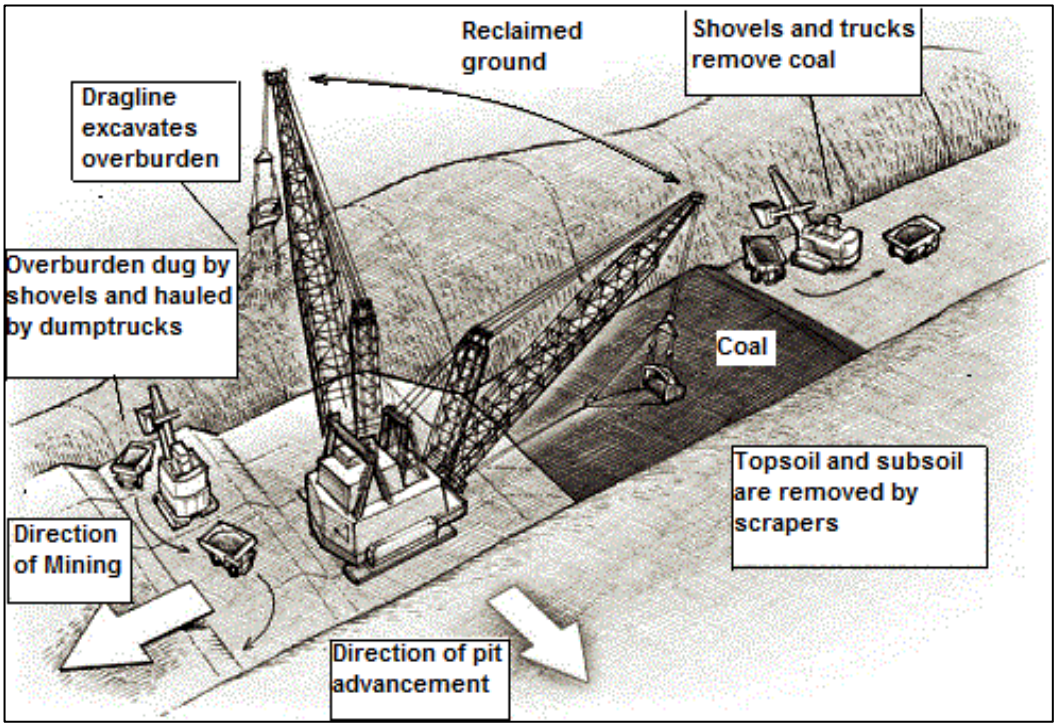

Figure 2.3 Simple Side Casting (Anonymous, 2010)

2.2 Dragline Productivity Factors

As in most earthmoving activities, two objectives should be managed also for an efficient dragline operation, (i) minimizing the cycle time and maximizing the

number of cycles and (ii) maximizing the payload of bucket (Vynne, 2008). Therefore, the detection of influential parameters and the related data in both cycle time and payload are important to criticize the productivity of a dragline operation. Demirel (2009) gathers these productivity factors into two groups, mine planning and operational factors. Mine planning and scheduling factors cover the subjects such as dragline operation geometry, suitability of the dragline for production rate, economical rehandle excavation volume, blast design satisfying the looseness of the formation, layering of coal, and bucket selection. On the other hand, operating factors handle the considerations such as availability of dragline for the operations, working conditions, suspended load, fatigue life of loading components on a dragline, cycle time, operator skill, and maintenance program. In this perspective, Rai's basic cyclic excavator formulation, as stated in Equation (2.1), presents a simple approach which is about the positive and negative effecting factors for monthly production of dragline (cited in Demirel, 2007).

$$O = \frac{B \times BF \times HS \times A \times J \times 3600}{(1 + S) \times C \times (1 + R)} \tag{2.1}$$

In Equation (2.1):

O = Monthly Production (m^3)
B = Bucket Size (m^3)
BF = Bucket Fill Factor (%)
HS = Scheduled Hours per Month (hrs)
A = Maintenance Availability (% of scheduled time machine is available for stripping/100)
J = Job Factor (% of time that machine is available for stripping)
S = Swell Percentage / 100
C = Average Cycle Time (sec)
R = Rehandle Ratio (%)

As in the Equation (2.1), cycle time of a dragline is a critical parameter which is reversely proportional with the dragline productivity. Minimizing cycle time and maximizing the number of cycles can be managed with reducing operational and mechanical delays such as idle, walking and fill times, swing and return rates, and spot time (Vynne, 2008). It is also clear that the efficiency is directly proportional with the role of bucket in the operation; bucket size and bucket fill parameters. These parameters determine the payload casted by dragline. The amount of payload is affected by the factors such as geology, blasting and looseness of the formation, resistance exhibited against the bucket, accuracy of weight monitoring system, bucket rigging, suspended load, specifications of the bucket, operator factor (Vynne, 2008). Therefore, formation specifications of the mine site and interaction of bucket with the formation are important to realize loading efficiency of the bucket. Studies about the bucket-formation interaction and bucket productivity can provide benefit to (i) increase the bucket payload, (ii) decrease the cycle time, (iii) prevent unexpected failures and fractures on the bucket components, and (iv) reduce the maintenance cost.

2.3 Dragline Productivity Studies

Global competition forces the mining companies to increase their productivities by controlling their capital and operational investments. At this point, determination of suitable mining method and scheduling, pre-evaluation of economic and security risks gain importance to measure the accuracy of the mid- or long-term plans for such a dynamic sector, mining. With developing technology, simulations supply realistic results in virtual environment and help the decision making mechanism for dragline operations. This part will review the previous computer-based researches about the productivity of dragline operation systems.

In the recent decades, many research studies about the dragline working efficiency have been carried out. These studies' topics can are divided into 3 main groups. They are mine planning and scheduling applications, productivity studies about loaded parts of dragline and virtual reality simulations to increase the skill of operator.

2.3.1 Dragline Productivity Studies through Mine Planning and Working Schedules

Computer-based studies have been performed to utilize in short-, mid- or long-term dragline mining plans and schedules, for decades. At one of them, Baafi *et al*. (1997) developed an integrated computer simulation model with DSLX computer language, to optimize the dragline operations. Three-dimensional geological model, assisted by a geological database, was formed. Complex multi-seam operations and distinct dragline methods were claimed to be scheduled and simulated in the model. Moreover, Erdem *et al.* (1998) searched about the synchronization of tandem dragline operation system, time management for operating and idle times of the two draglines and its effect on the efficiency of total operation. The draglines were denominated as dependent and independent dragline. Independent dragline was the free one in its advance way. The model aimed to reduce unoperated time of both dependent and independent draglines and to satisfy the synchronization between each other. In another study, Erdem *et al.* (2004) studied on a three-dimensional computational model assisting to choose optimal dragline digging mode for direct side-casting method. According to the hierarchical structure of the model, the program initiated with the determination of the spoil type depending on the coal seam inclination. Then, it progressed with the identification of spoil placement such as Dump-Near-Set (DNS) and Dump-Near-Dig (DND). By the execution of the model, several pit configurations could be obtained for a dragline by changing pit width values. In addition, Erdem *et al.* (2005) handled the simulation of three fundamental dragline stripping techniques; box cut opening, direct side casting and extended benching. In the research, it was tried to investigate the effects of overlapping cones on spoil geometry along the direction of both dragline advance and mining advance. Furthermore, Genç (2006) performed a research about dragline operations in Western Anatolia. During the study, single dragline, tandem dragline and dragline-shovel-truck combinations were compared according to cost/capacity relationships. Dragline methods in Western Anatolia Pits were illustrated with three-dimensional animations. Productivity of dragline was tried to calculate numerically with the help of working parameters. Also, Cobcroft (2007) performed a virtual

reality program. It was indicated that this program was practically used in Australian open-cast mines to organize short-, mid-, long-term mine plans. It was claimed that program had the ability to combine truck-excavator, dragline and bulldozer operations and optimize the overall mine plan in the field. In addition, it was stated that the program could provide cycle time of dragline, maximum excavation depth of dragline, maximum spoil height, and volumetric calculations for stripping rate.

2.3.2 Dragline Productivity Studies through Operator Training

Another investigation field for dragline productivity is about the training of dragline operator in a virtual excavation environment. Training of an inexperienced operator is not a simple work. It is required a six-month training to bring a dragline operator to a proficient level (Corke *et al*., 2006). This situation can cause a time loss and financial loss up to 2500 $/hour (Williams, 1997). Moreover, such an operator can lead to both machinery and environmental risks in the mine site. Due to the overloading conditions of dragline parts, some catastrophic failures can occur (Figure 2.4). This situation can cause long time-breakage and delay in mining plans.

Irrespective of the experience factor, it can also be observed productivity difference between experienced operators up to 20 percent (Corke *et al.*, 2006). Under all of these conditions, simulation-based training tools are important to provide both experienced and inexperienced operators with the opportunity to practice different dragline stripping scenarios in an environment away from the risk. In this field, some specific simulation companies, Immerse Technologies, 5DT, ThoroughTec, VortexSim presents three-dimensional virtual dragline applications. In Turkey, there is not such a training simulation for dragline. Carrying out simulation study in this direction, within the university or the private sector, is significant for the efficient control of earthmovers.

Figure 2.4 Dragline Boom Failure (Davis, 2010)

2.3.3 Dragline Productivity Studies through Improving Machinery Parts

Third common search topic for the dragline productivity is about the front-end parts of dragline during excavation and their effects over the productivity. A dragline is an earthmover which is operated with its long and heavy boom in a range of curvilinear area. Different amounts of forces and inertias are applied to distinct parts of machine during digging, hoisting, revolving and dumping cycles. Ideally, dragline should be controlled so that maximum amount of payload could be carried within minimum cycle time without catastrophic failure or damages on the mechanism. Since these types of failures and damages can cause long-term breaks and loss of time and production, the investigation and simulation of the loaded parts of dragline are critical to analyze their effects over the dragline performance. Several studies for different components of dragline have been practiced in recent years. These researches mostly concentrate on the topics about boom structure, rigging mechanism, bucket, and its apparatus.

In a study about dragline booms, Dayawansa *et al*. (2006) described stress and failures in the weld joints of the booms. A solid model of the boom was created, which was made of structural tubular elements. Three-dimensional stress analysis of the boom components was performed. Effective forces on the boom were detected, which appeared due to the self-weight of boom, weight of the bucket acting through the hoist ropes, suspension ropes, and the inertia of angular accelerations. In the study, crack propagation in the boom was investigated. In another research, Demirel (2007) modeled the front-end assembly of dragline with dynamic and kinematic variables in order to find maximum loads over the parts and yield stress of the boom. Figure 2.5 illustrates the two-dimensional vector loop presentation of the front-end assembly, used in the analysis of stress values during hoisting and dragging of the bucket and rotation of boom. Discrete Element Method (DEM) and Simultaneous Constraints Method were used to formulate the kinematics of dragline and bucket-material interactions, respectively.

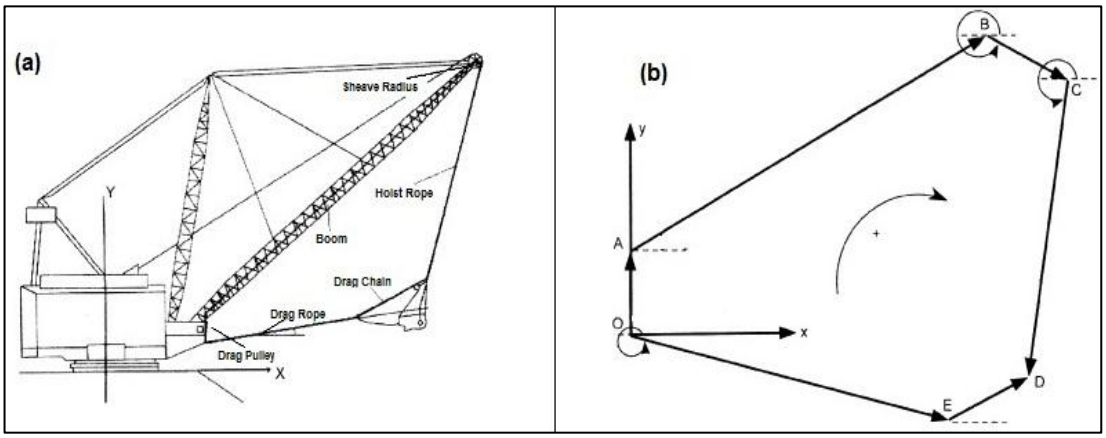

Figure 2.5 Dragline Kinematics (a) Dragline Front-End Assembly (b) Vector Loop Presentation (Modified after Demirel, 2007)

In addition to dragline boom, researches about dragline bucket and rigging system are equally critical, since dragline contacts the formation with the help of bucket. Draglines make overburdening operation with their large earth digging buckets, some of which can remove earth more than 108 m^3 (140 yd^3) at once (Gilewicz, 1999). The

bucket of dragline is mounted to the truss-structured boom with supporting wire ropes. Movement of the bucket is carried out by a number of chains and ropes, called rigging mechanism (Figure 2.6). The rigging mechanism mainly ballasts the bucket. Furthermore, wire ropes support the vertical and horizontal movements of the bucket. There are two types of ropes, hoist rope and drag rope, which are powered by electric or diesel type motors. While the hoist rope helps the suspending bucket to move upward and downward, the drag rope pulls the bucket horizontally. In a dragline operation, all external stresses appearing on the component of the dragline arise from the interaction between formation and bucket. Therefore, design and simulation of the bucket and its apparatus are important for the overall efficiency of the dragline.

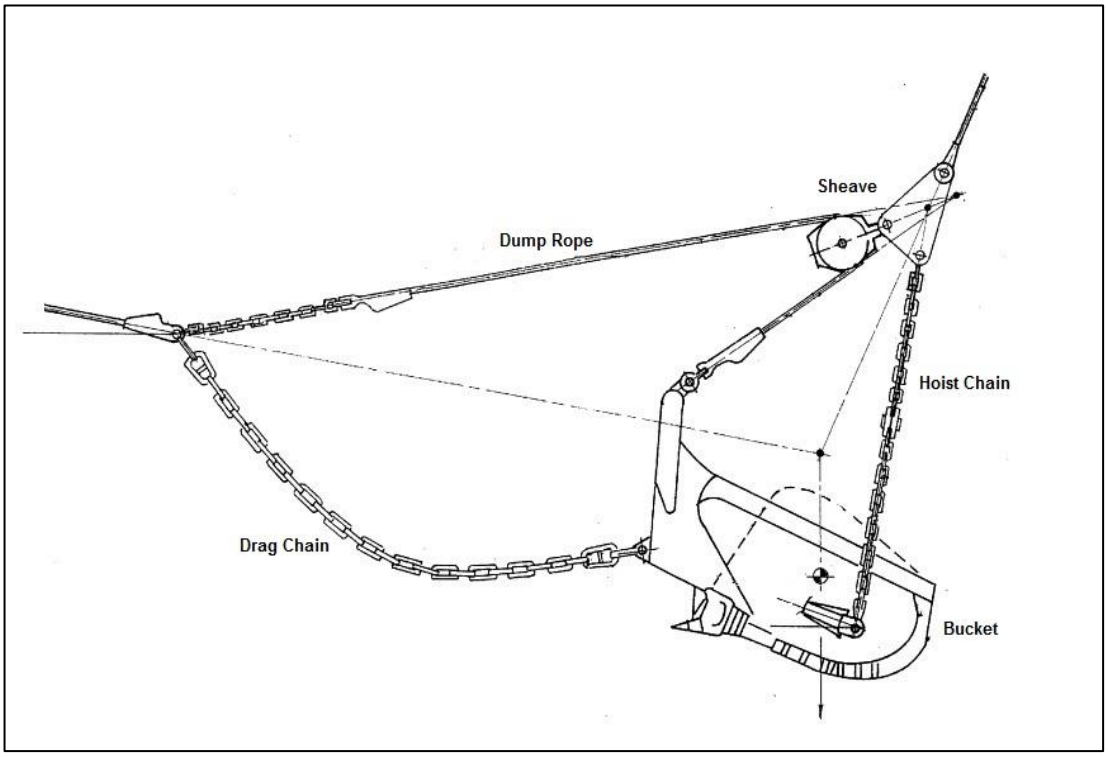

Figure 2.6 Dragline Bucket and Rigging Mechanism (Modified after Ridley, 2004)

Design of a dragline bucket includes the dimensional and weight parameters depending on the selection of lip type, shape of the tooth and its number, bucket

rigging mechanism, and it affects the overall productivity of dragline operation (Özdoğan, 2003) Therefore, many research studies have been carried out to improve the bucket and rigging system of dragline. Ridley and Algra (2004) classified the investigations about the productivity studies for bucket and rigging mechanism into four main groups: Optimization of bucket filling, improvement of rigging system, testing of bucket kinematically, and automation of scooping.

About the bucket filling, O'Beirne (1997) tried to find the effects of changes on rigging mechanism in the bucket efficiency. Within the scope of the investigation, differences between rigging system utilizations in Australian mines, influences of rigging parts such as hoist rope, dump rope, chain for the bucket efficiency were analysed. Moreover, Kavetsky (1999) developed a computational tool to use in the design and optimization of bucket and rigging system. Some computational modules were created to prepare a CAD environment for bucket design, to create two-dimensional bucket and rigging mechanism models, to determine material particle specifications, and to validate and display the program results. In another dragline bucket productivity investigation, Townson (2001) searched the optimization bucket payload of dragline. To achieve this, different mechanical and finite element models were created and it was validated with site test measurements of a Bucyrus type dragline. In the study, it was aimed to analyze the relationship between bucket filling and idle time which occurs due to the high wearing. As an example to the simulations about dragline bucket, Coetzee *et al*. (2007) used DEM and Material-Point Method (MPM) to analyze the load in the bucket part of the excavator. During the digging period, flow of the material over the bucket of excavator and maximum stresses on the tooth were discussed, as visualized in Figure 2.7. In another work about buckets, Cleary (2008) searched and compared the filling performances of two different trademarks of dragline bucket with the help of DEM. Besides the investigation about material swelling during the filling, erosion effects of the particles on the wearing were also tried to be guessed from the kinetic energy changes and particle collision angle.

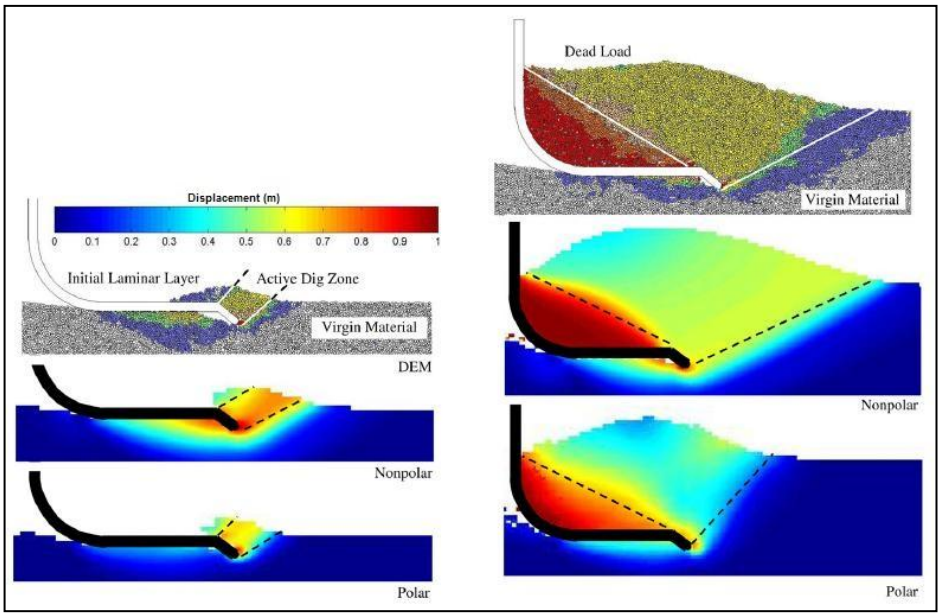

Figure 2.7 Shear Zone Theory at Different Displacements (Coetzee, 2007)

As relevant with the improvement of rigging system, Rowlands (2000) informed about universal rigging system which is different from the conventional rigging with its distinct hoisting rope configuration. A dragline prototype with a 1:250 scale was tested for this purpose. After experiments, it was observed that universal rigging system provides benefits with a decrease in capital cost of rigging components, cost of installation, duration of idle time, and an increase in possible dumping height and chopping reach. It was also claimed that this system was able to limit the transient forces on the dragline with its semi-automatic control. Moreover, Meyers and Leslie (2001) worked about the effects of the pivot point variations of an universal rigging mechanism, drag, front hoist, and rear hoist points, over the performance of bucket. In the study, total mass reduction and new mass distribution of both bucket and payload, load variations according to new configurations of ropes were discussed and performances of conventional rigging and universal rigging were compared.

Concerning with the kinematics of the dragline bucket, Srour (1999) claimed that it was created a simulation model identifying bucket and its rigging system with the help of a data set. It was expressed that this model had the ability to solve non-linear equations for the static balance of the bucket and rigging. It was also stated that

the model could assess the carrying angle and static force distribution on the system when any change about the bucket and rigging mechanism was introduced to the model. Furthermore, Ridley *et al.* (2004) tried to explain the bucket and rigging dynamics of dragline with a numerical model and simplified laboratory experiments. In the study, dynamic model was described the perturbation of the bucket from static equilibrium. Static pose of dragline bucket and rigging with a contour set of equal bucket carry angle was defined as in Figure 2.8. Initial angular accelerations were determined with the help of hoist and drag rope tensions and this static load. After computation process, solutions of the numerical model were compared to the experimental results.

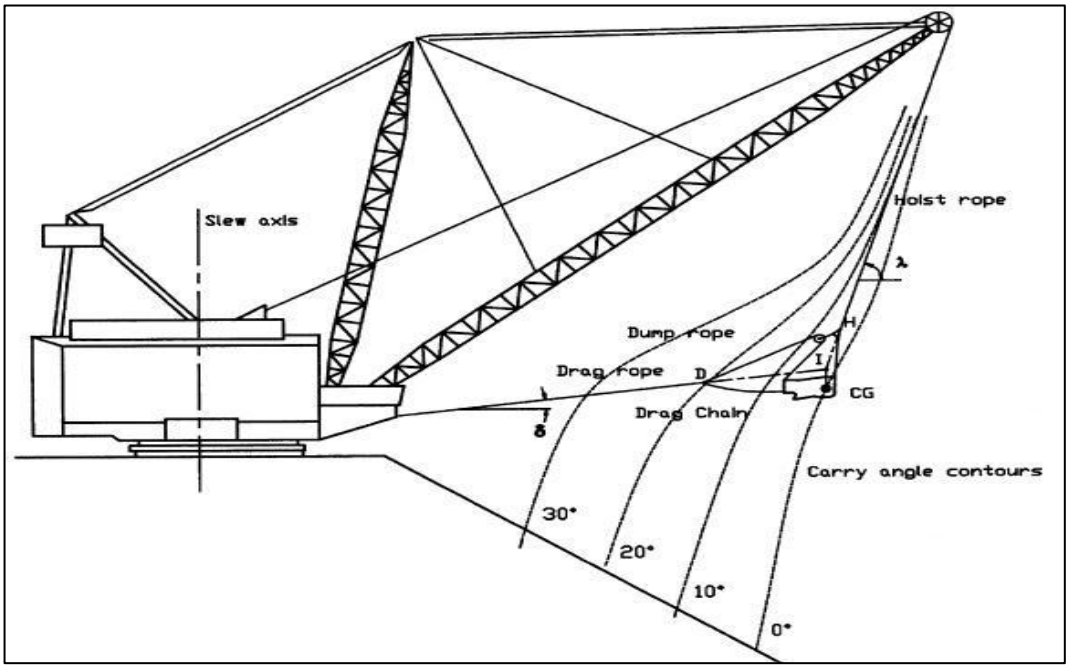

Figure 2.8 Dragline Layout Showing Constant Carry Angle Contours (Ridley, 2004)

About the automation of dragline, Lever and McAree (2003) aimed to draw a roadmap for determining the requirements of the scooping automation in open-cast mines. In this perspective, topics were detected and surveyed to enhance the productivity and to reduce the number of failures with the help of advance sensor technology, mine-wide information system, existing sensor systems on the sites.

In addition to researches about boom, bucket and rigging system, investigations about bucket teeth is of vital importance. Since, dragline buckets use teeth mounted to the front lip to penetrate and cut the formation for earthmoving activity. A typical tooth is either single-part with wedge shape or two-parts consisting of tooth holder and tooth point (Figure 2.9). For two-part teeth, there is a nose part in front of bucket lip to weld the removable tooth holders on it and to mount the replaceable tooth points to the holders. As Ryerson (1980) indicated, the assembly of these two parts extends about 66 cm from the lip part in 46 m^3 (60 yd^3) buckets where it extends forwardly about 76 cm from the lip part in 92 m^3 (120 yd^3) buckets. Moreover, Ryerson (1980) express that a 25 cm width bucket tooth point can weigh up to 68 kg, tooth holder 177 kg and tooth base 385 kg to overcome the high level of formation stress during the digging and to resist the breakages on the tooth assembly. In the thesis study, single-part tooth with wedge shape is used. Detailed expressions for the model's teeth are in Chapter 3.2.

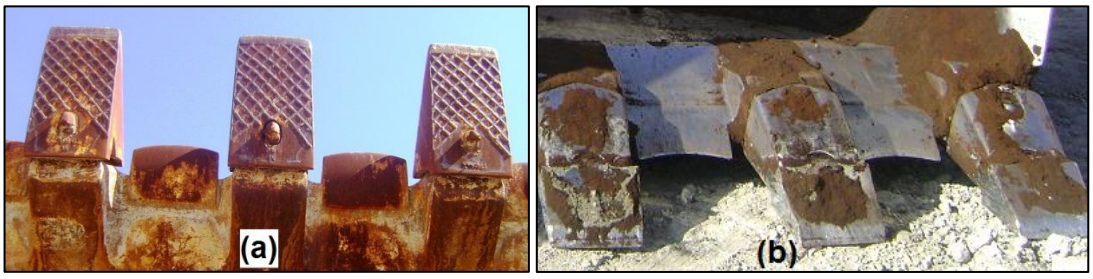

Figure 2.9 Dragline Bucket Teeth (a) Single Part (b) Double Part

2.4 Finite Element Applications for Earthmoving Activities

2.4.1 General Information about Finite Element Analysis

Finite Element Analysis (FEA) is a computational simulation technique providing different opportunities to analyze physical conditions such as displacement, strain and stress, force, velocity, acceleration, mass on solid bodies, using a numerical

identification called finite element. FEA drives complex configurations of points named as node. It generates adjoining grids named as mesh, using the nodes. The mesh has a network formation where each adjacent node is connected to each other. This mesh network involves material and structural specifications in order to identify how the structure will respond for different analysis conditions. As an example to FEA application, a blade cutting operation is illustrated in Figure 2.10.

Structural analysis in FEA contains linear and nonlinear models. Linear models utilize simple parameters and suppose that the deformation of material is not plastic. On the other hand, nonlinear models can analyze the stress on the material when elastic capability of it is exceeded. Therefore, stress values in nonlinear models continue to change with plastic deformation.

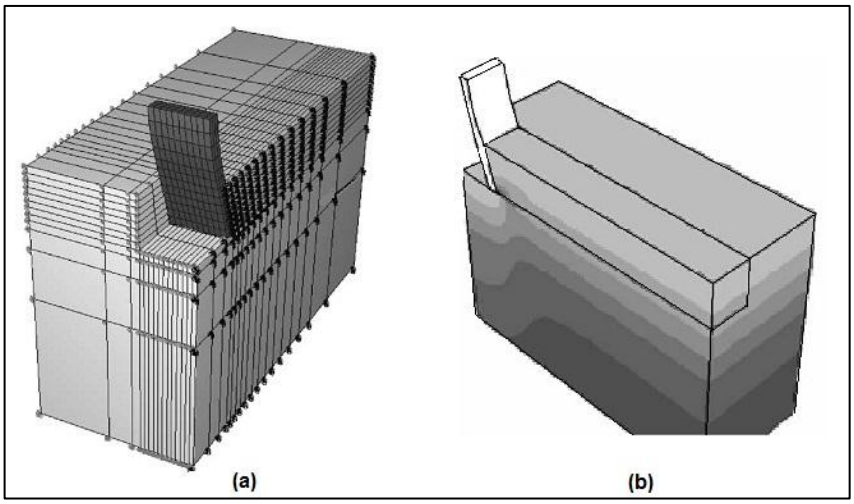

Figure 2.10 Finite Element Analysis (a) Meshing (b) Stress Distribution (Abo-Elnor *et al*., 2004)

2.4.2 FEA Applications for Earthmoving Actions

An earthmoving action expresses the shape of interaction between the formation and the digging tool. This interaction is mainly affected by formation specifications such as density, internal friction angle, external friction angle, cohesion and adhesion.

Earthmoving factors form a very complex phenomenon. Since, formation can exhibit either isotropic or anisotropic behavior. If it is anisotropic, formation specifications change largely with the direction of effective forces inside the formation, and it is hard to estimate such a behavior. Moreover, it is clear that compactness of the formation can fully change the formation manner on the digging tool. All dynamics of the formation are required to be known to see the full interaction between tool and formation. However, it is hard to identify complete effect of the formation on the tool. Under these conditions, it is better to characterize the tool-formation interaction most closely to the reality, with some assumptions.

Dealing with the bucket moving into the formation, different types of questions can be investigated. In literature, researches about the bucket utilization are divided into the topic as the settlement and movement of the formation, forces exerted during sweeping, amount of filling into the bucket, and resistive forces of formation against the tool. Because of its complexity, simple analytical models cannot answer to such problems. Computational integrations can be required to evaluate these earthmoving actions.

Above mentioned topics can be solved by utilizing FEA. It yields a technique to model systems consisting of many differential elements. Many investigators have used FEA to address issues related to earthmoving actions. At one them, Yong and Hanna (1977) worked about productivity of a flat blade moving in clay formation for a distances smaller than one foot. It was claimed that they improved a method that presents particular information about the stress and deformation of the formation due to the excavation forces. It was stated that the method provided benefit at the estimation of forces exerted by both the tool and the formation. Mounem and Nemenyi (1999) created an elastic-perfectly plastic formation model and used FEA to simulate the formation cutting process of a subformation with different geometries. Fielke (1999) performed a computational model expressing the effect of cutting edge geometry over the tillage forces. This two dimensional finite element model was supported by the experiment findings. Mootaz *et al.* (2003) performed the three-dimensional simulation of narrow blade-formation interaction in a FEA solver,

by assuming that formation behaves elastic. They verified formation failure zones vertically and horizontally to eliminate convergence problem induced because of large blade movement. The model was validated by providing the ultimate shear stress zones in the formation after computing the software and matching it with the predefined formation failure areas. In a two dimensional approach, Davoudi *et al.* (2008) insisted that a model which is capable of estimating draft forces during tillage was created in FEA software. Moreover, in many research, brittle behavior and plasticity of formation during the cutting process was analyzed (Chi and Kushwaha, 1989; Raper and Erbach, 1990; Aluko and Chandler, 2004; Aluko, 2008).

Besides FEA, the reader can prefer to investigate DEM for the tool-formation interaction modeling, while it is specifically good for the simulation of granular materials and for analyzing the relationship between inter-particle and particle-tool behaviors (Cleary, 1998; Owen *et al*., 2002; Hofstetter, 2002).

2.5 Earthmoving Action of a Dragline Bucket within the Formation

An earthmover performs two main earth digging mechanisms such as cutting and penetration, according to their digging tool geometries and/or formation displacement abilities. When the shape of the digging tool is handled, a bucket mainly consists of two parts as shown in Figure 2.11. Initially, a bucket has a rectangular shape floor component, named as the separation plate as stated with A in Figure 2.11. With the help of this plate, a bucket is able to move the formation by pushing or dragging (dragline bucket) it to the failure state. Secondly, the bucket has another mechanical component, teeth, as stated with B in Figure 2.11. Bucket teeth penetrate the formation media to relieve digging mechanism.

Dragline buckets are common overburden stripping tools used in the open-cast mines. In a dragline, chain and rope combination gives axial motion to the bucket and determine the digging direction. The motional varieties provide the earthmover fully benefit from the separating and penetration ability of the bucket. Depending on the interaction conditions between bucket tips and the formation, the movements into

the formation can be achieved into two different ways for the dragline, cutting, penetration.

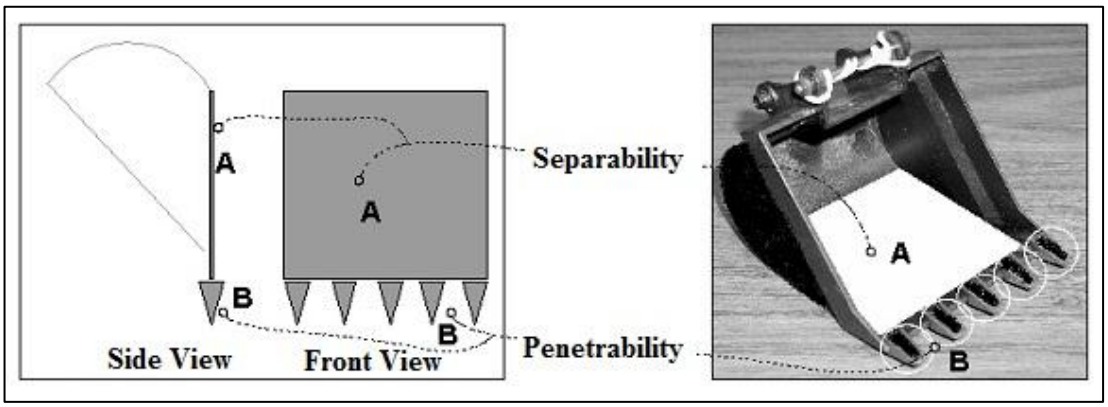

Figure 2.11 Penetration and Separation Parts of a Bucket

Figure 2.12 illustrates the kinds of earthmoving actions for a dragline bucket. As seen in Figure 2.12, the bucket firstly penetrates the formation with the help of its own weight and then, cut it along the operation direction. Figure 2.13 shows the orientation of a dragline bucket with the formation during the operation.

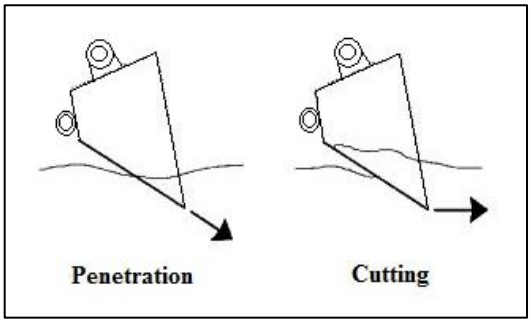

Figure 2.12 Fundamental Earthmoving Actions for Shovel (Modified after Blouin, 2001)

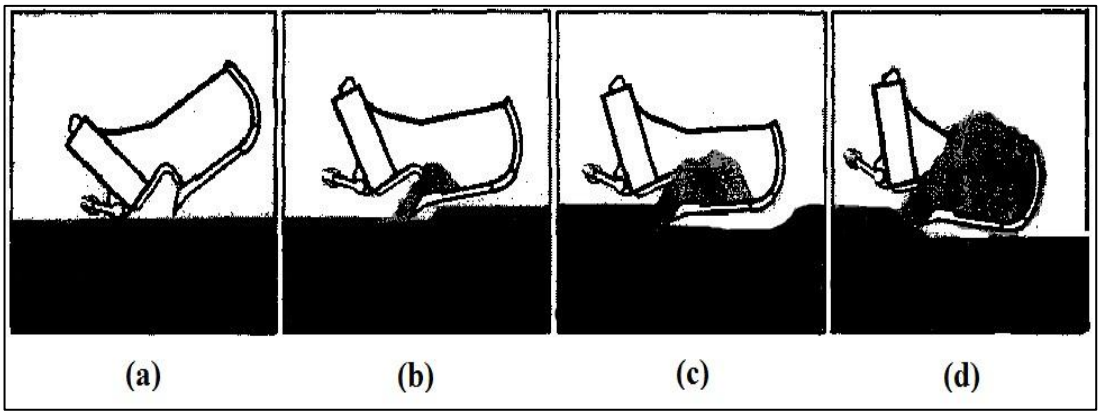

Figure 2.13 Dragline Bucket Earthmoving Actions (Özdoğan, 2003)

In the earthmoving operations, it is required to estimate resistive forces against the tool to provide the stress distribution on the tool and to limit the earthmover velocity and torques which are necessary for an efficient operation. As Blouin (2001) stated, penetration exhibits similarity to cutting theory in bucket actions. Therefore, cutting force theories were utilized in the thesis study to estimate the resistance of formation against the dragline bucket.

2.6 Tool-Formation Cutting Resistance Models for Earthmoving Activities

This part examines distinct models for the estimation of force amount required to move a plate buried into the formation. To achieve the movement of a plate, the formation is required to displace. It is essential that a failure surface appears between the moving formation in front of the plate and stagnant formation body. The force required to "fail" the formation and pull a tool is generally named as draft force. The force models discussing in this part are mainly concerned with the formation strength and conditions that manages the formation failure. All models are 2-D and conditions of plane strain are assumed for all of them. Besides, formation in the models is assumed to be homogeneous and isotropic.

2.6.1 Background on the Cutting Resistance Models

Interaction between cutting tool and formation can be described with the help of external and internal forces in the excavation area. One of the effective forces is the force exhibited by the formation against tool. To understand the condition better, it is required to discuss the types of lateral earth pressures back and front of the cutting tool. Weber (n.d) states that lateral earth pressures are divided into three categories, (i) active earth pressure, (ii) passive earth pressure, (iii) at rest earth pressure. At rest earth pressure appears on the plate when there is no lateral movement. On the other hand, active and passive earth pressures are effective when lateral displacement takes place. In Figure 2.14, there is an illustration of active and passive force on the plate. When the plate moves away from the formation, environment for the active pressure evolves. With the displacement of plate, formation wall behind the plate is free to move outward and formation mass is activated under shear strength conditions. On the other side, passive earth pressure is initiated with the compression of formation in front of the moving plate. Lateral pressure continues to rise until the passive earth pressure is maximized.

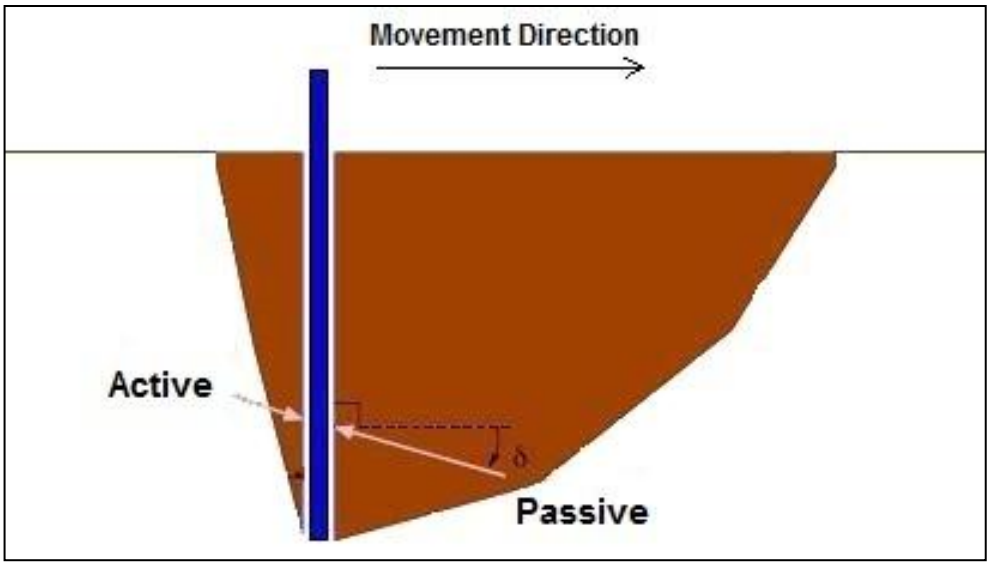

Figure 2.14 Active and Passive Pressure Acting on the Plate Embedded in Formation

There are two common theories utilized to investigate the lateral earth pressures, Coulomb's and Rankine's Theories (Craig, 1997). While the Rankine's Theory mainly pays attention to plastic equilibrium and stresses in the formation body during the shear failure, the Coulomb's Theory focus on the stability between the failure plain and an earth-retaining plane (Craig,1997). Application of Rankie's Theory requires a failure environment with no adhesion and no friction between the plane and the formation. It is also limited to vertical walls. Coulomb's Theory is also similar to Rankie's Theory. However, formation-wall friction angle can be taken into the account only in the Coulomb's Theory. Furthermore, wall subjected to lateral pressures do not have to be vertical in the theory. Most of the earthmoving theories use the basics of Coulomb's formation mechanics equations.

2.6.2 Empirical Approaches for the Cutting Resistance Models

The question about the resistance of formation during the machine cutting operation has been one of the primary interests in surface mining and construction machinery, aerospace earthmoving, and agricultural tillage fields. At that point, empirical approaches can help to find beneficial information about this question. Some researchers have tried to calculate cutting resistance of the formation based on empirical outcomes for distinct earthmoving machines (Alekseeva *et al*., 1985; Zelenin *et al.*, 1986; Nedoredzov, 1992, and Hemami *et al.*, 1994).

A number of the empirical approaches for estimating a cutting tool-formation force were made by Zelenin, *et al.* (1986). At one of the studies, cutting resistance model was formed for a bucket without teeth. The model takes into account the factors such as condition of formation, cutting conditions and geometry of the digging tool as shown in Equation (2.2).

$$P = 10C_0e^{1.35}(1 + 2.6b)(1 + 0.0075\alpha_c)(1 + 0.03s)\alpha_0 k \qquad (2.2)$$

In Equation (2.2), P is cutting resistance, C_0 is compactness coefficient, e is cutting depth in cms, b is bucket width in m, α_c is angle of cutting in degrees, s is bucket cutting surface thickness in cms, α_0 is tip angle coefficient, k is cutting-type coefficient.

In empirical models, different types of indices are suggested based on the system of earthmoving machines and resistive forces existing between the formation and the machine. They can be approximately predicted by quantitative basic equations. Since this type of model generally aims to offer analytical tools for machine design, it is not obvious how to infer for random mechanisms and formation conditions. Even though the empirical models predict the earth-moving resistance of the formation, they are lack of representing the process of excavation. Analytical approaches were utilized instead of empirical models to calculate the earth-cutting force of dragline bucket due to:

i. They are not analytical models so they are not fully capable of providing the needs of earth-moving simulations. For instance, it is hard to obtain how to embody a case in the formula where an overburden is located on the top of the expected cutting zone.

ii. It is not clear what types of resisting force base are involved in the empirical model.

iii. The models are not referred in terms of general geotechnical parameters such as internal friction angle (φ) and cohesion (c). This terminological usage is required to reflect formation properties to the model correctly.

iv. Since the models depend on experimental outcomes, the validity of the models is directly related to how the estimated formulations resemble the original experiment conditions.

2.6.3 Analytical Approaches for the Cutting Resistance Models

Models used for the force estimation in earth-moving activities aim to find mathematical approaches for the counter force behavior of formation on the moving

tool. These models can be divided into 3 main categories according to the types of the earth-moving activities, penetration, cutting, and loading. Draglines perform the excavation operations with dragging, hoisting, and swing functions. It cuts the formation with its dragging function. Therefore, resistive force models for the cutting action are critical to estimate the stresses over the bucket.

In this perspective, Blouin *et al.* (2001) presented a review study about the force prediction models for earth-moving tasks. In the review, it was emphasized that three-dimensional cutting models are apart from the two-dimensional cutting models with their side effect factors. However, Blouin *et al.* (2001) also stated that there is negligible relationship between side effect findings of analytical three-dimensional models and those of a real bucket and Blouin *et al.* (2001) also indicated that it can be utilized from two-dimensional models in force calculation of bucket digging process. Therefore, two-dimensional models will be analyzed and discussed under this title.

In the two-dimensional models, forces on the surface of the cutting plate are calculated in two-dimensional perspectives (Figure 2.15). For instance, Osman (cited in Blouin *et al.*, 2001) utilized from the logarithmic approach to formulate two-dimensional cutting action. Both the behavior of heavy medium without surcharge and cohesion and the behavior of weightless medium with surcharge and cohesion were included in the model as equation components. The resultant cutting force is calculated as stated in Equation (2.3).

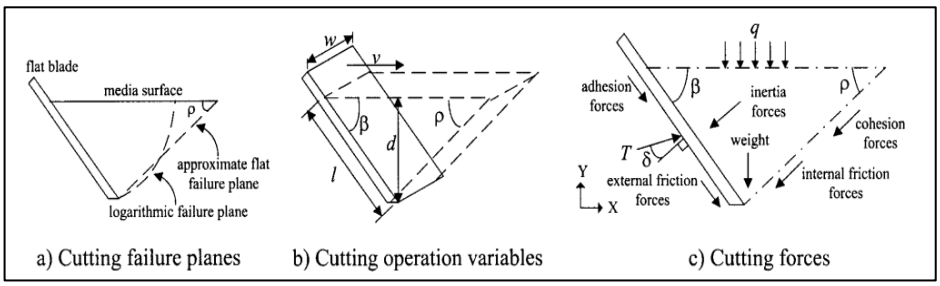

Figure 2.15 Failure Plane in Formation Cutting (Blouin *et al.*, 2001)

$$T = w\left[\left(0.5\gamma t^2 tan^2(45 + 0.5\rho)d_1 + \frac{e^{2w \cdot tan\rho} - 1}{4\ tan\rho} {r_0}^2 \gamma d_2 + qttan^2(45 + 0.5\rho)d_4\right) {d_3}^{-1} + \left(0.5(r_1^2 - r_0^2)\frac{c}{tan\rho} + 2ct\ tan(45 + 0.5\rho)\, d_4 + \frac{qt}{sin(45 - 0.5\rho)} d_5 + C_a l d_7\right) d_6^{-1}\right] \quad (2.3)$$

In Equation (2.3), T is resultant cutting force, γ is specific weight, w is tool width, d is tool depth, l is tool length, c is cohesion, C_a is adhesion, t is depth of Rankine Zone, ρ is shear plane angle, r_0 is curvature radius, and $d_1, \dots, d_7$ are graphical distances.

Projection of the resultant cutting force on the horizontal plane is in Equation (2.4).

$$H = Tsin(\beta + \delta) \quad (2.4)$$

In Equation (2.4), H is horizontal force, β is rake (cutting) angle, and δ is external friction angle.

Unlike Osman's formula, Gill and Vanger Berg (cited in Blouin *et al.*, 2001) insert the influence of weight and inertia factors to the cutting force calculation as in Equation (2.5).

$$H = N_0 sin\beta + \delta N_0 cos\beta + kw \quad (2.5)$$

In Equation (2.5), N_0 is inertia factor and the parameter k is related to the wearing factor of the material. It is taken into consideration in case of high wearing. Therefore, re-arranged version of the formula is given in Equations (2.6) and (2.7).

$$H^* = H - kw = N_o sin\beta + \delta N_o cos\beta \quad (2.6)$$

In Equation (2.6):

$$H^* = \left[\gamma \frac{\sin(\beta+\rho)}{sin\rho}\left(l + \frac{dcos\beta + \rho}{2\,sin\rho} + \frac{dsin(\beta+\rho)tan\beta}{2\,sin\rho}\right) + \frac{c}{sin\rho\,(sin\rho + \phi cos\rho)} + \frac{\gamma v^2 sin\beta}{gsin(\beta+\rho)(sin\rho+\phi cos\rho)}\right] . \frac{wd(sin\beta + \delta cos\beta)(sin\rho + \phi cos\rho)}{\sin(\rho+\beta)\,(1-\phi\delta) + \cos(\rho+\beta)\,(\phi-\delta)} \quad (2.7)$$

In Equation (2.7), ϕ is internal friction angle, v is tool speed, and g is gravitational acceleration.

Swick and Perumpral (cited in Blouin *et al.*, 2001) improved Gill and Vanden Berg's model and created an analytical model which covers effects of adhesion, cohesion, surcharge, weight, and inertia. Swick and Perumpral's model (1988) is shown in Equation (2.8).

$$T = \frac{wd}{\sin(\beta+\phi+\rho+\delta)}\left[\frac{-C_o \cos(\beta+\phi+\rho)}{sin\beta} + \frac{\gamma d^2}{4}(cot\beta + cot\rho)\,sin(\phi+\rho) + \frac{qd}{2}(cot\beta + cot\rho).sin(\phi+\rho) + \frac{c\,cos\phi}{sin\rho} + \frac{\gamma v^2\,sin\beta\,cos\phi}{g\sin(\beta+\rho)}\right] \quad (2.8)$$

In Equation (2.8), C_o is compactness and cutting index.

Finally, horizontal force in the model is calculated as in Equation (2.9).

$$H = Tsin(\beta + \delta) \quad (2.9)$$

McKyes's earthmoving model (cited in Blouin *et al.*, 2001) is the most complete form of two-dimensional earthmoving theories which contains factors of weight, cohesion, adhesion, surcharge, and inertia. Simple version of the model is in Equation (2.10).

$$T = w\left(\gamma g d^2 N_\gamma + cdN_c + C_a dN_{ca} + qdN_q + \gamma v^2 dN_a\right) \tag{2.10}$$

In Equation (2.10), N_γ is weight coefficient, N_c is cohesion coefficient, N_{ca} is adhesion coefficient, N_q is surcharge coefficient, and N_a is inertia coefficient.

Detailed expressions of N_γ, N_C, N_{Ca}, N_q, N_a in McKyes's Model are given in Equations (2.11), (2.12), (2.13), (2.14), and (2.15), respectively (cited in Worley and Saponara, 2008).

$$N_\gamma = \frac{(cot\rho + cot\beta)[sin\theta \cot(\beta + \phi) + cos\theta]}{2\cos(\rho + \delta) + \sin(\rho + \delta)\cot(\beta + \phi)} \tag{2.11}$$

$$N_C = \frac{1 + cot\beta \cot(\beta + \phi)}{\cos(\rho + \delta) + \sin(\rho + \delta)\cot(\beta + \phi)} \tag{2.12}$$

$$N_{Ca} = \frac{1 - cot\rho \cot(\beta + \phi)}{\cos(\rho + \delta) + \sin(\rho + \delta)\cot(\beta + \phi)} \tag{2.13}$$

$$N_q = 2N_\gamma \tag{2.14}$$

$$N_a = \frac{tan\beta + \cot(\beta + \phi)}{[cos(\rho + \delta) + \sin(\rho + \delta)\cot(\beta + \phi)]} + (1 + tan\beta cot\rho) \quad (2.15)$$

Extended form of McKyes's Model (1985) is visualized in Equation (2.16).

$$T = \frac{wd}{\cos(\beta + \delta) + \sin(\beta + \delta)\cot(\rho + \phi)} \left[\frac{\gamma g d(cot\beta + cot\rho)}{2} + q(cot\beta + cot\rho) + c(1 + cot\rho\cos(\rho + \phi)) + C_a.(1 - cot\beta\cot(\rho + \phi)) + \frac{\gamma v^2(tan\rho + \cot(\rho + \phi))}{1 + tan\rho\, cot\beta}\right] \quad (2.16)$$

Horizontal force acting in McKyes's earthmoving model (1985) is in Equation (2.17).

$$H = Tsin(\beta + \delta) \quad (2.17)$$

In the thesis study, passive force existed on the bucket due to the interaction with the formation was estimated by McKyes's the earth moving formulation (1985) in Equation (2.10).

2.6.4 Cutting Resistance Model Applications

Formation cutting involves the mechanical failure of formation, which usually occurs in the shear mode along internal rupture surfaces in the formation, and often at the boundary between the cutting tool surface and the formation (McKyes, 1985). In the modeling of tool-formation environment, methods like finite and discrete element solutions, geometric simulation and the passive earth theory are applicable to

estimate interactions forces (Offei and Frimpong, 2009). In concern with the passive earth theory, Ericsson (2000) simulated the excavation of wheel loader in software. The author divided the resistive forces of formation against the bucket as cutting, penetration, inertial forces and mass flow, and utilized from MyKyes's method to calculate approximate counter force in the formation during the cutting operation.

Besides the theoretical models, some laboratory studies have been executed to optimize the bucket cutting. Maciejewski and Jarzebowski (2002) carried out the digging process of bucket in a laboratory stand. They basically performed the operation with a cutting tool into the formation, mounted on the hydraulic cylinders which measure the horizontal, vertical, and rotational forces during the process. With theoretical predictions and experimental observations, they modified the parameters such as shape of cutting tool, digging trajectory, and the angles of tool-formation interaction angle. Specific energy measurements in the cylinders were taken as indicator for the effect of parametric changes on overall digging efficiency.

In the thesis study, stress values on the dragline bucket during horizontal cutting action were investigated. Resistive earth pressure on the digging teeth during the action was determined using McKyes's cutting theory (1985). Parameters in the theory were provided using three different formation data with different compactness.

2.7 Summary of the Literature Review

A comprehensive literature survey has been carried out to collect information about previous studies about dragline earthmoving operation and theories behind this phenomenon. These researches prepared a background for the thesis subject, investigation of stresses on the dragline bucket with FEA. The literature search started with the general information about dragline utilization on the world open-cast mines and dragline stripping methods. Then, it proceeded with the investigation of productivity factors which effect the efficiency of dragline in the field and review of the previous studies about dragline productivity.

The productivity researches about dragline were surveyed in three main groups, mine planning and scheduling, operator training, and dragline machinery parts. After overview of dragline and productivity, literature search advanced in a more specific field. In this part, it was tried to create a basis for dragline bucket simulation. To achieve this, components of finite element analysis, principles of earthmoving operations and factors of formation-tool interaction period were analyzed.

After literature survey, it was observed that there was a lack of enough research study about stress investigation on an operating dragline bucket. At that point, this thesis study aims to contribute to the literature, with three dimensional dragline bucket simulation and stress value investigation on the bucket.

CHAPTER 3

SOLID MODELLING OF DRAGLINE BUCKET

3.1 Computer-Aided Design of a Dragline Bucket

Computer-Aided Design (CAD) presents many advantages over hand drawing techniques in mechanical modeling. A part or assembly model can be easily monitored three-dimensionally on a computer. Shape of the models can be practically modified by changing the geometrical dimensions. This computer-aided system allows the user to illustrate the spatial relationships between the parts and to view the model a large range of representations. It prepares the model for simulation in a virtual environment. Mechanical simulations in CAD environment test the model by computing the dynamic relationships among the parts. For instance, one of the common simulations, stress test, measures the nodal modifications, and distortions on the model under distinct types of stresses. It uses the displacement of meshes or grids to guess the strain and stress components. In design and simulation steps, geometrical relationships on the parts, settlements of the parts in the system, material properties and finite element patterns should be assigned as close as possible to the reality, to get the most efficient and realistic results.

To create and simulate a model related to dragline productivity, it is required to investigate and criticize the working parts of a dragline and their effects on the productivity (Figure 3.1). At first, a typical dragline consists of swivel control cabinet placed on a fixed base. An outwardly extending boom is fixed axially to the cabinet. Winch assembly on the sides of the cabinet controls the bucket movements by releasing or retrieving ropes. Two pairs of ropes in different duties, hoist and drag ropes, provide the connection between control cabinet and rigging mechanism of bucket. Hoist rope lies along the boom up to the sheave on the farthest point of boom

and lies down to the rigging and bucket assembly. Drag rope is located between the drag winch and rigging and bucket assembly. Within the dragline working components, the most stress exposed parts against the resistive forces of the formation are bucket elements and rigging mechanism. Determination of the stress and strain components on these parts is critical to hold a view about the excavation efficiency of dragline. These investigations can provide benefit to (i) detect the critical yielding points on the bucket components, (ii) develop more effective maintenance plans, (iii) decrease the maintenance cost, and (iv) increase the availability and productivity of the bucket. In this regard, this thesis study is focused on the modeling and simulation of the bucket and rigging mechanism of dragline, where dragline contacts with the formation and resistive forces are ultimate.

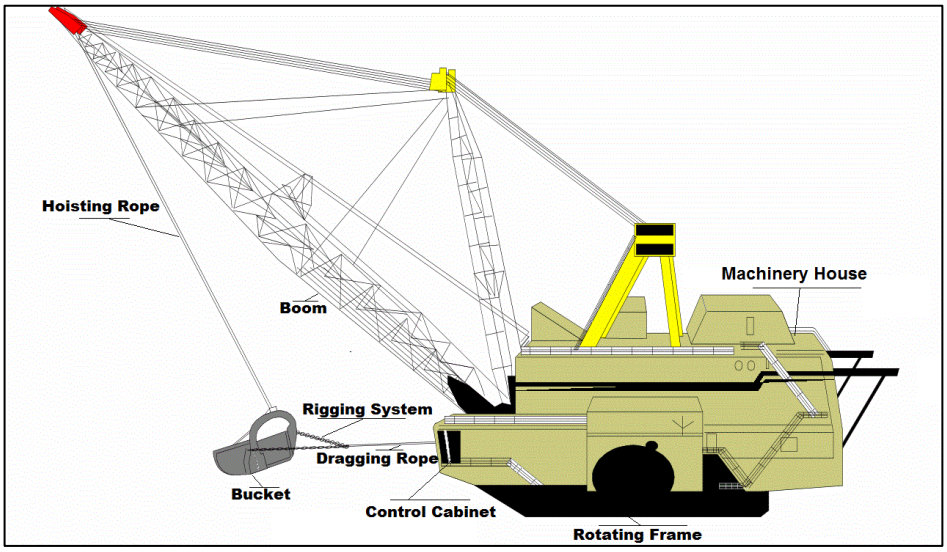

Figure 3.1 Components of a Walking Dragline (Anonymous, 2004)

3.2 Geometry of Main Bucket Body and Tooth

Dragline bucket has a massive shape compared to other excavator buckets, being able to remove 23 m^3 (30 yd^3) to 134 m^3 (175 yd^3) overburden at once (Gilewicz, 1999). Due to its own weight (weight of a dragline bucket with a capacity of 50 m^3 is approximately 100 tons), resistance of the formation against the bucket and heavy

payload, high level of stresses emerge on the bucket and its rigging system. In this regard, a careful description of the bucket model with a proper geometry is essential to simulate these stress components on the bucket.

Dragline bucket and rigging assembly contain main bucket body itself and a mechanism named as rigging which means the combination of chains, steel strands and constituents fulfilling the work of suspending and supporting the bucket (Figure 3.2). A dragline bucket main body can be defined as a combination of a back wall, two side walls, floor wall, arch and lip elements that create a space to gather the partially loose or soft material during excavation.

Figure 3.2 Bucket and Rigging Mechanism in the Operation (Esco Dragline Buckets, 2010)

Figure 3.3 illustrates the elements of the main body. Main body design basically consists of the geometrical association of floor, back and side walls, arch, drag and hoist elements. Each wall of the bucket shows differences with their dimensions, slopes and orientations in the body. The side walls on the bucket are slightly inclined outward. These sidewalls provide rearward space with an upward tapering. The back wall exhibits convex configuration with its curved structure. Front sides of the side walls and floor wall are integrated with the lip part. Rope and chain assemblies, used

for pulling and releasing the bucket, and digging teeth are attached to the lip with the help of connecting links.

Mechanical design of any machinery part combines the determination of geometry and material that represent its functions. An adequate design of the bucket system should lay out the explicit role of the bucket during excavation. Design process contains the steps such as creation of layouts, sketches of design elements, behavior of the elements toward each other (constraints) and assembles of the machine parts. Design of a particular part starts with the gathering data about its geometry. In this study, geometry of each element on the main bucket body was formed using available data of existing buckets. Measurements on an original dragline bucket in a mine site and official catalog information were utilized to generate the overall geometries. Solid form of the dragline bucket and rigging mechanism were performed in Solidworks (Solidworks Co., 2009).

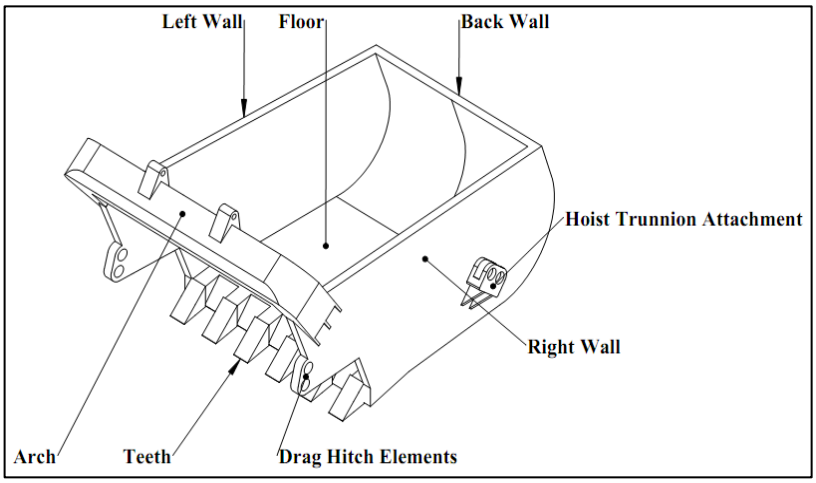

Figure 3.3 Dragline Bucket Elements

Figure 3.4 presents general view of the bucket solid model from different sights. As seen, the bucket has a mount opening of 4.32 m and consists of six digging teeth, each one have a 0.35 m in width. Furthermore, the bucket body extends 4.88 m in the length, 3.05 m in the height, and also it expands from the back to the front.

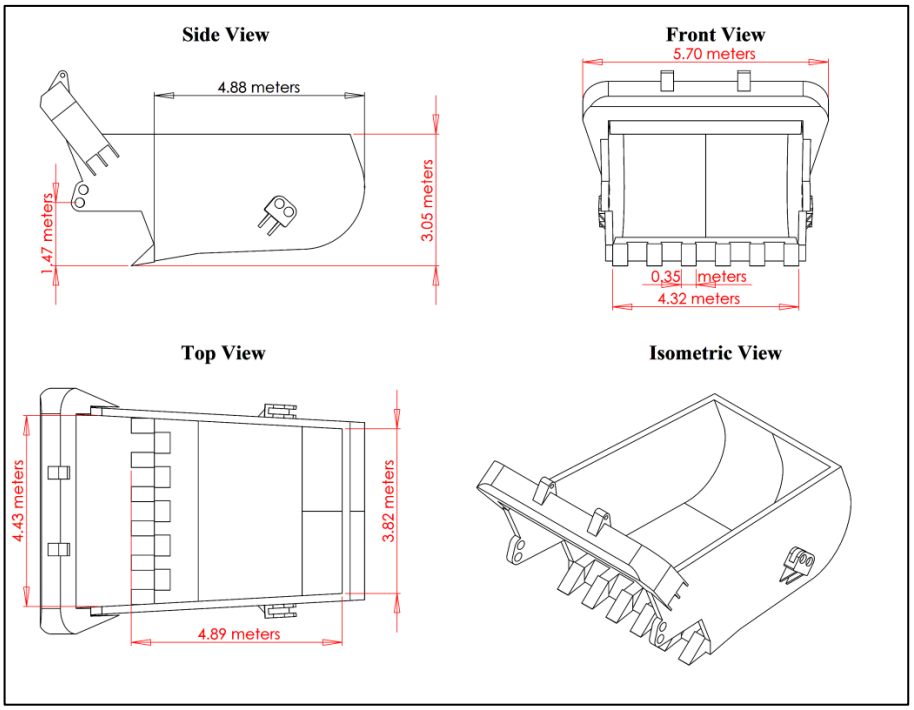

Figure 3.4 Dragline Bucket from Different Perspectives

Representation of sketch parameters used in the design of main bucket body is introduced in Figure 3.5 and Figure 3.6.

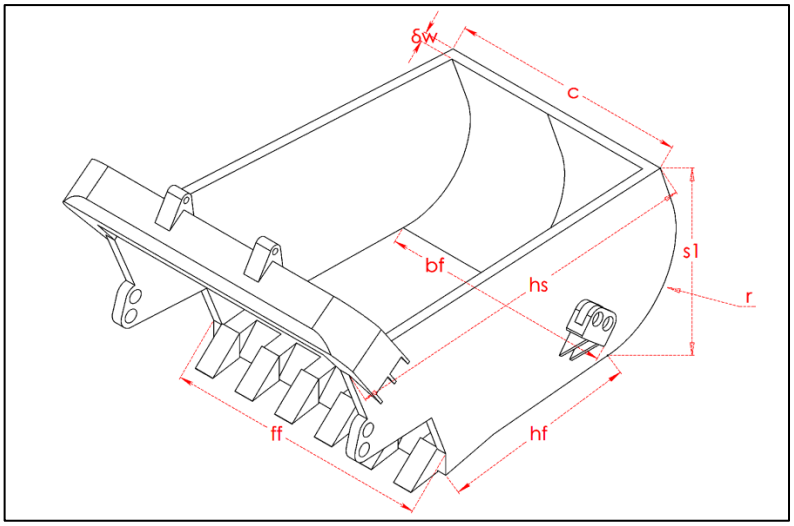

Figure 3.5 Basic Parameters of Dragline Bucket Body

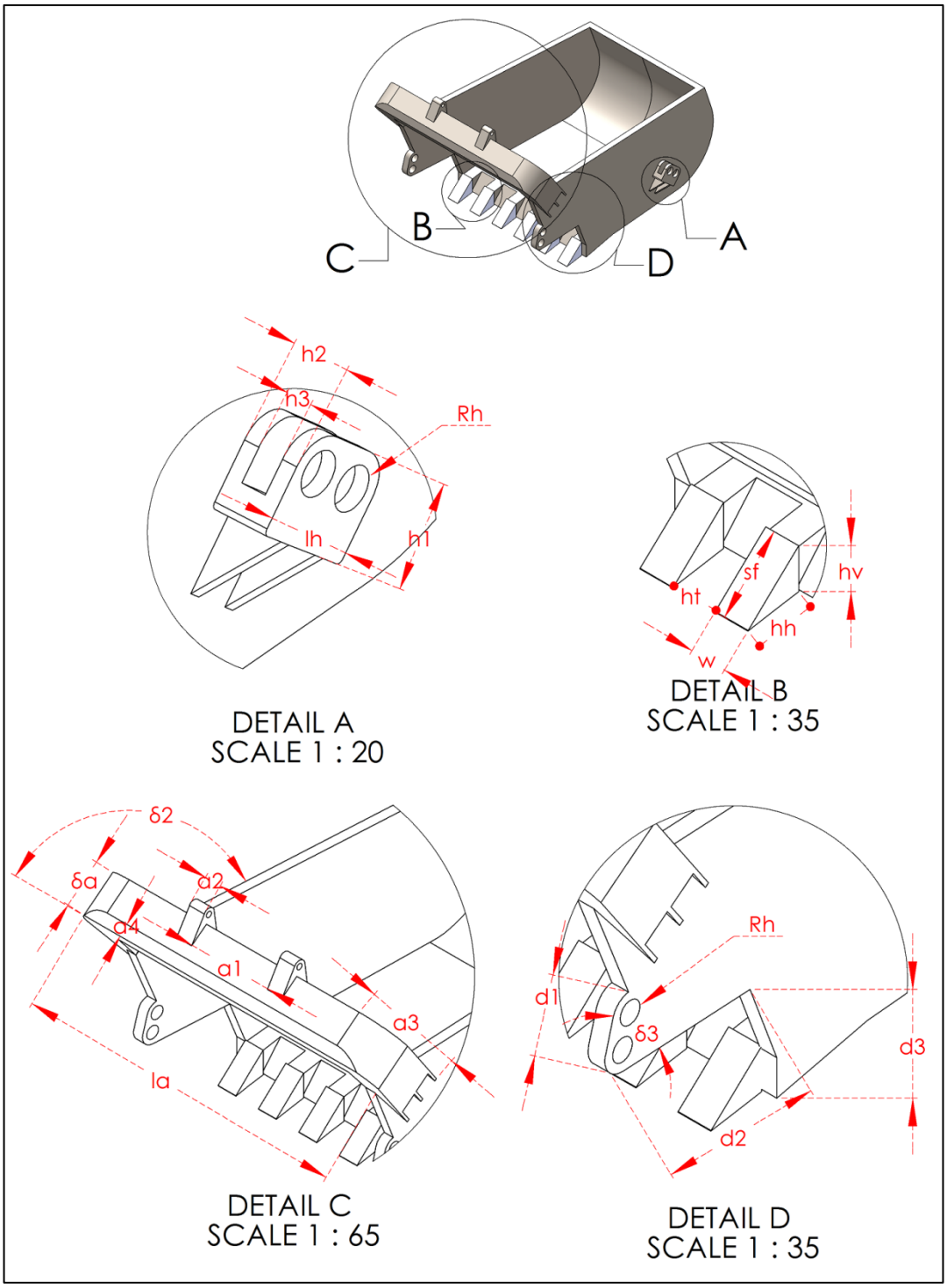

Figure 3.6 Parameters of Dragline Bucket Body Elements

Identification of the dimensions stated in Figure 3.5 and Figure 3.6 is shown in Table 3.1.

Table 3.1 Dimensions of Dragline Bucket Body Parameters

Elements	Parameters	Notation	Value
Back Wall	Length (Top)	c	4149 mm
	Thickness	δ_w	186 mm
Floor	Length (Horizontal)	h_f	3433 mm
	Width (front)	f_f	4647 mm
	Width (back)	b_f	4270 mm
	Thickness	δ_f	176 mm
Side Wall	Height (Vertical)	s_1	2700 mm
	Length (Top)	h_s	6605 mm
	Back Radius	r	1450 mm
	Thickness	δ_f	176 mm
Arch	Arch Length	la	5700 mm
	Arch Angle	δ_2	128^0
	Distance Btw. Rope Attach.	a_1	1488 mm
	Thickness of Rope Attach.	a_2	292 mm
	Slant Height (from Main Body)	a_3	2215 mm
	Chamfer	a_4	240 mm
	Thickness	δ_a	730 mm
Drag Hitch Element	Slant Height (front)	d_1	655 mm
	Width (bottom)	d_2	1430 mm
	Height from floor	d_3	1157 mm
	Bottom Angle (front)	δ_1	74^0
	Thickness	δ_d	176 mm
Hoist Chain Linkup	Length	l_h	639 mm
	Height	h_1	502 mm
	Width	h_2	300 mm
	Width (Opening)	h_3	135 mm
	Radius (Pin)	R_h	110 mm

Sketch values of digging tooth are stated in Table 3.2, separately.

Table 3.2 Dimensions of Dragline Bucket Tooth Parameters

Element	Parameters	Notation	Value
Teeth	Number of Teeth	K	6 units
	Distance Between Teeth	h_t	445 mm
	Width	w	349 mm
	Slant Length	s_f	744 mm
	Attach Distance Horizontal	h_h	545 mm
	Attach Distance Vertical	h_v	421 mm

3.3 Geometry of Dragline Bucket Rigging Mechanism

Conventional design of a dragline bucket rigging mechanism contains two dragging lines attached to the lip of the bucket for pulling the bucket filled with excavated material, a couple of hoisting lines attached to the sides of the bucket with pins for descending and elevating the bucket and a couple of dumping rope for discharging the loaded bucket. In general, hoist lines consists of a couple of chain assembly and two metal spreader located between the chain assemblies to keep them away from each other and away from the sides of bucket. For easily discharging the material from the bucket, dump ropes lines are connected to the arch of bucket with the trunnions, lies around the rotating pulleys which are linked to hoisting lines and finishes at the connection link of drag lines.

The bucket is lowered by the operator to the formation and it is then dragged toward the cabinet of the dragline. During dragging, teeth of the lip part of bucket sink into the formation with the effect of bucket's weight and fracture the formation. Lifted material flows inside and fills the bucket. Loaded bucket is elevated by the rigging mechanism and dumped to the spoil after the rotation of dragline. In order to visualize these working parts of dragline, a complete illustration of bucket and

rigging mechanism elements is shown in Figure 3.7. Explanation of these elements and quantities of them in the assembly are also stated in Table 3.3.

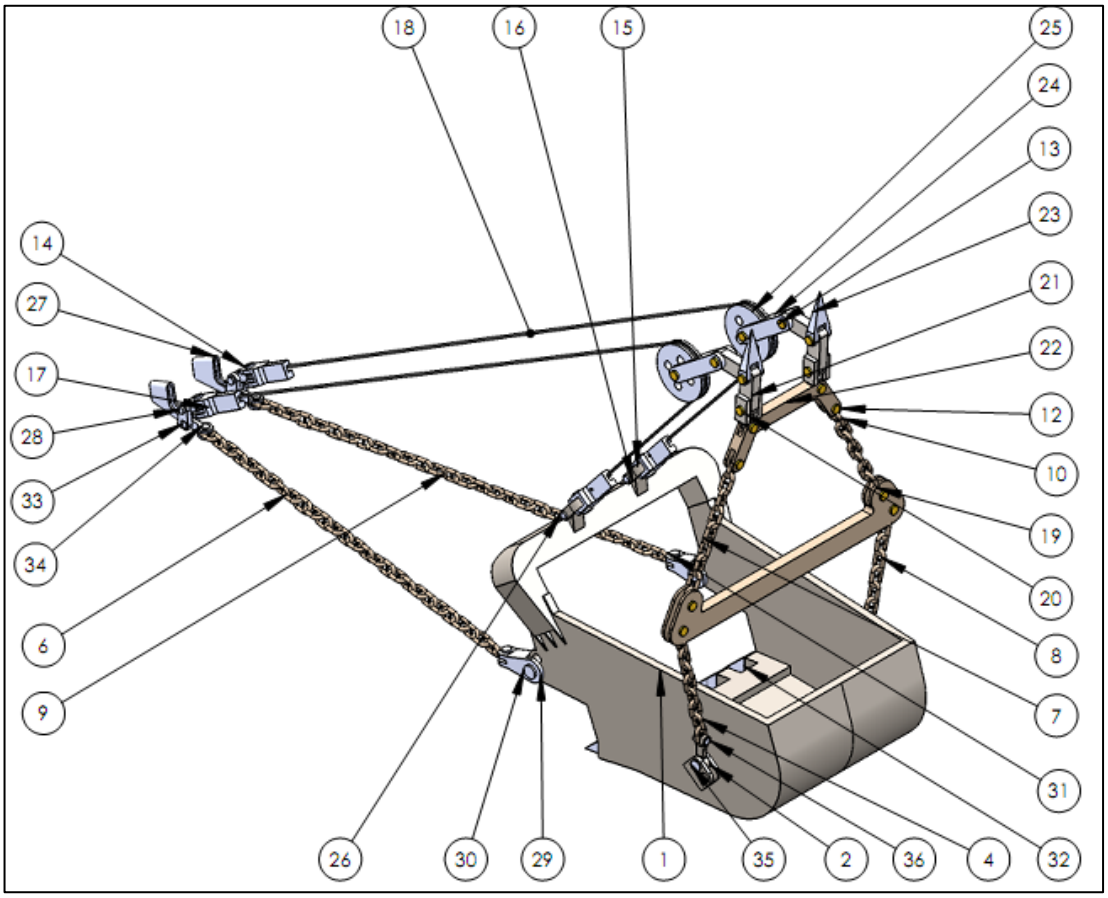

Figure 3.7 Elements of Dragline Bucket and Rigging Mechanism

Dragline rigging mechanism can be divided into three categories according to their tasks in the system. They are named as hoisting system, dragging system, and dumping system. Each system has different task to move the bucket. While dragging system transmits the pulling force to move the digging bucket close to the control cabinet, hoisting system transfers upward and downward force to the bucket. On the other hand, dumping system provides the filling and discharging action of the bucket.

Table 3.3 Identification of Dragline Bucket and Rigging Mechanism Elements

Item Number	Part Number	Quantity
1	Bucket Main Body	1
2	Trunnion Link	2
4	Chains (Hoisting, Right Lower Side)	9
6	Chains (Dragging, Right Side)	29
7	Chains (Hoisting, Right Upper Side)	9
8	Chains (Hoisting, Left Lower Side)	9
9	Chains (Dragging, Left Side)	29
10	Chains (Hoisting, Left Upper Side)	9
12	Pin (Spreader)	8
13	Pin (Hoist Shackle and Sheave)	8
14	Pin (Dump Socket)	4
15	Dump Rope Socket	4
16	Connecting Link 1	2
17	Connecting Link 2	4
18	Wire Rope	2
19	Lower Spreader	1
20	Hoist Link	2
21	Hoist Shackle	2
22	Upper Spreader	1
23	Rope Socket	2
24	Sheave Retainer	2
25	Dump Sheave	2
26	Pin (Connecting Link)	2
27	Drag Dump Link	2
28	Pin (Drag Dump Link)	2
29	Connecting Link 3	2
30	Pin (Connecting Link 3)	2
31	Pin (Connecting Link 3-2)	2
32	Tooth	6
33	Pin (Drag Dump Link 2)	2
34	Pin (Connecting Link 4)	2
35	Pin (Trunnion Link)	2
36	Pin (Trunnion Link 2)	2

In Figure 3.8, parts of dragline rigging system in charge of hoisting the bucket are shown with their parameters. In this part, trunnions are attached to the both sides of

bucket main body with the help of the pins. Two chain assemblies exist between the trunnions and the metal spreader. This lower spreader serves as a suspensive part which keeps the chain assemblies away from the sides of bucket main body. Therefore, it prevents wearing and fracture due to the collision between chains and the bucket body during an earthmoving procedure. Other two chain assemblies are placed among lower spreader and upper spreader. Upper spreader is the connection place of dumping system and hoisting system of the rigging mechanism. Design parameters belonging to the hoisting system can be checked from Table 3.4.

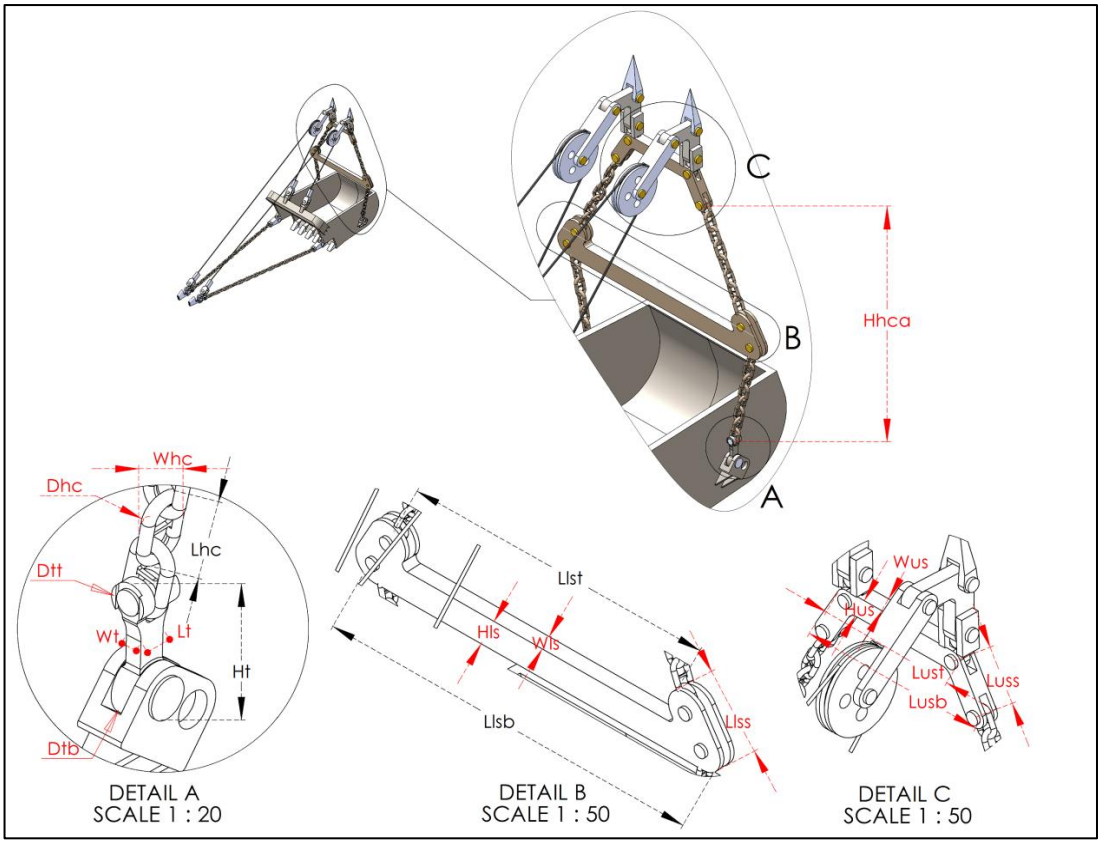

Figure 3.8 Hoisting Elements of the Rigging Mechanism

Another rigging mechanism, dragging system, is most stress-sustained section of a dragline rigging mechanism. Since, impulse and response loads against the resistance of the formation emerge here.

Table 3.4 Dimensions of the Rigging Mechanism Hoisting Elements

Elements	Parameters	Notation	Value
Hoist Chain	Length	L_{hc}	510 mm
	Diameter	D_{hc}	75 mm
	Width	W_{hc}	290 mm
	Number of Chains in Hoist System		36 units
	Height of Assembly (Vertical)	H_{hca}	6298 mm
Trunnion	Length	L_t	170 mm
	Diameter (Bottom Connection)	D_{tb}	350 mm
	Diameter (Top Connection)	D_{tt}	220 mm
	Width	W_t	100 mm
	Height	H_t	875 mm
Lower Spreader	Top Length	L_{lst}	5086 mm
	Bottom Length	L_{lsb}	6342 mm
	Slant Length (Connection)	L_{lss}	1191 mm
	Height	H_{ls}	489 mm
	Width	W_{ls}	250 mm
Upper Spreader	Top Length	L_{ust}	2092 mm
	Bottom Length	L_{usb}	2892 mm
	Slant Length (Connection)	L_{uss}	800 mm
	Height	H_{us}	325 mm
	Width	W_{us}	250 mm

As shown in Figure 3.9, the dragging section basically contains two chain assemblies, which are connected to the lip of bucket with the connection links and extend to the dump links. The dragging chain assembly is longer (10.31 m slant length; 10.17 m horizontal length) than hoisting chain assembly (6.3 m vertical height). Dump link, stated as Detail A in Figure 3.9, is the part where dragging and dumping system come together. This links are fastened to the wire ropes outside of the rigging mechanism, which are directly controlled by the winches on the both sides of dragline cabinet. Parametric explanations of the dragging system's parts are

indicated in Table 3.5.

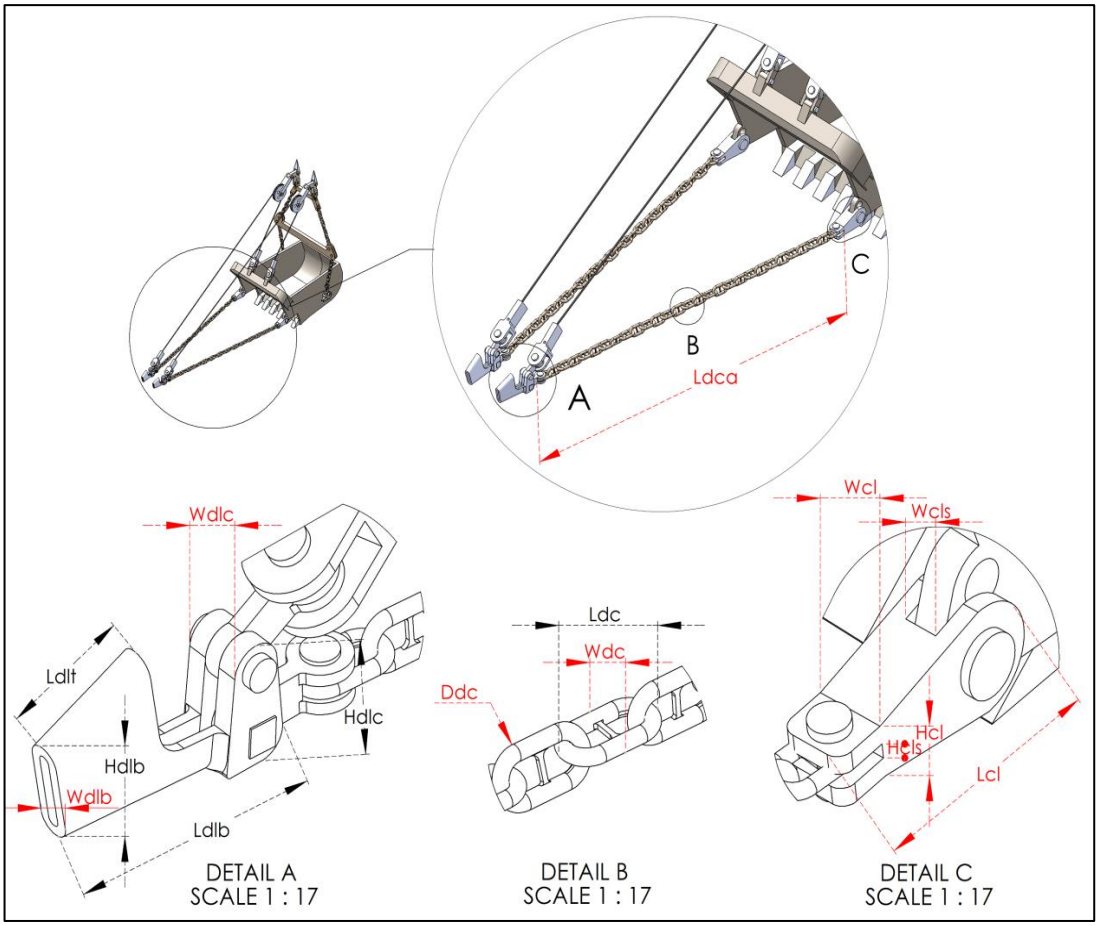

Figure 3.9 Dragging Elements of the Rigging Mechanism

During the operation, dragline leaves the bucket away from itself with a swing angle and drags it back with the aid of winches. After the bucket gets full of material, head of the bucket is tilted upward with stretching dump rope and it is tilted downward on the spoil site with realizing dump rope. In this dumping system, as shown in Figure 3.10, wire ropes go around the sheaves and they provide a bond between dump link and main bucket body. Sheaves are fixed to the sheave retainer. The retainer is an adapter between dumping and hoisting system of the rigging mechanism. From catalogs of manufacturers, 45 mm wire rope is suitable such a bucket with a 50 m^3 (65 yd^3) volume. Length of the each wire rope is about 22.27 m. Wire rope ensures the connection with both dump link and bucket main body with the help of trunnions.

Parameters of the parts and their dimensional values are specified in Table 3.6.

Table 3.5 Dimensions of the Rigging Mechanism Dragging Elements

Elements	Parameters	Notation	Value
Drag Chain	Length	L_{dc}	510 mm
	Diameter	D_{dc}	75 mm
	Width	W_{dc}	290 mm
	Number of Chains in Drag System		58 units
	Slant Length of Chain Assembly	L_{dca}	10307 mm
Drag Chain Dump Link	Length (Bottom)	L_{dlb}	1183 mm
	Length (Top)	L_{dlt}	579 mm
	Width (Back)	W_{dlb}	160 mm
	Height (Back)	H_{dlb}	480 mm
	Width (Connection)	W_{dlc}	300 mm
	Height (Connection)	H_c	541 mm
Drag Chain Connecting Link	Length	L_{cl}	1195 mm
	Height	H_{cl}	265 mm
	Height (Spacing)	H_{cls}	75 mm
	Width	W_{cl}	350 mm
	Width (Spacing)	W_{cls}	176 mm

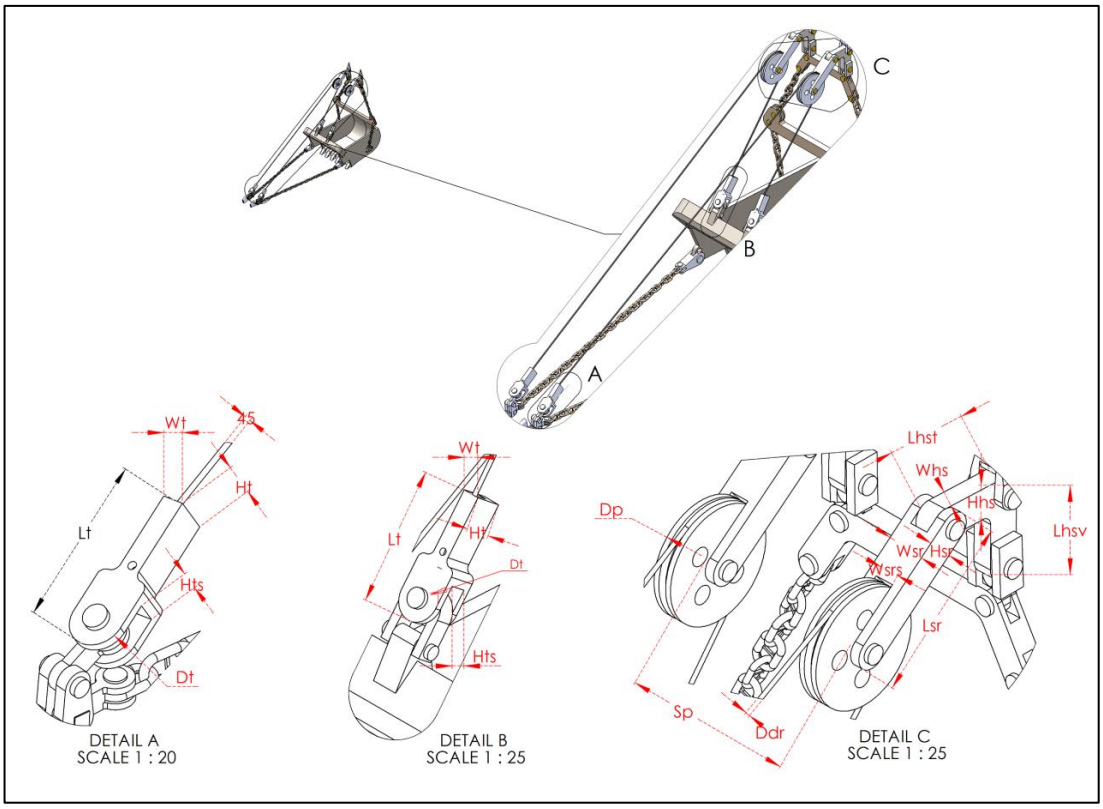

Figure 3.10 Dumping Elements of the Rigging Mechanism

Table 3.6 Dimensions of the Rigging Mechanism Dumping Elements

Elements	Parameters	Notation	Value
Pulley	Pulley Diameter	D_p	1260 mm
	Spacing Between Pulley Center	S_p	1922 mm
Sheave Retainer	Length	L_{sr}	1740 mm
	Width	W_{sr}	434 mm
	Width (Spacing)	W_{srs}	217 mm
	Height	H_{sr}	340 mm

Table 3.7 Dimensions of the Rigging Mechanism Dumping Elements (Cont'd)

Elements	Parameters	Notation	Value
Hoist Shackle	Length (top)	L_{hst}	1113 mm
	Length (vertical)	L_{hsv}	1113 mm
	Width	W_{hs}	217 mm
	Height	H_{hs}	340 mm
Dump Rope	Diameter	D_{dr}	45 mm
	Length of Rope in Dump System		22272 mm
Trunnion	Length	L_t	1325 mm
	Diameter	D_t	450 mm
	Width	W_t	180 mm
	Height	H_t	350 mm
	Height (Spacing)	H_{ts}	80 mm

General dimensions of bucket and rigging assembly from different views can be investigated in Figure 3.11 and solid design of the model in Figure 3.12.

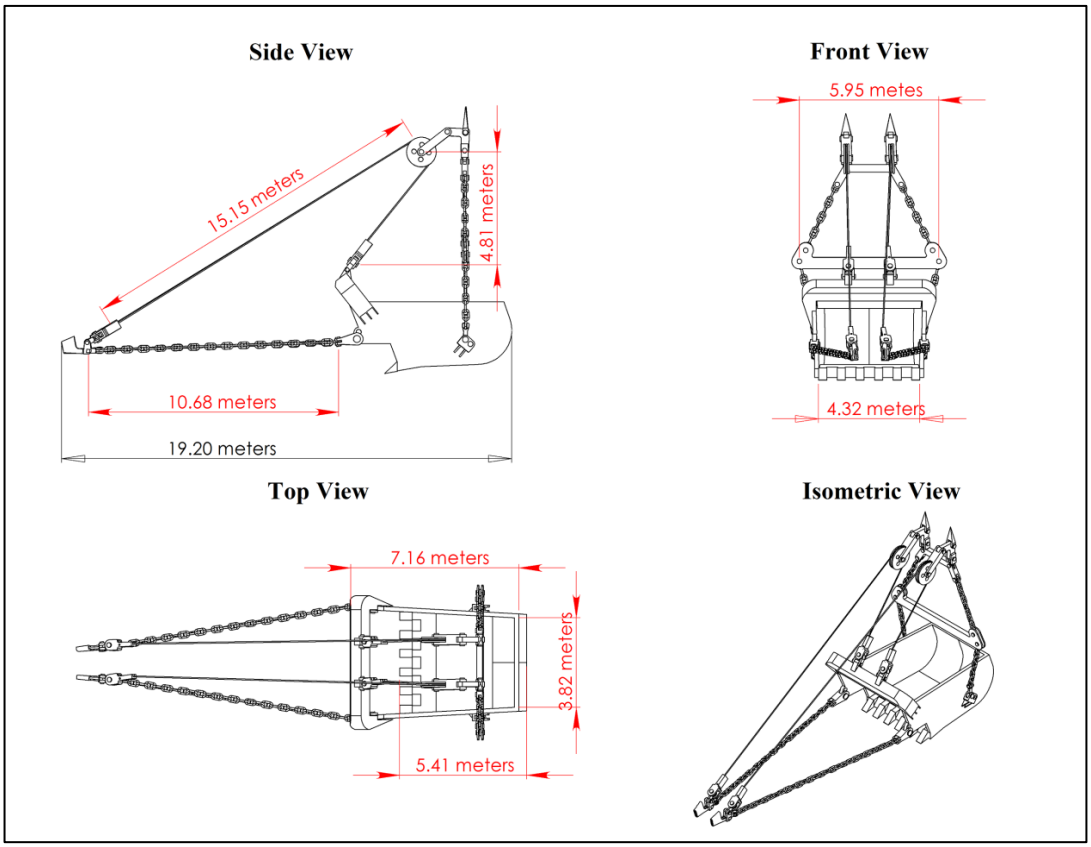

Figure 3.11 Dragline Bucket and Rigging Mechanism from Different Perspectives

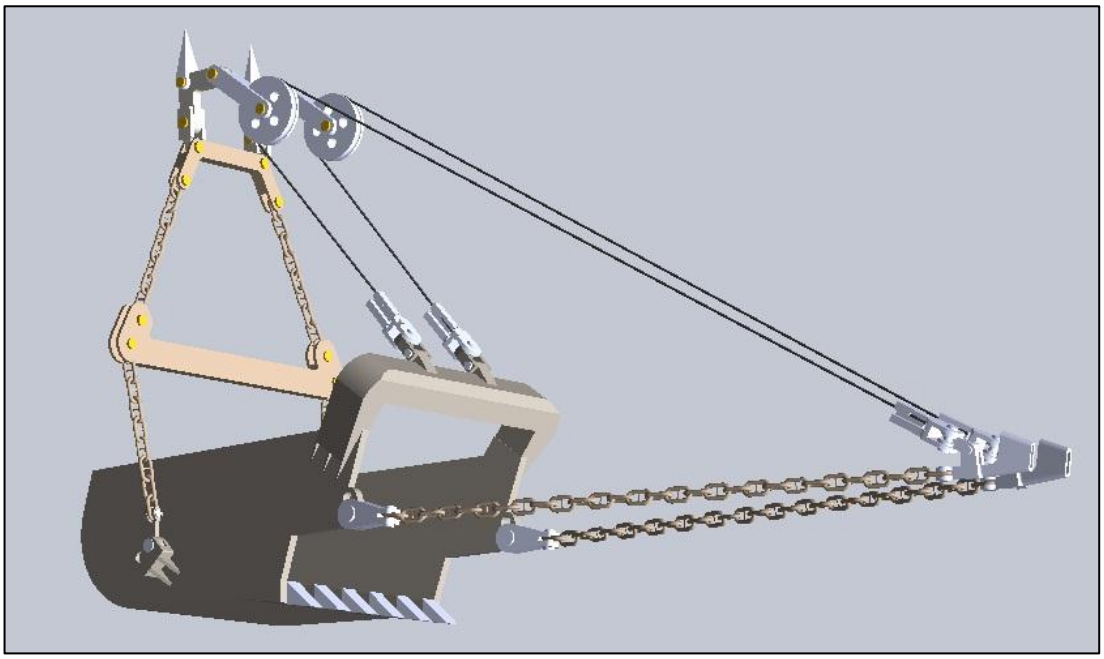

Figure 3.12 Solid Model of Dragline Bucket and Rigging Mechanism

CHAPTER 4

DIGGING SIMULATION OF WALKING DRAGLINE BUCKET

4.1 Resistive Force Calculations

4.1.1 Formation Specifications

In order to effectively estimate a bucket action into the formation, it is essential to find the resistive forces of the formation against the bucket. In this regard, it is required to know the principles behind the contradictory response of the formation, to calculate these earthmoving forces. A dragline bucket constitutively performs the earthmoving process with penetration and cutting actions. It initially penetrates the formation and cuts it until filling its volume with loose material. Since, bucket penetration mechanism shows similar principles with bucket cutting mechanism, cutting theory was utilized to calculate the resistive force in the thesis study.

As discussed in Chapter 3, different types of analytical and theoretical approaches are available for the cutting force estimation. These models contain parameters related to formation specifications and tool-formation interaction properties. In the thesis research, formation data were directly taken from the study performed by Mouazen and Nemenyi (1999) with the authors' permissions. Table 4.1 illustrates the specifications belonging to three different conditions of the same formation, very compacted, compacted and loose. These formation specimens have homogeneous particle distributions and different mechanical specifications.

Table 4.1 Formation and Tool-Formation Specifications (Mouazen and Nemenyi, 1999), by Author Permissions

Specifications	**Units**	**Values**		
		Very Compacted	*Compacted*	*Loose*
Formation Material Properties				
Bulk Density	kg/m^3	1840	1731	1610
Cohesion	kPa	20.4	15.5	15.3
Internal Friction Angle	degree	34.0	31.8	30.3
Poisson's Ratio		0.385	0.359	0.339
Modulus of Elasticity	kPa	11356	8067	4939
Tool-Formation Properties				
Formation-Metal Friction Angle	degree	25.0	23.0	22.0
Formation-Tool Adhesion	kPa	0.0	0.0	0.0

4.1.2 Cutting Force Calculation

Cutting tools vary according to their contact widths from wide to narrow. For instance, a tillage machine uses narrow-width cutting blade to move the formation while a dozer earthmover utilize its wide-width blade. Cutting force approaches change according to the width factor. If the cutting blade is not very wide, a large amount of material moves to the sides of plane which causes the side effect. Two-dimensional cutting methods exhibit approaches for wide-blade operations without considering the side effect. These methods assume that the operation is carried out on the infinitely-wide plate. On the other hand, three-dimensional techniques include the side effect for narrow-blade cutting. However, a bucket does not show side effect behavior like a blade although bucket cutting edge is not infinitely wide (Blouin, *et al.*, 2001; McKyes, 1985). Since, bucket sides cause the cutting material to move the inside and two-dimensional approach become convenient for this situation (McKyes, 1985), two-dimensional models were utilized to calculate the resistive forces on the bucket teeth.

As indicated in the Equation (2.10), total resistive force on the teeth can be estimated from the forces related to the weight of removing formation, cohesion between formation-formation interaction, adhesion between tool-formation interaction, surface surcharge pressure and inertia inside the formation (Figure 4.1). In this thesis study, resistive forces such as adhesion, surcharge, and inertia forces were neglected in the calculation of total resistive force. On the formation failure surface, there is a potential perpendicular pressure, q, due to a loose surcharge rising there. This extra pressure can occur because of any probable loading on the surface, whether from a machine or the existence of a loose material whose weight must be supported by the surface. In the study, this type of force was neglected. Moreover, adhesion force can be described as the force of attraction between different materials. In the study, formation and the bucket teeth are two distinct materials and interaction between them was assumed zero. In addition, effect of inertia is released when formation is accelerated from resting state to a specific velocity (Abo-Elnor *et al.*, 2004). Since constant velocity bucket movement was applied in the study, inertial force was also neglected.

Weight of removing formation body can be assumed to contribute a negligible resistance on the total resistance when the cutting operation is achieved in the shallow depths (McKyes, 1985). However, in the study, bucket operates in a 512 mm depth (Figure 4.2). It evokes a remarkable load on the teeth. Therefore, weight of the formation body was included to the earth passive pressure formula. Furthermore, cohesion is one of the fundamental factor which headlight the interaction between formation-formation. It can be defined as a force due to attraction between the formation particles. If there is not cohesion, no fragmentation observes in the formation and particles behave independently of each other. Thus, cohesion force was taken into account of resistive force calculation. Therefore, weight and cohesion were taken as two factors utilized in the determination of formation resistive forces in the study.

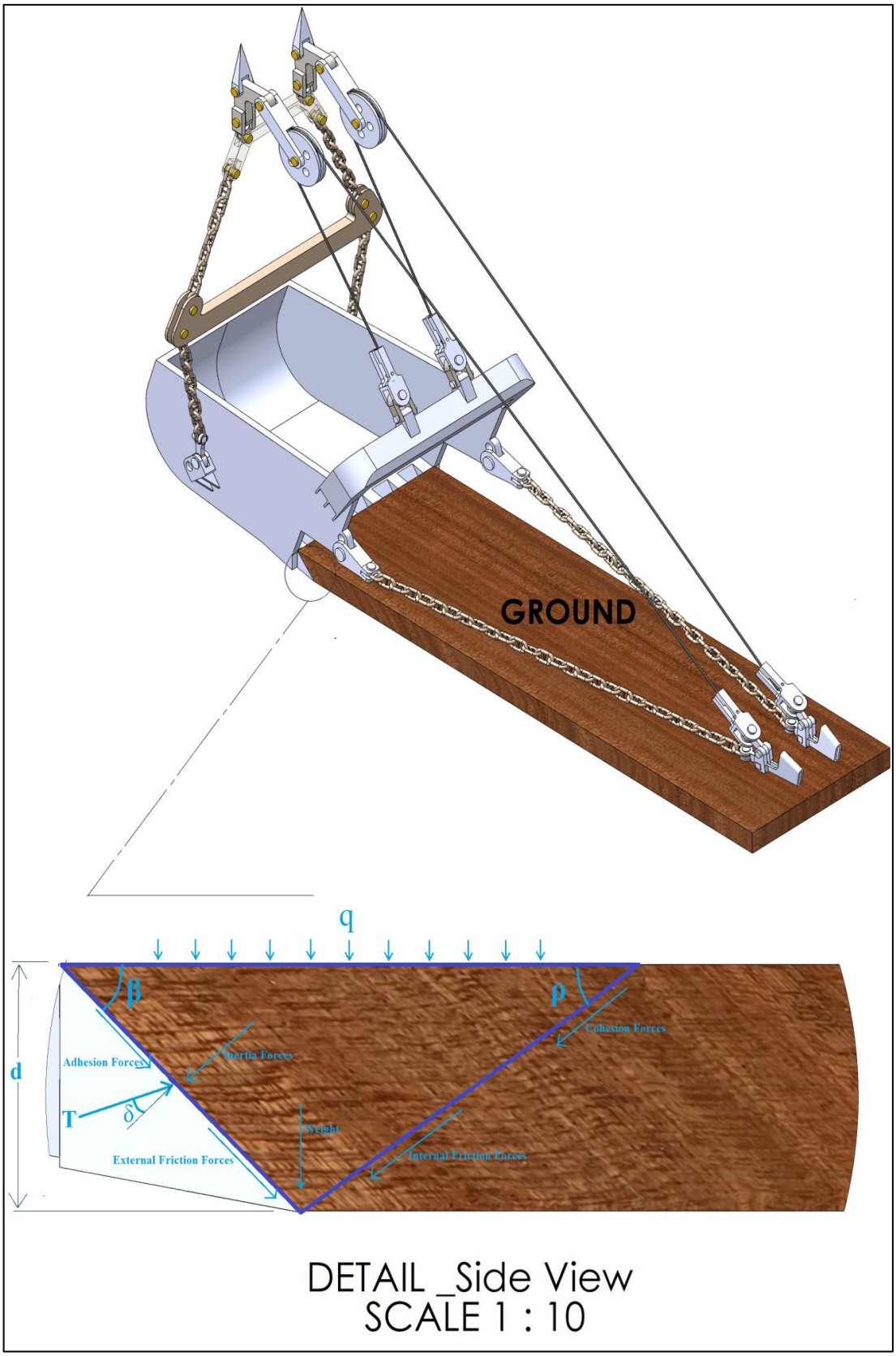

Figure 4.1 Resistive Forces between the Bucket Teeth and the Formation

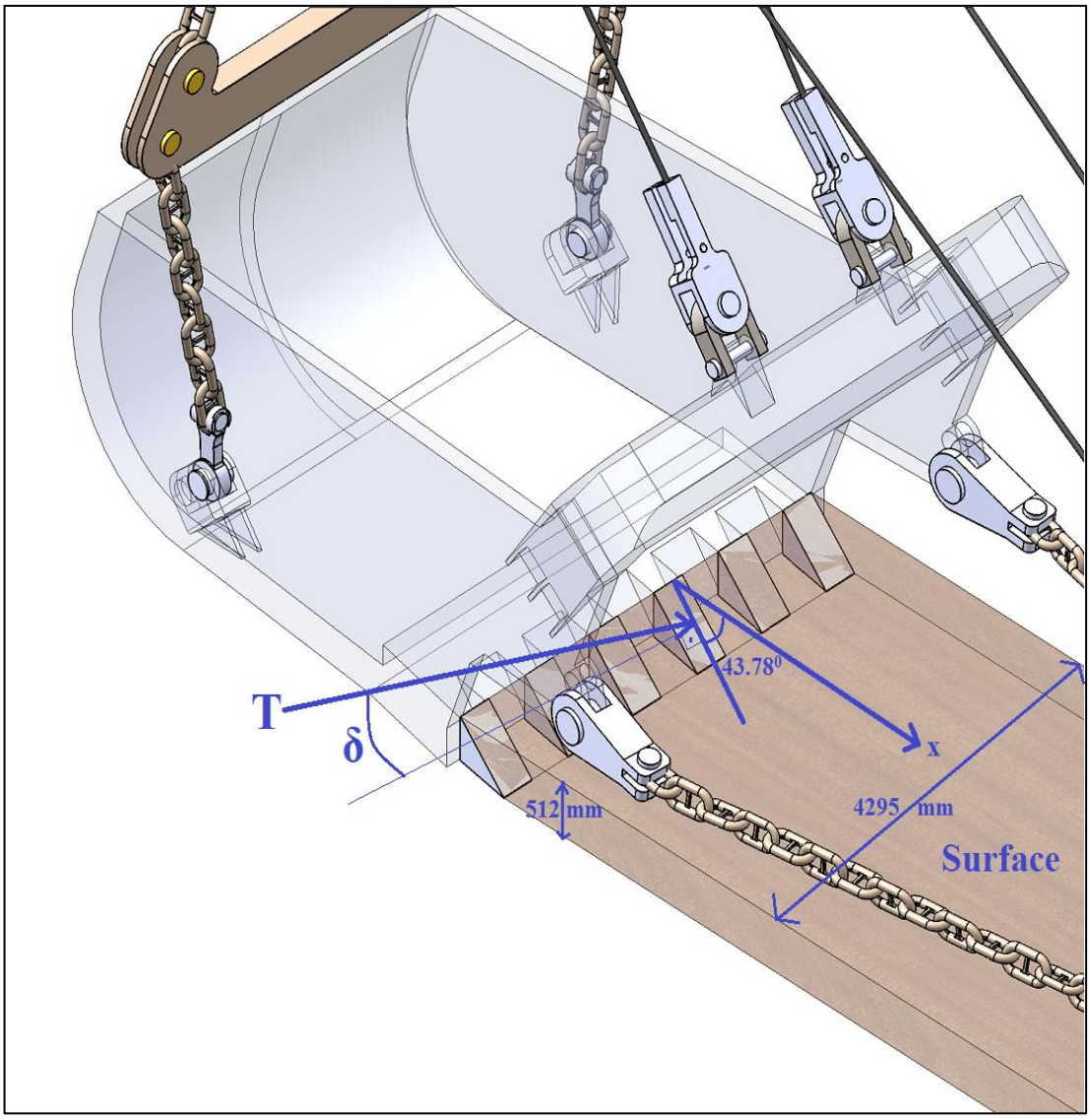

Figure 4.2 Orientation of Total Resistive Force on the Bucket

According to the proposed model, re-arranged version of the cutting force equation, Equation (2.10), is given as follows:

$$T = w(\gamma g d^2 N_\gamma + c d N_c) \tag{4.1}$$

In Equation (4.1):

w = Cutting Width (m)

γ = Formation Density ($^{t}/_{m^3}$)

g = Gravitational Acceleration ($^{m}/_{s^2}$)

d = Depth of Work (m)

c = Formation Cohesion Strength (kPa)

N_γ = Weight Factor

N_c = Cohesion Factor

As mentioned in Chapter 4.1.1, formation specifications stated in Equation (4.1) were taken from the study of Mouazen and Nemenyi (1999) by authors' permissions. In addition to these data, N_c and N_γ factors were provided from the charts generated by Hettiaratchi and Reece (1974). Mckyes (1985) states that Hettiaratchi's charts for N-factors can be used efficiently for the rapid solution of passive earth pressure formulas. Charts only give N-factors for the situations of $\delta=0$ and $\delta=\Phi$. Therefore, to find N-factors for a specific δ value, Equation (4.2) is used as stated below. This equation provides a linear relationship between N-factors and external friction angle.

$$N = N_0 + (N_\phi - N_0)\frac{\delta}{\phi} \tag{4.2}$$

In Equation (4.2):

δ = External Friction Angle

ϕ = Internal Friction Angle

N = N Factor for a Specific External Friction Angle

N_0 = N Factor where External Friction Angle is zero

N_ϕ = N Factor where External Friction Angle is Equal to Internal Friction Angle

Calculation of the resistive force for very compacted formation type which is stated in Table 4.1, is explained below.

Predetermined data to use in Equation (4.1) are indicated in Table 4.1 and Figure 4.2, except for N_γ and N_c. Weight factor, N_γ, and cohesion factor, N_c, are determined from the charts as follows:

Calculation of N_γ:

From Figure A.1 (see Appendix A), for external friction angle (δ) is 0^0, internal friction angle (Φ) is 34.0^0, and rake angle of the cutting teeth (α) is 43.78^0:
N_0 is calculated as 0.99.

From Figure A.2 (see Appendix A), for external friction angle (δ) is equal to internal friction angle, internal friction angle (Φ) is 34.0^0, and rake angle of the cutting teeth (α) is 43.78^0:
N_ϕ is calculated as 2.00.

From Equation (4.2); for $\delta=25^0$,

$$N\gamma = 0.99 + (2.00 - 0.99)\frac{25}{34} = 1.7326$$

Calculation of N_c:

From Figure A.3 (see Appendix A), for external friction angle (δ) is 0^0, internal friction angle (Φ) is 34.0^0, and rake angle of the cutting teeth (α) is 43.78^0:
N_0 is calculated as 0.85.

From Figure A.4 (see Appendix A), for external friction angle (δ) is equal to internal friction angle, internal friction angle (Φ) is 34.0^0, and rake angle of the cutting teeth (α) is 43.78^0:

N_ϕ is calculated as 3.30.

From Equation (4.2); for $\delta=25^0$,

$$\text{Nc} = 0.85 + (3.30 - 0.85)\frac{25}{34} = 2.6515$$

Data for the cutting force equation (Equation (4.1)), are tabulated in Table 4.2.

Table 4.2 Cutting Force Equation Data for the Very Compacted Formation

Specification	Symbol	Value
Cutting Width	w	4.295 m
Formation Density	γ	1.840 t/m^3
Depth of Work	d	0.512 m
Gravitational Acceleration	g	9.810 m/s^2
Formation Cohesion Strength	c	20.400 kPa
Weight Factor	Nγ	1.733
Cohesion Factor	Nc	2.652

Finally, from the Equation (4.1), total cutting force,

$$T = \left[\left(1.84\,{}^{t}/_{m^3}\right)\left(9.81\,{}^{m}/_{s^2}\right)(0.512\ m)^2\ (1.7326) + (20.4\ kPa)(0.512\ m)(2.6515)\right]\ x\ 4.295m \cong 154\ kN$$

at an attack angle of 21.22^0 to the horizontal (90^0- δ - α).

Unit force for each tooth = 154 kN / 6 teeth = 25.667 kN

Area of a single tooth contact surface = 210000 mm^2

Pressure on the surface of single tooth in terms of N/mm^2 or MPa

$= 25667N/210000mm^2 = 0.122\ MPa$

As a result, normal pressure on a single tooth,

$P_n = P_t x cos\delta = 0.122 x cos25 = 0.111\ MPa$

Normal pressures on the digging tooth for other formation types, compacted and loose formations in Table 4.1, were calculated with same steps mentioned above. All date utilized for the very compacted, compacted and loose formation materials and resultant cutting forces for each formation type are tabulated in Table 4.3.

Table 4.3 Cutting Forces According to the Formation Types

		Values for the Formation Types		
		Very Compacted	Compacted	Loose
Cutting Width	w	4.295 m	4.295 m	4.295 m
Depth of Work	d	0.512 m	0.512 m	0.512 m
Formation Density	γ	1.84 t/m^3	1.73 t/m^3	1.61 t/m^3
Gravitational Acceleration	g	9.81 m/s^2	9.81 m/s^2	9.81 m/s^2
Formation Cohesion Strength	c	20.4 kPa	15.5 kPa	15.3 kPa
Internal Friction Angle	Φ	34.0^0	31.8^0	30.3^0
External Friction Angle	δ	25.0^0	23.0^0	22.0^0
Weight Factor	N_γ	1.7326	1.6037	1.4529
Cohesion Factor	N_c	2.6515	2.4050	2.2658
TOTAL CUTTING FORCE	T	154.0 kN	112.6 kN	102.1 kN
Attack Angle to Horizontal		21.22^0	23.22^0	24.22^0
Number of Teeth		6	6	6
Total Cutting Force per Tooth		25.667 kN	18.767 kN	17.017 kN
Contact Area of a Tooth		0.21 m^2	0.21 m^2	0.21 m^2
TOTAL PRESSURE ON TOOTH	P_t	0.122 MPa	0.089 MPa	0.081 MPa
External Friction Angle	δ	25.0^0	23.0^0	22.0^0
NORMAL PRESSURE ON TOOTH	P_n	0.111 MPa	0.082 MPa	0.075 MPa

4.2 Pre-processing Steps in the Simulation Environment

Abaqus is a finite element software, having the capability to solve both linear and non-linear problems containing issues such as elasticity, plasticity and large deformations. Abaqus/CAE is the special version of Abaqus which holds the properties of both Abaqus/Standard and Abaqus/Explicit. It allows the pre-processing and post-processing steps of the model. Pre-processing is the first stage of the analysis, involves different steps to generate a model with parts, characterize material properties, identify boundary and loading conditions, mesh the assembly with variable element types.

4.2.1 Transferring the CAD Model into the Simulation Environment

In the modeling and simulation of the model, two softwares were used in the thesis study, Solidworks and Abaqus. Solidworks (Solidworks Co., 2009) was preferred to create the solid models of bucket and the rigging mechanism. Geometries of the solid models were formed with the help of available data of existing buckets. Relationships between the parts were created with the help of constraints in Solidworks assembly module. Besides, Abaqus (Simulia, Version 6.9-2) was chosen as a multi-functional simulation tool. Moreover, these two software companies are partner under the name of Simulia. Combined utilization of these two softwares is possible with the help of an add-in program, named as Associative Interface for Solidworks. This add-in simply provides the transfer of a Solidworks model to Abaqus environment. During the transfer, all database of the model which includes the geometry of the parts, relationships of parts in the assembly, appearance properties are conveyed to Abaqus software.

After installing the add-in to Solidworks, an icon of Abaqus appears in the main menu bar. After activating the add-in in both programs, a port with same code emerges. Then, the command, Export to Abaqus, provides the transmission of model data from Solidworks to Abaqus, simultaneously. As shown in Figure 4.3, 36 units of solid parts and 167 instances belonging to them were transferred to Abaqus.

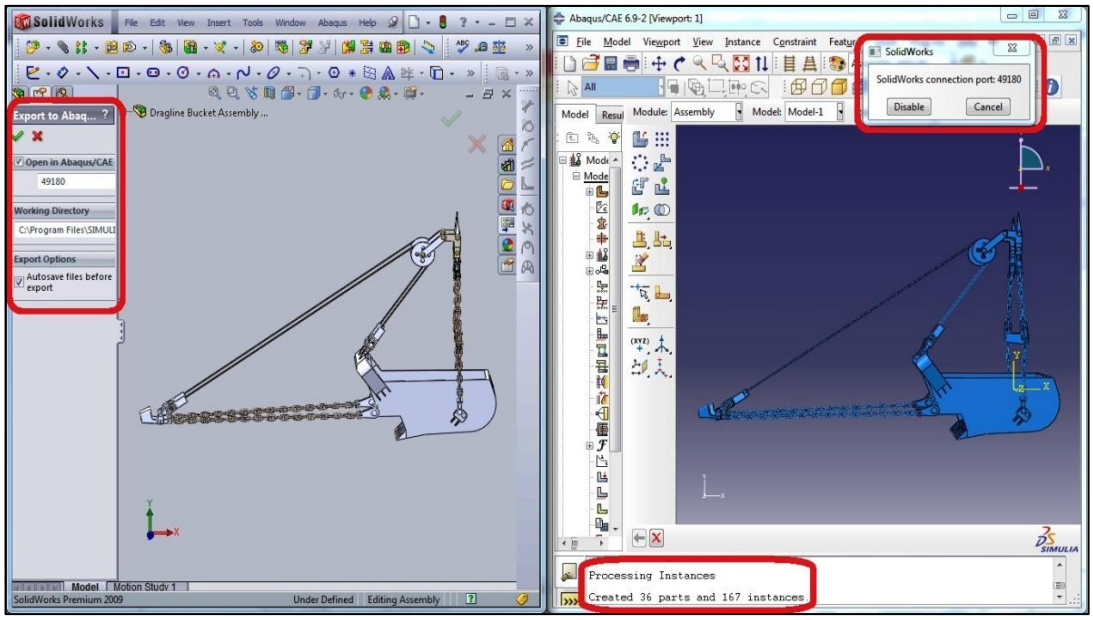

Figure 4.3 Transferring Three-Dimensional Model from Solidworks to Abaqus

A bucket-rigging mechanism combination includes lots of connection points in the assembly and curved surfaces on the parts. This situation causes complexities and inaccuracies in the simulation, and a long simulation time as a result. To eliminate the possible inaccuracies due to the irregular shape of the model, to decrease the simulation time, and to focus on the main interaction area, only main bucket and tooth parts were simulated in Abaqus. The rigging mechanism was not included in the simulation.

Moreover, before starting the simulation, some modifications were made on the main bucket model as shown in Figure 4.4. Curved surfaces of the bucket arch were reduced; chamfer edge of the arch and trunnion attachment holes on the two sides of bucket body were eliminated. By this way, it was aimed to avoid possible bad mesh configuration on the curvatures. Since, bad mesh configurations and the resultant errors on finite elements can lead to undesirable simulation results.

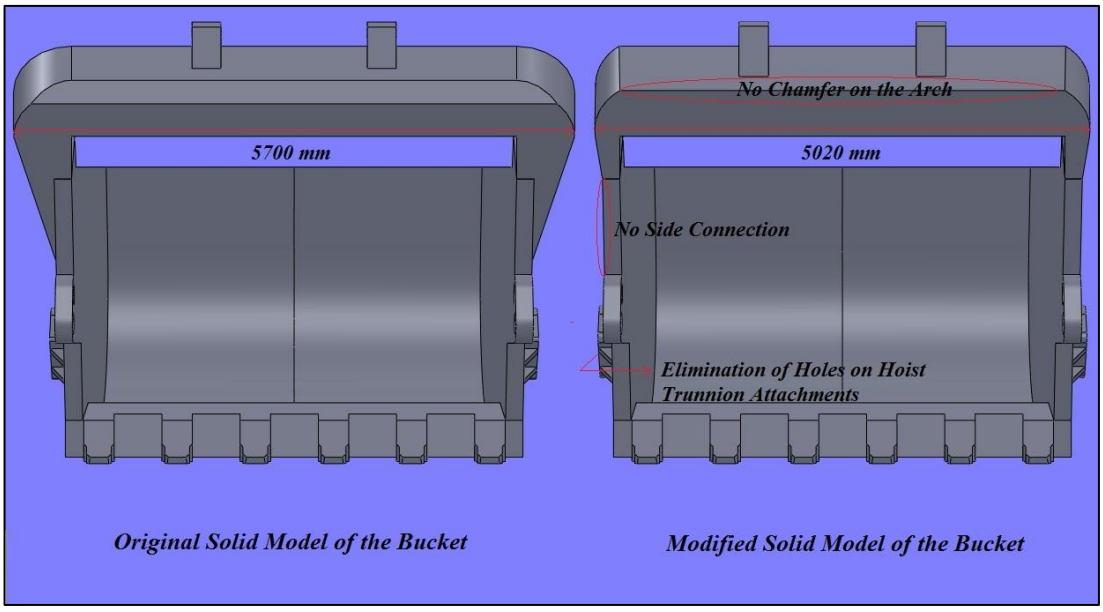

Figure 4.4 Modifications on the Solid Bucket Body Before the Simulation

4.2.2 Material Property Assignment

Property module in Abaqus is used to identify specifications of different materials employed in the model. Materials can be characterized according to their various behaviors such as general, mechanical, thermal, acoustic, and electrical. Moreover, different numbers of behavior types can be combined in the characterization of a single material. In this thesis study, materials were defined as elastic-perfectly plastic. In elastic-perfectly plastic material, strain remains constant after yield stress (Figure 4.5). To introduce this specification to the program, density as a general property, elasticity and plasticity as mechanical properties were committed as input data. Path followed in the thesis study to define material property is shown in Figure 4.6.

In the simulation, two different types of cast steel were used to identify the material properties, GS-25CrMo4 and GS-70 (C. H. Gür, personal communication, January 11, 2011). While GS-25CrMo4, which has greater yield strength, was assigned to the digging teeth, GS-70 was utilized to characterize the mechanical properties of main

bucket body. Material specifications are stated in Table 4.4. After the determination of material specifications, it is required to set material distribution type on the parts. It can be managed with the help of section toolbar. Section toolbar combines material with section property. In the study, sections for the cast steels were selected as homogeneous. Therefore, the distribution of material properties over each section of the parts was homogeneous.

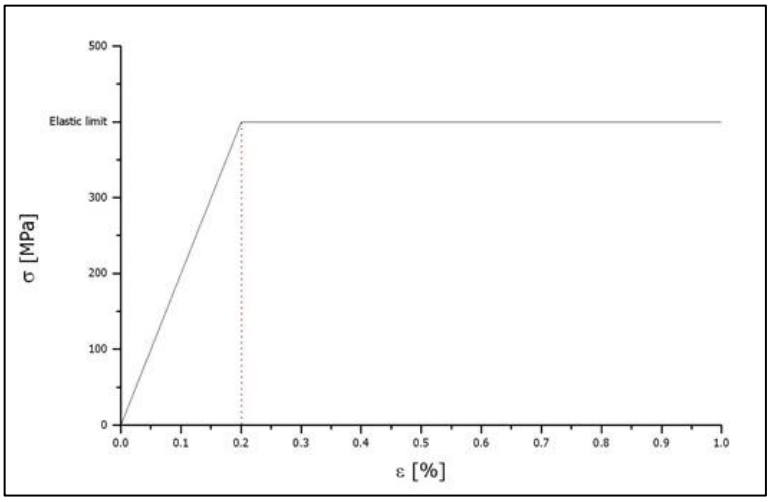

Figure 4.5 Stress-Strain Diagram for an Elastic-Perfectly Plastic Material

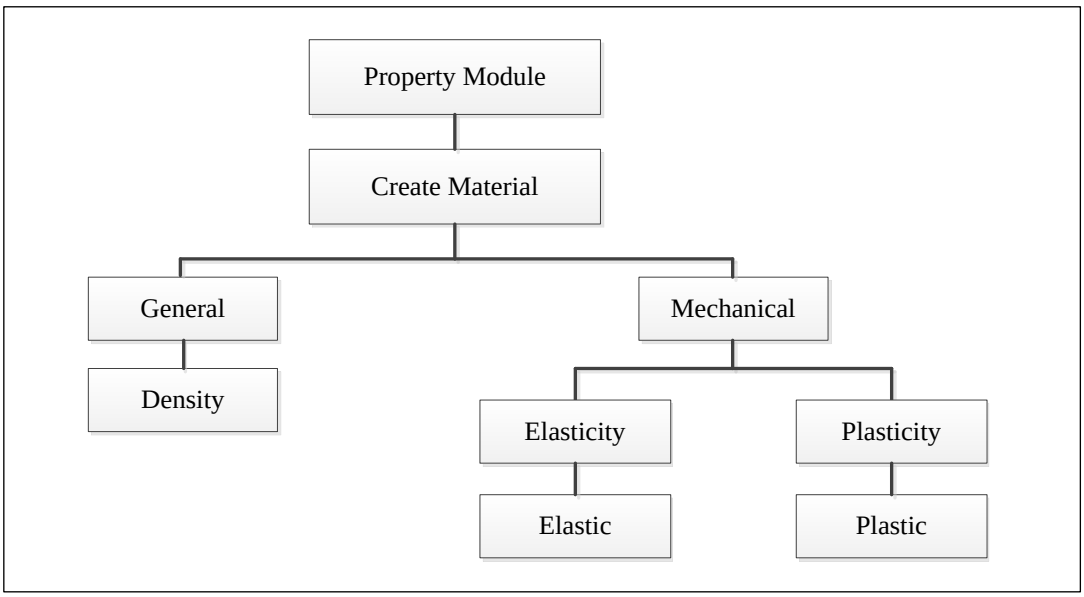

Figure 4.6 Flowchart of Material Definition in the Study

Table 4.4 Material Specifications for the Solid Model (Matbase, 2011)

Material	General	Elasticity		Plasticity
	Density (kg/m^3)	Young's Modulus (N/m^2)	Poisson's Ratio	Yield Stress (N/m^2)
Cast Steel (GS-25CrMo4)	7800	$205x10^9$	0.30	$510x10^6$
Cast Steel (GS-70)	7850	$200x10^9$	0.29	$410x10^6$

4.2.3 Element Type Selection and Creating Mesh

Mesh is one of the most important factors of the simulation since accuracy and efficiency of the simulation depend on mesh quality of model parts.

Figure 4.7 illustrates the meshing procedure applied in the study.

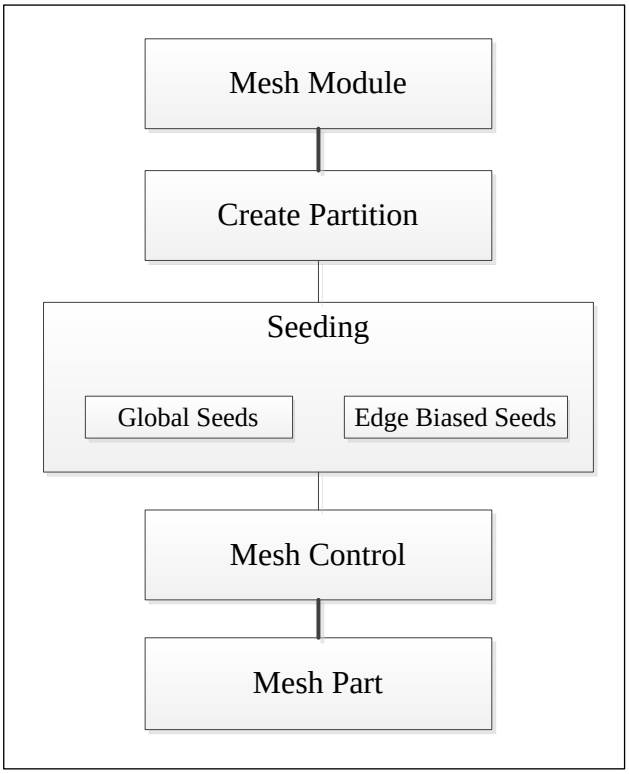

Figure 4.7 Flowchart of Mesh Definition in the Study

As seen in Figure 4.7, it was avoided to create direct meshes on the model. Some parts of the assembly were partitioned to make more sensitive analysis on these particular places. Partition property allows creating more susceptible seeding in the partitioned sides. As indicated in Figure 4.8, highlighted edges have denser in seeds, compared to the other edges. Especially, during an earthmoving operation, contact area where external forces exist should be investigated in more details to make a better stress analysis. On the study, bucket teeth and bucket arch were partitioned to perform more accurate investigation on these parts. Since, a dragline uses its bucket teeth to contact with the formation and also utilizes drag and hoist chains attached to the bucket arch to draw back the bucket. Resistive forces appear here much more than the other parts of bucket.

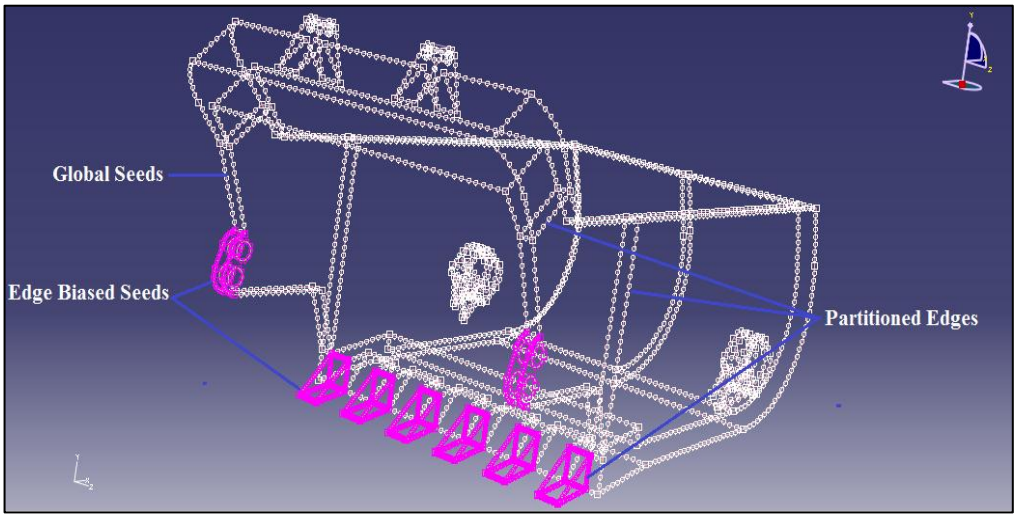

Figure 4.8 Mesh Seeding

After defining the nodes on all edges of the model, it is required to determine appropriate element type which connects the nodes and creates three-dimensional solid network. Different types of finite elements can be investigated from Figure 4.9.

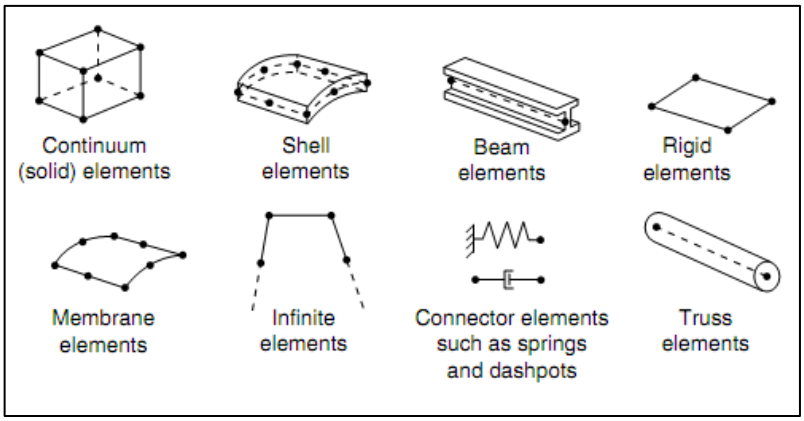

Figure 4.9 Common Elements Used in Stress Analysis (Abaqus 6.9 User's Manual, 2009)

Through the element types, continuum elements are the general three-dimensional volume elements of Abaqus. As shown in the Figure 4.9, continuum elements do not contain two-dimensional structural elements like other types. A solid continuum element can be used in a shape of quadrilateral, hexahedral, triangular, and tetrahedral according to the dimension and kind of the analysis. In the study, 4-node linear tetrahedron continuum element, denoted as C3D4, was used due to its flexibility to create three-dimensional elements in curved surfaces (Figure 4.10).

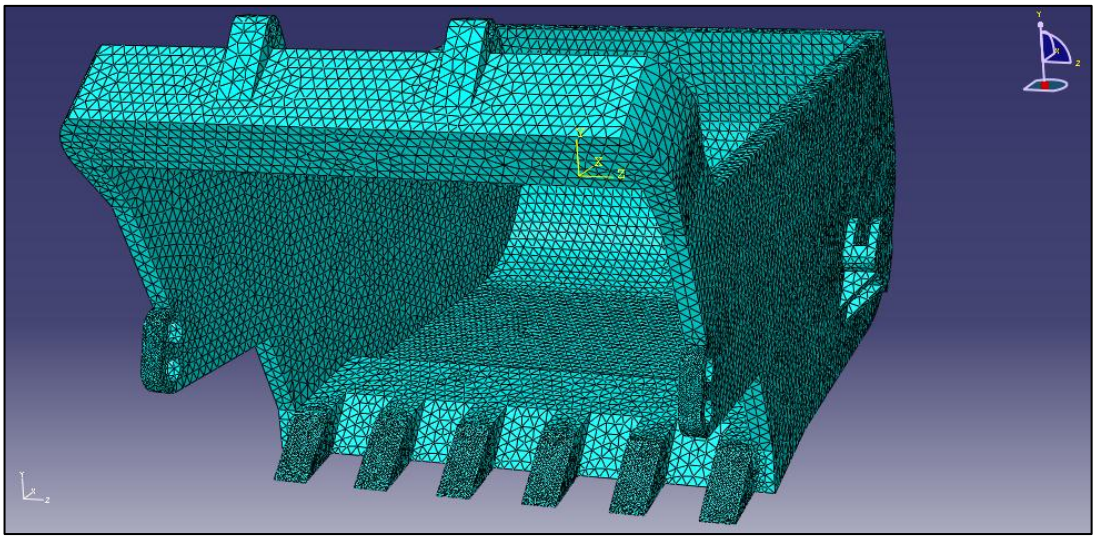

Figure 4.10 Mesh Body of the Bucket

4.2.4 Determination of Analysis Type

Step module in Abaqus serves to divide simulation into the phases to follow the analysis history. To achieve this, a proper analysis type according to the aim of problem should be introduced. The type can be chosen through the analyses such as buckling analysis, heat transition analysis, dynamic stress analysis, and static stress analysis. In this research study, static stress analysis was taken as analysis type to focus on the critical loading times instead of whole cutting operation. Figure 4.11 shows flowchart to create step used in the thesis study.

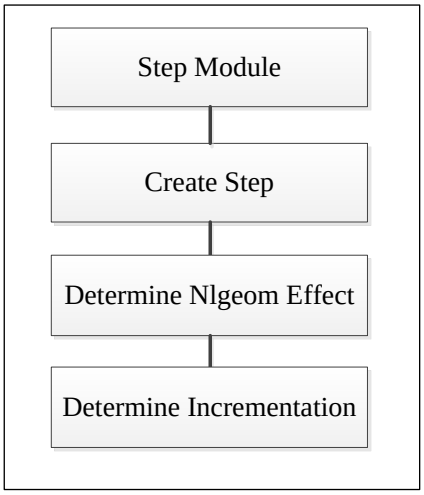

Figure 4.11 Flowchart of Step Definition in the Study

Abaqus allows two kinds of static simulation, Static General and Static Riks. A special type of static analysis, Static Riks, was introduced to the program, which prevents the instabilities due to the geometrical nonlinear conditions. Static Riks can perform buckling and collapse situations in the model. Furthermore, in step definition, Nlgeom command was also activated against the possibility of nonlinear effect with large deformation and displacement. Moreover, Abaqus contains a time-dependent response in the analyses, thus, the solution generally is determined as a series of increments with iterations to reach equilibrium in each increment. Increment numbers are stated in Chapter 4.3.

4.3 Case Studies and Loading-Boundary Conditions

Under load module in Abaqus, the program provides the identification of load and boundary condition cases. In a model, load can be created in the form of concentrated force, body force, moment, pressure, and gravity. Besides, boundary conditions can be determined to assign the degree of freedom for each element in terms of symmetry, displacement, and motion.

In the thesis research, two case studies for stress investigation on the bucket were carried out. The case studies focused on the horizontal cutting action of dragline bucket (Figure 4.1). Material specifications and mesh properties remained constant during both of the simulations. Only boundary conditions were changed to define the cases in the simulation environment. Each case was repeated for each formation type stated in Table 4.1. Boundary conditions of the cases are given below.

i. In the first case, floor of the bucket was fixed in all directions and cutting forces were applied to the teeth to detect single effect of cutting force on the empty bucket (Figure 4.12-a). For this case, bucket was assumed to be in an equilibrium state with the formation at time is zero, and stable at that time. Increment number was given as 10 to obtain a short-term static simulation.

ii. In the second case, tips of the digging teeth were fixed in all direction except of movement direction and cutting force applied to the teeth to investigate the stress distribution on a moving bucket (Figure 4.12-b). A velocity, 0.5 m/sec, was given to the drag hitch elements of the bucket in –x direction. Also, 0.015 m/sec velocity was given to the back of floor in –y direction. Uniform gravity force was also introduced to the program. Increment number was given as 40 to observe a long simulation.

As mentioned above, the cases were repeated for each formation types, very compacted, compacted, and loose. For each one of them, different normal pressures were applied to dragline bucket teeth as 0.111 MPa, 0.082 MPa, and 0.075 MPa, respectively.

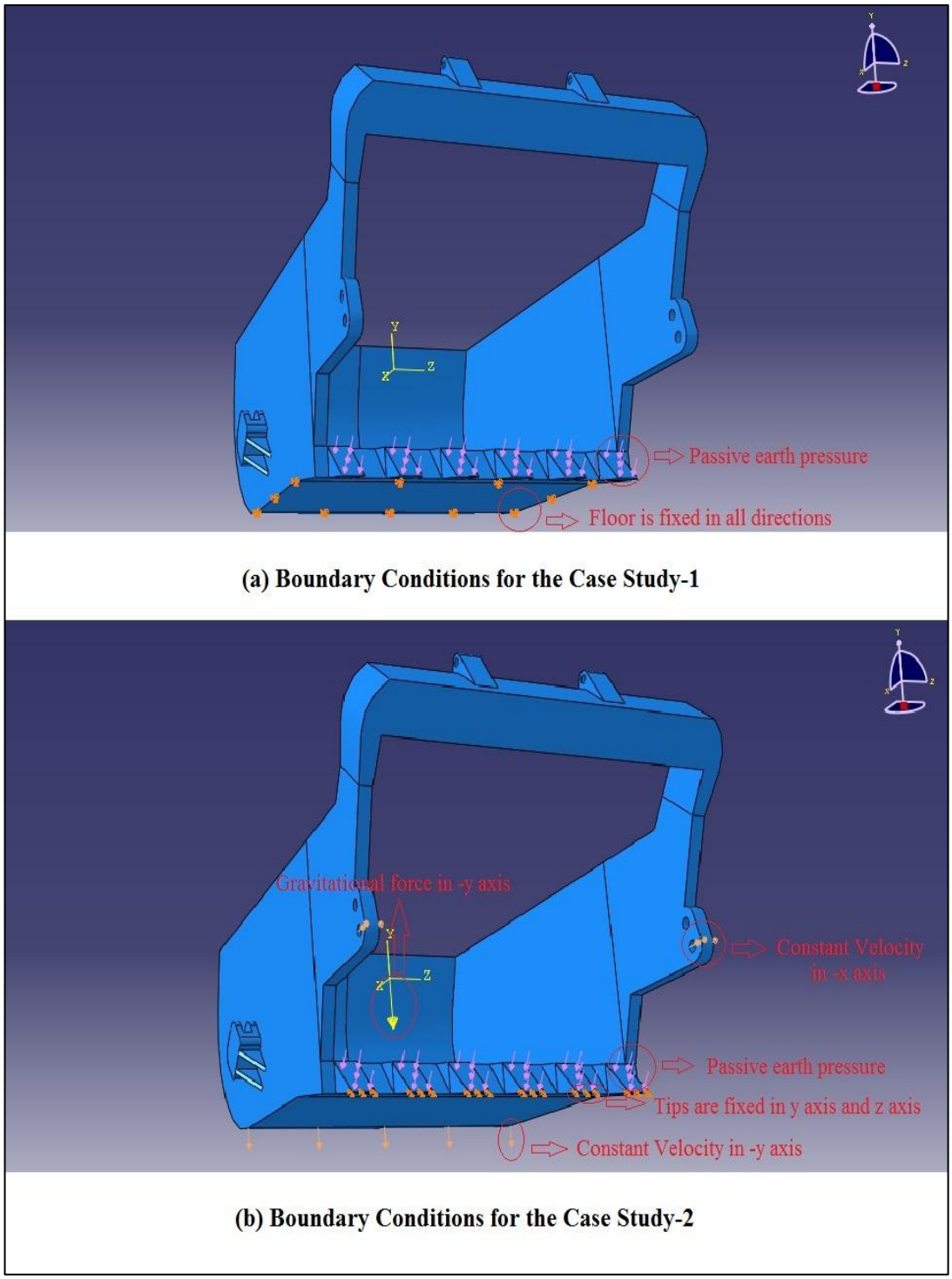

Figure 4.12 Boundary Conditions for (a) Case Study-1 (b) Case Study-2

In the illustration of simulation results, the Von Mises stress values were utilized for both Case-1 and Case-2. The Von Mises stress criteria can be defined as in Equation (4.3):

$$\sigma_{mises} = \sqrt{\frac{(\sigma_1 - \sigma_2)(\sigma_1 - \sigma_3)(\sigma_2 - \sigma_3)}{2}} \tag{4.3}$$

4.4 Sensitivity Analysis for the Formation Specifications in Stress Investigation

A sensitivity analysis basically helps to understand how the individual parameters of the model affect results of whole model. It determines how sensitive the model to modifications in the values of model variables. In the thesis study, cutting force equation (Equation 4.1) utilizes different formation specifications such as density, cohesion, internal friction angle, and external friction angle. To detect the sensitivity of the model for each parameter, parametric value for each one was changed within +/- 20% interval while other parameters were kept constant. Very compacted formation specifications in Table 4.1 were taken as initial starting parametric values as change is 0 %. Re-arranged values of the parameters in the change intervals are given in Table 4.5.

Table 4.5 Parametric Values in +/- 20% Change Interval

% Change	Density (t/m^3)	Cohesion (kPa)	Internal Friction Angle (Degree)	External Friction Angle (Degree)
20	2.208	24.48	40.8	30.0
10	2.024	22.44	37.4	27.5
0	1.840	20.40	34.0	25.0
-10	1.656	18.36	30.6	22.5
-20	1.472	16.32	27.2	20.0

For each change in a single parameter, a new normal pressure (P_n) value is calculated. For instance, P_n calculation is expressed below for the +20% change in density.

From Equation (4.1),

$$T = \left[\left(1.84\,{}^{t}/_{m^3}\,(1+E)\right)\left(9.81\,{}^{m}/_{s^2}\right)(0.512\,m)^2\,(1.7326) + (20.4\,kPa)(0.512\,m)(2.6515)\right]\,x\,4.295m$$

E= +20%:

$$T = \left[\left(1.84\,{}^{t}/_{m^3}\,(1+0.2)\right)\left(9.81\,{}^{m}/_{s^2}\right)(0.512\,m)^2\,(1.7326) + (20.4\,kPa)(0.512\,m)(2.6515)\right]\,x\,4.295m = 161.2\,KN$$

Unit force for each tooth = 161.2 kN / 6 teeth = 26.867kN
Area of a single tooth contact surface = 210000 mm^2
Pressure on the surface of single tooth in terms of N/mm^2 or MPa
$= 26867N/210000mm^2 = 0.128\,N/mm2$
$P_n = P_t x cos\delta = 0.128 x cos25 = 0.116\,MPa$

By repeating the calculations for each variable at every change level (20%, 10%, -10%, -20%), new normal pressure values (P_n) are found as in Table 4.6.

It should be noted that graphical checks are required for $N\gamma$ and N_c in any change in internal and external friction angles. Therefore, Table A.1, Table A.2, Table A.3, Table A.4 in Appendix A should be utilized in calculation of $N\gamma$ and N_c, as explained in Chapter 4.1.2. Moreover, all numerical details in P_n calculations can be investigated in Table B.1, Table B.2, Table B.3, and Table B.4 in Appendix B.

According to new P_n values, a total of seventeen different simulations, the main simulation at 0% change and other sixteen simulations, were performed in Abaqus

where each one of them included five iterations. Structures of the simulations were identical with the Case-2 in Chapter 4.3, expect for the normal pressures on the teeth. It was aimed to find which one of the parameters mostly effects the stress values in the simulation results.

Table 4.6 P_n-Values According to New Parametric Values

% Change	P_n-Values for Change in Density	P_n-Values for Change in Cohesion	P_n-Values for Change in Internal Friction Angle	P_n-Values for Change in External Friction Angle
20	0.1160	0.1280	0.1465	0.1377
10	0.1134	0.1194	0.1269	0.1242
0	0.1109	0.1109	0.1109	0.1109
-10	0.1084	0.1023	0.0961	0.0979
-20	0.1058	0.0938	0.0843	0.0853

CHAPTER 5

RESULTS AND DISCUSSIONS

5.1 Case-1: Stress Investigation on a Stable Dragline Bucket

This case was carried out to understand the single effect of the earth resistive force on a dragline bucket. Size and durations of the simulations for Case-1 are stated in Table 5.1.

Table 5.1 Problem Size and Job Time Summary for Case-1

Problem Size		
Number of Elements	Number of Nodes	Total Number of Variables in the Model
199062	45318	135954

Job Time Summary (Sec)		
Very Compacted Formation Analysis	Compacted Formation Analysis	Loose Formation Analysis
703.4	429.5	656.3

As seen in Table 5.1, three different loading conditions were applied normal to the tooth surfaces. Floor of the bucket was fixed in all directions since it is assumed that bucket was stable for a short time at the initial interaction with the formation. Each simulation consisted of 10 iterations. Resultant stress contour distributions for three different formation resistances are as in Figure 5.1.

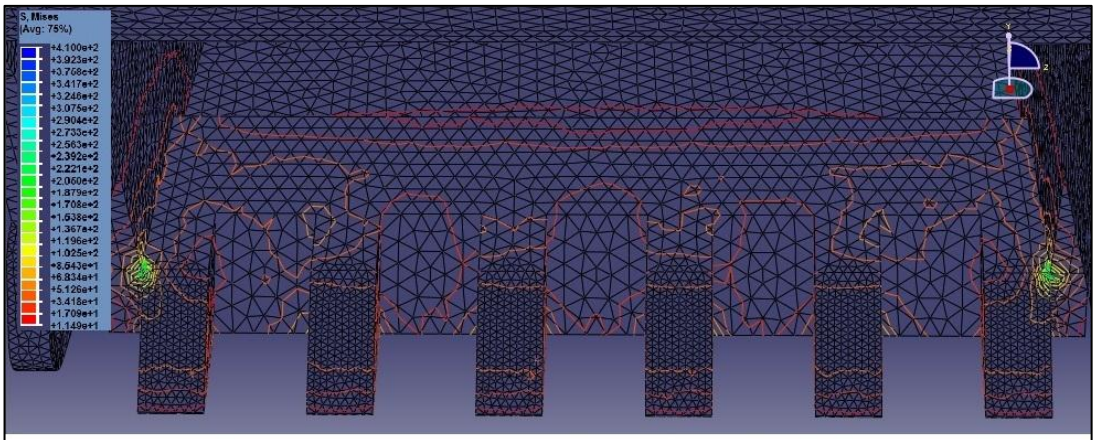

(a) Stress Distribution for the Very Compacted Formation

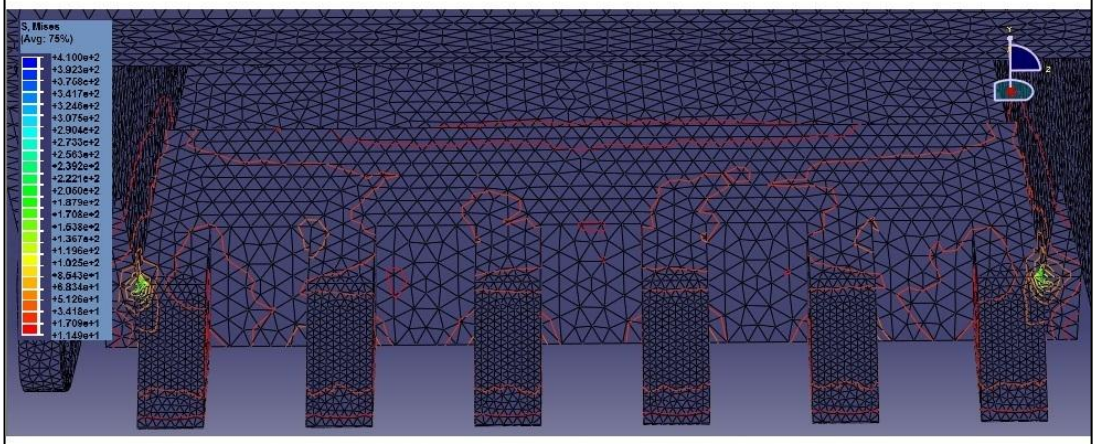

(b) Stress Distribution for the Compacted Formation

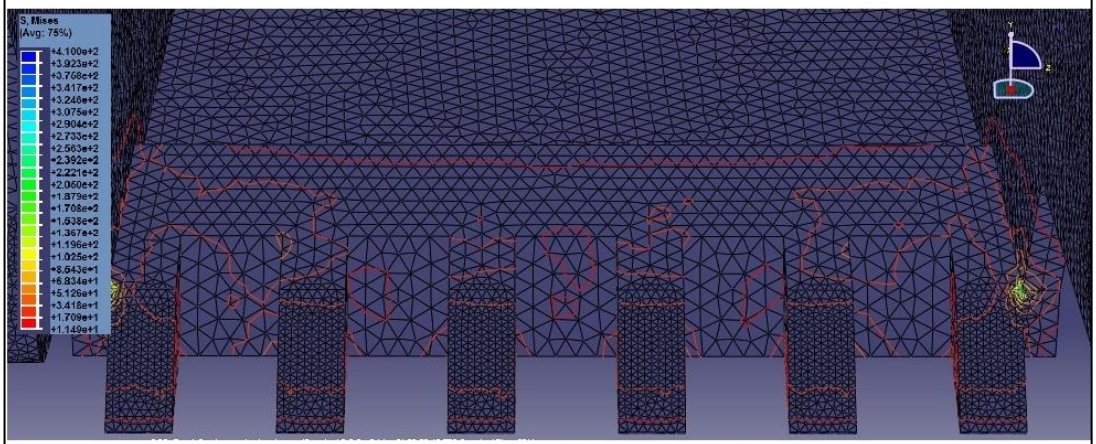

(c) Stress Distribution for the Loose Formation

Figure 5.1 The Von Mises Stress Contours According to the Formation Types for Case-1

As illustrated in Figure 5.1, the Von Mises stresses accumulated at the lower edges of the bucket lip. Element-130463 on the one of these critical edges was selected for a detailed investigation (Figure 5.2).

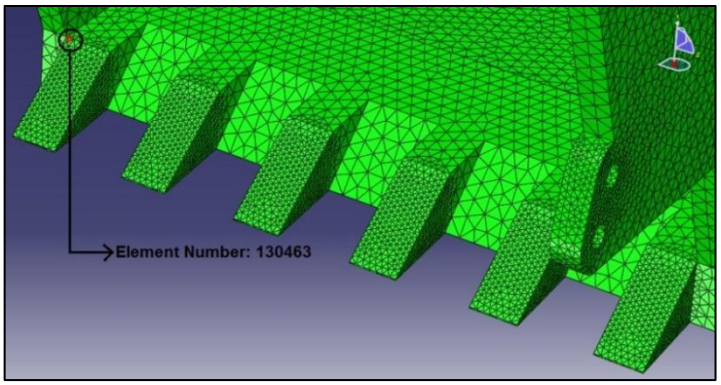

Figure 5.2 Presentation of Element-130463

Iteration-dependent stress increase on the element-130463 is shown in Figure 5.3 for very compacted formation, in Figure 5.4 for compacted formation, and in Figure 5.5 for loose formation.

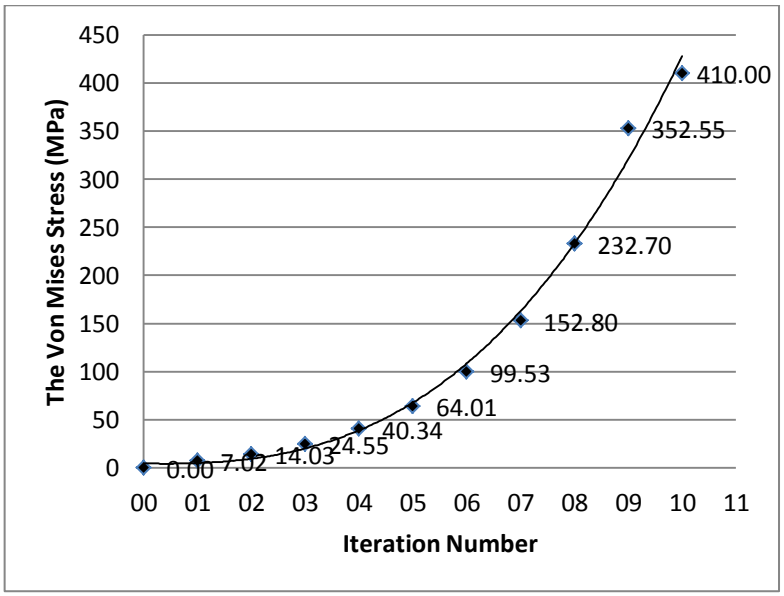

Figure 5.3 Stress Change on Element-130463 for the Very Compacted Formation

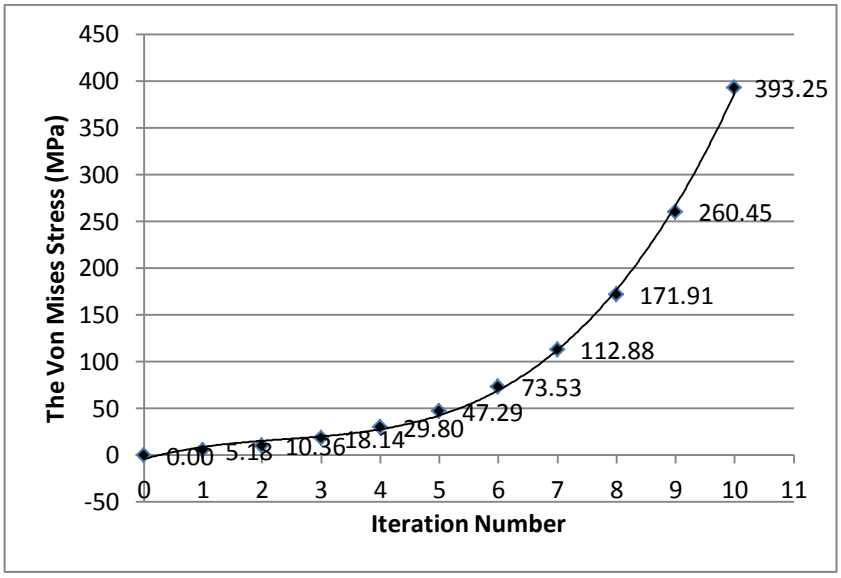

Figure 5.4 Stress Change on Element-130463 for the Compacted Formation

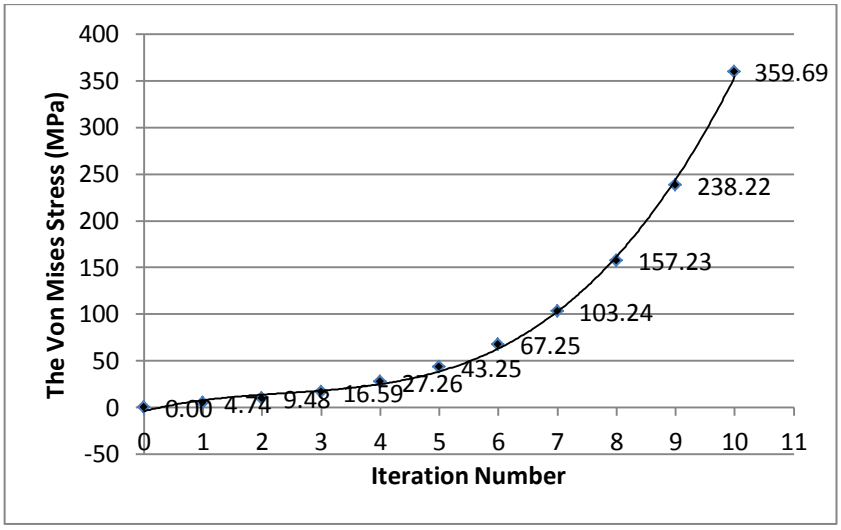

Figure 5.5 Stress Change on Element-130463 for the Loose Formation

As seen in the Figure 5.3, Element-130463 reach the yield point for the very compacted formation type since the yield strength of the bucket material is 410 MPa. In the other analysis for the compact and the loose formation types, stresses are in the critical levels, 393.25 MPa and 359.69 MPa, respectively.

5.2 Case-2: Stress Investigation on a Moving Dragline Bucket

Case-2 was performed to analyze stress formations on a horizontally moving dragline bucket. Size and durations of the simulations for Case-2 are stated in Table 5.2.

Table 5.2 Problem Size and Job Time Summary for Case-2

Problem Size		
Number of Elements	Number of Nodes	Total Number of Variables in the Model
199062	45318	135954

Job Time Summary (Sec)		
Very Compacted Formation Analysis	Compacted Formation Analysis	Loose Formation Analysis
4386.1	5452.4	4496.5

Same loading conditions in Case-1 were applied for Case-2. However, boundary conditions were different from Case-1. In Case-2, tips of teeth were only allowed to move in –x direction. Also, back floor of the bucket was fixed in z-direction. Constant velocities were given to drag hitch element as 0.5 m/sec in –x direction and back floor as 0.015 m/sec in –y direction. Moreover, gravitational force was included in the simulation. Each simulation consisted of 50 iterations. After the procedure was completed, colored visualizations for simulation stress contours were determined for three different formation resistances as in Figure 5.6. Simulation results showed that there were some overloading conditions on the bucket elements and yield points as an outcome of overloading. Figure 5.7 shows the the yielding points on the bucket occur on drag hitch elements and tips of teeth.

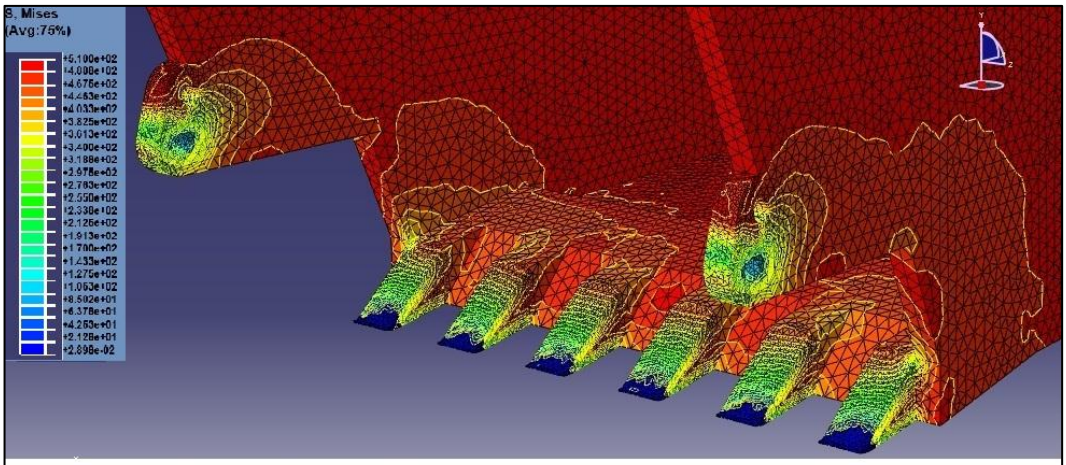

(a) Stress Distribution for the Very Compacted Formation

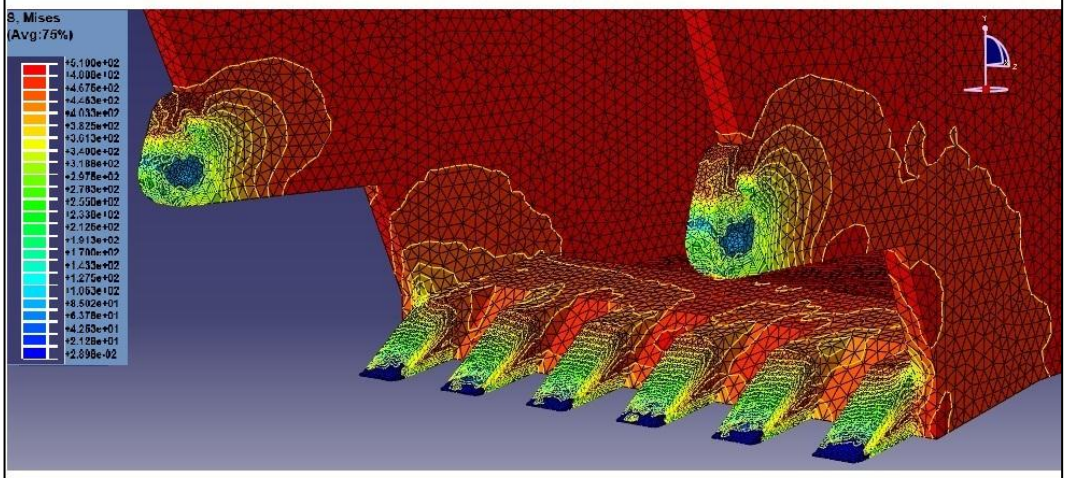

(b) Stress Distribution for the Compacted Formation

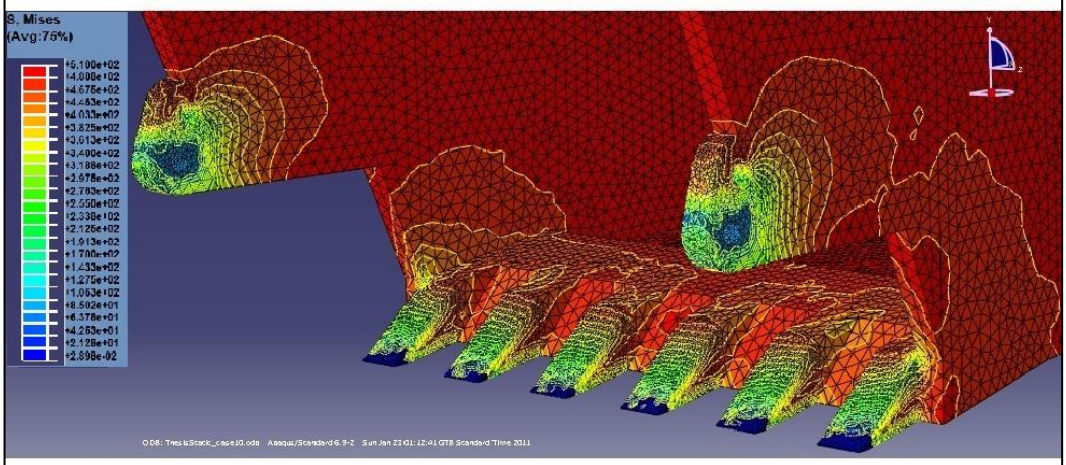

(c) Stress Distribution for the Loose Formation

Figure 5.6 The Von Mises Stress Contours According to the Formation Types for Case-2

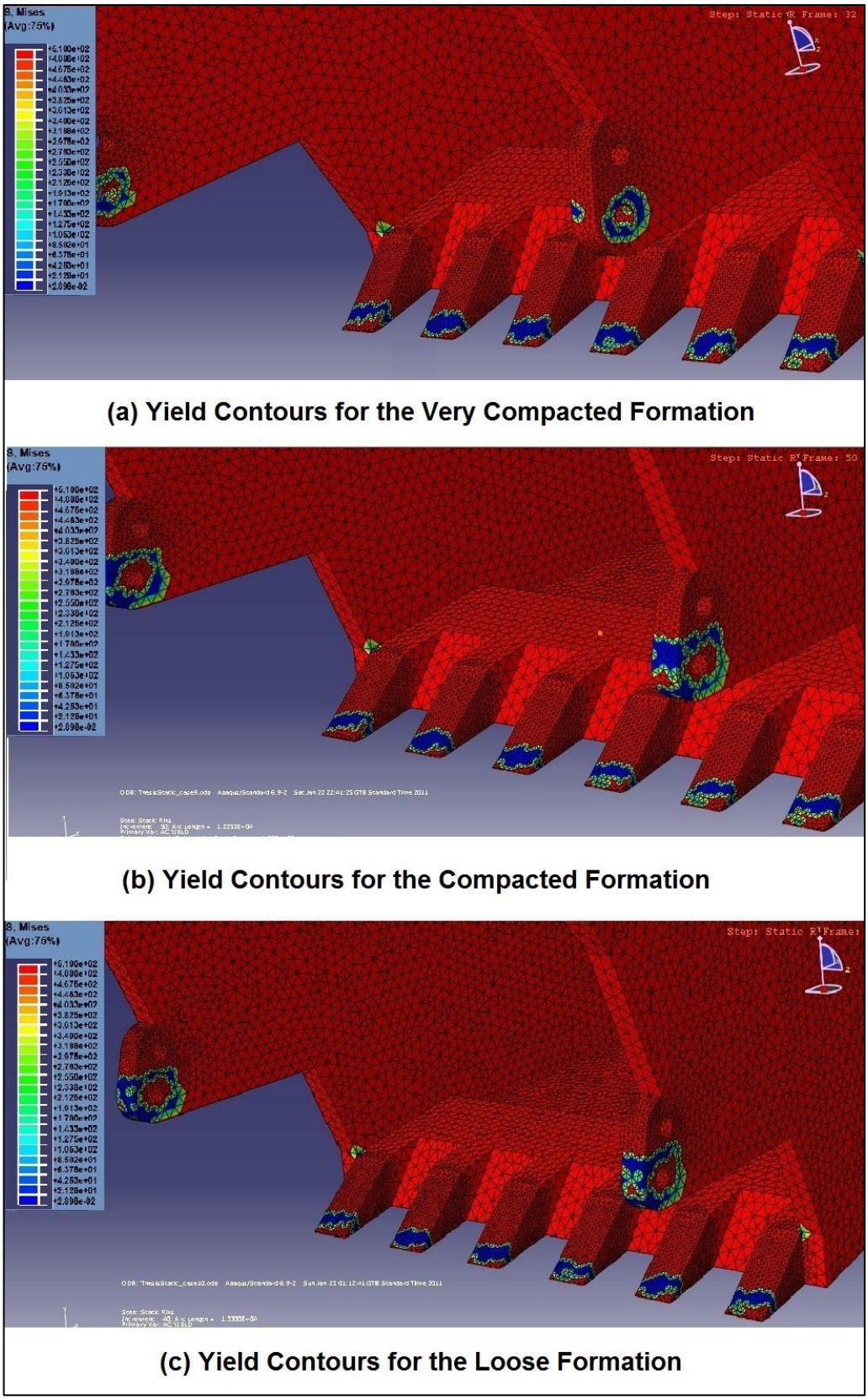

Figure 5.7 Yielding Contours According to the Formation Types for Case-2

After the execution simulations, some elements were selected to visualize the effect of stress on the deformation. As indicated in Figure 5.7, bucket regions are closest to failure in drag hitch part and digging teeth elements. These parts are exposed to large plastic failure and more sensitive to the changes in stress. Therefore, Element-24753, on the tooth tip, and Element-5858, on the drag hitch part, were selected as representative analysis elements (Figure 5.8 and Figure 5.9).

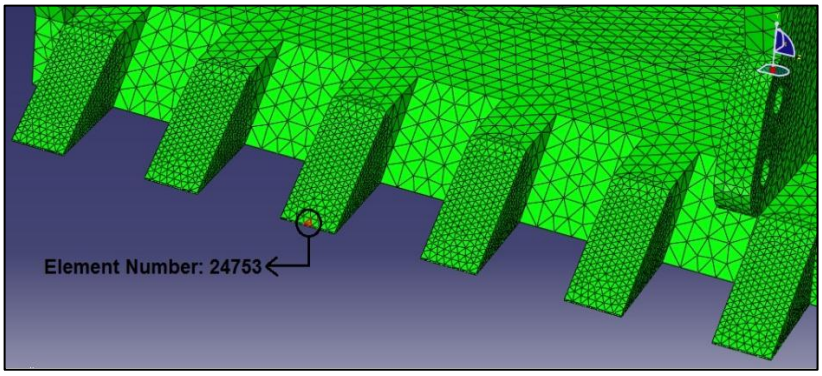

Figure 5.8 Presentation of Element-24753

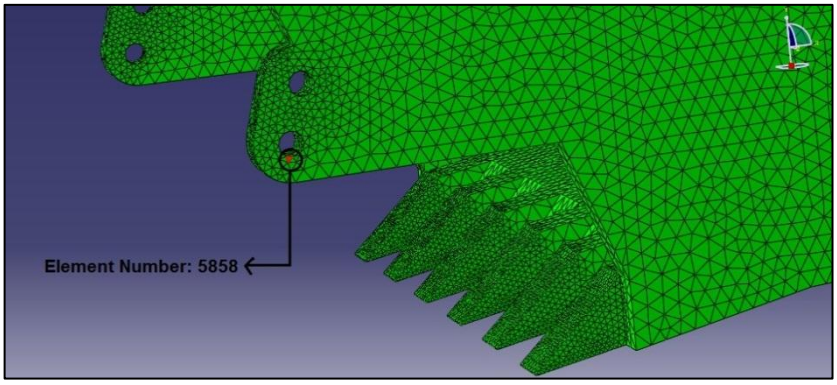

Figure 5.9 Presentation of Element-5858

Initial analyses were performed on Element-24753. As indicated in Figure 5.10 for the very compacted formation, in Figure 5.11 for the compacted formation, and in Figure 5.12 for the loose formation type, stresses on the Element-24753 at the end of simulations were greater than the yield strength, 510 MPa for the tooth material.

Some volumetric deformations were detected as 34 % for the very compacted formation type, 20% for the compacted formation type, and 13 % for the loose formation type. From graphs, it is clear that amount of deformation increase with the compactness of the formation.

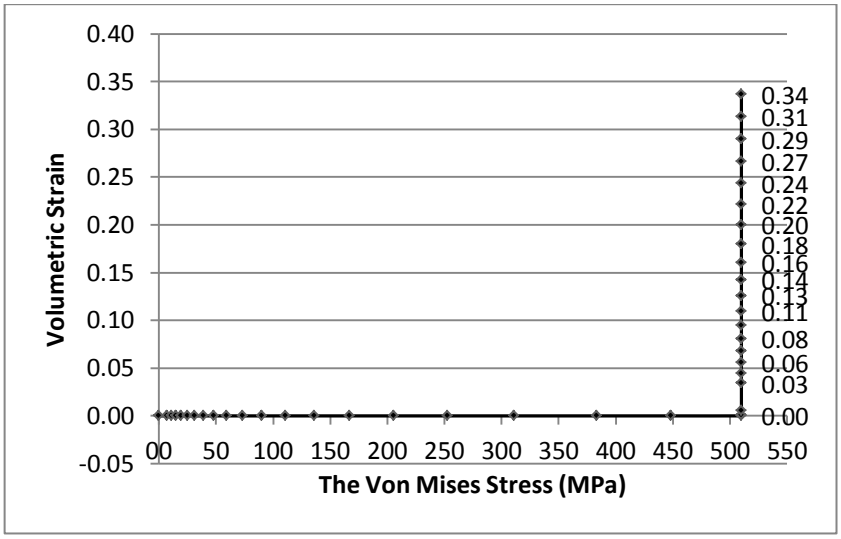

Figure 5.10 Stress and Strain Curve of Element-24753 for the Very Compacted Formation

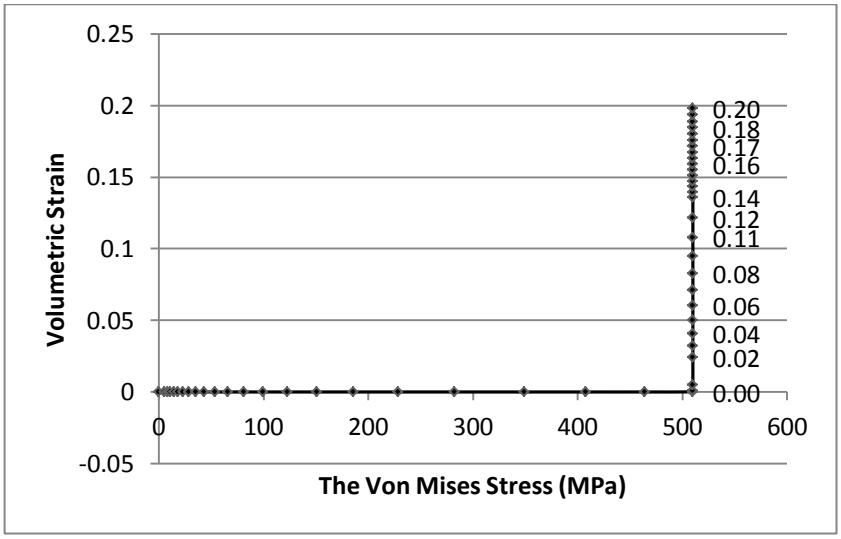

Figure 5.11 Stress and Strain Curve of Element-24753 for the Compacted Formation

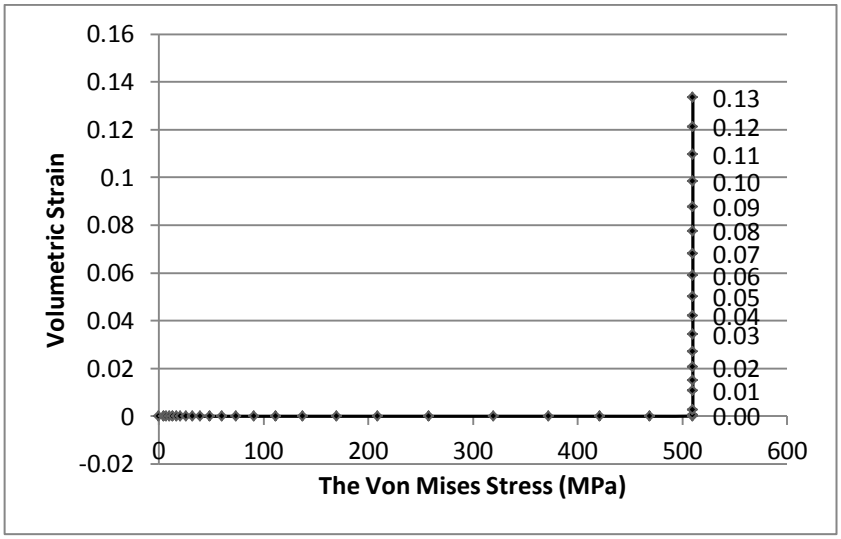

Figure 5.12 Stress and Strain Curve of Element-24753 for the Loose Formation

Other stress-strain investigations were carried out on the drag hitch element, Element-5858. Volumetric deformation amounts for the very compacted, compacted and loose formation were obtained as 0.08 %, 0.8%, and 1%, respectively, as indicated in Figure 5.13, Figure 5.14,and Figure 5.15.

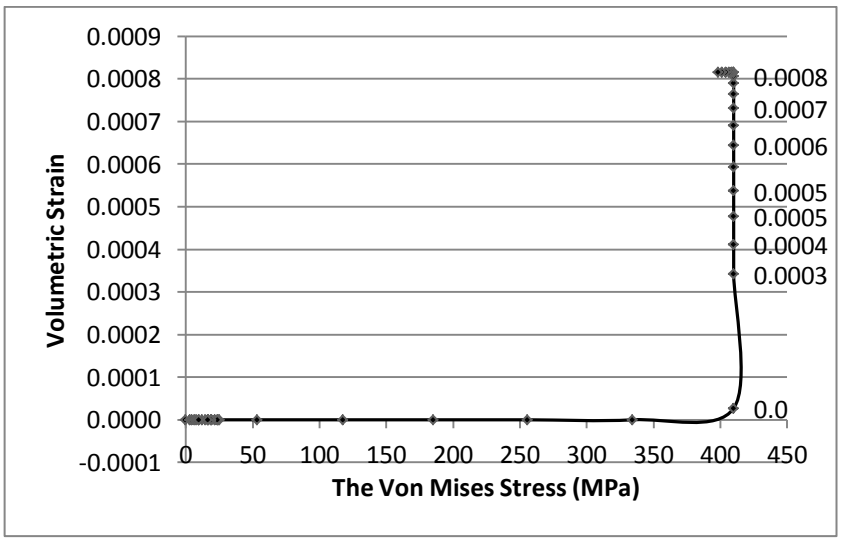

Figure 5.13 Stress and Strain Curve of Element-5858 for the Very Compacted Formation

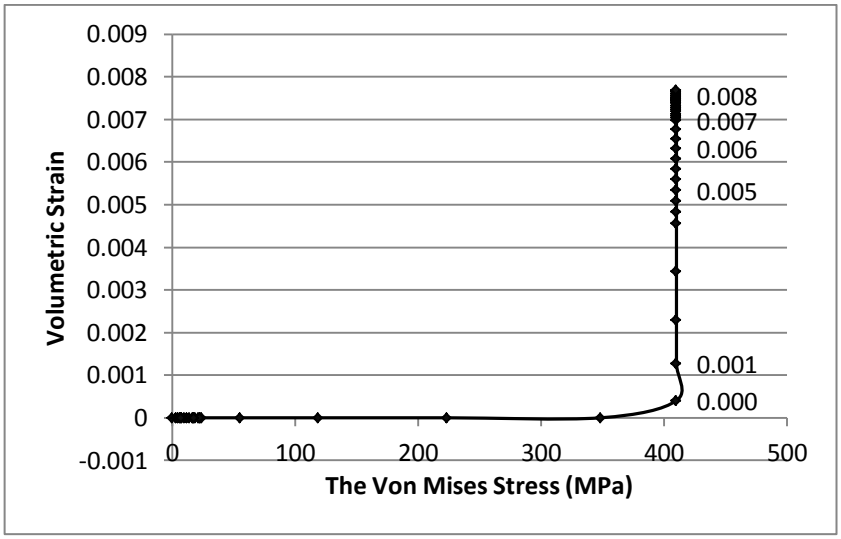

Figure 5.14 Stress and Strain Curve of Element-5858 for the Compacted Formation

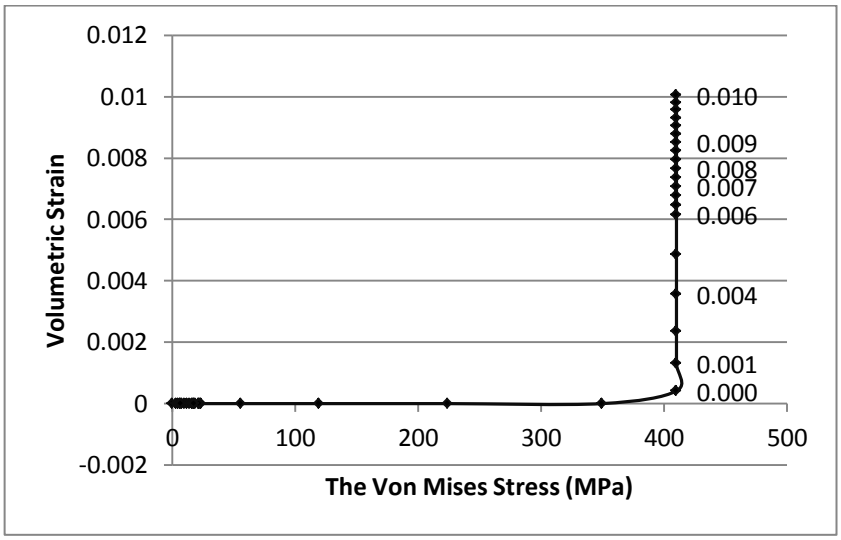

Figure 5.15 Stress and Strain Curve of Element-5858 for the Loose Formation

As seen in the stress-strain curves of Element-5858, largest plastic deformation on the drag hitch part occurs in loose formation type analysis, contrary to the expectations. This situation is due to that failure on the teeth elements occurs in later period in loose formation analysis and stress continues to accumulate on drag hitch elements. On the other hand, resistive stress on the teeth cause rapid failure on the

compacted and very compacted formations earlier and stresses on the drag hitch elements are relaxed. Therefore, accumulation of stresses on the drag hitch elements occurs more slowly.

5.3 Sensitivity Analysis for Formation Parameters

In addition to the stress-strain analysis on the dragline bucket, it was also performed a sensitivity analysis to observe that how the changes in formation specifications could effect the stress formations on the bucket element. Formation properties in the sensitivity analysis were taken as density, cohesion, internal friction angle, and external friction angle. To achieve this, Element-24753 in Figure 5.8 was set as representative element for this analysis.

Table 5.3 illustrates resultant pressure values on Element-24753 as the outcomes of the simulations. As seen in the table, twenty different simulations, five for each formation specification, were performed to find how the specification changes in the range of $\pm$20 % influence the stress values (Figure 5.16).

Table 5.3 The Von Mises Stress Values on the Element-24753 after 5th Iteration

% Change	Stress for Density (MPa)	Stress for Cohesion (MPa)	Stress for Internal Friction Angle (MPa)	Stress for External Friction Angle (MPa)
20	26.18	28.92	33.27	31.20
10	25.57	26.97	28.66	28.03
0	24.99	24.99	24.99	24.99
-10	24.40	22.98	21.55	21.96
-20	23.80	21.01	18.82	19.05

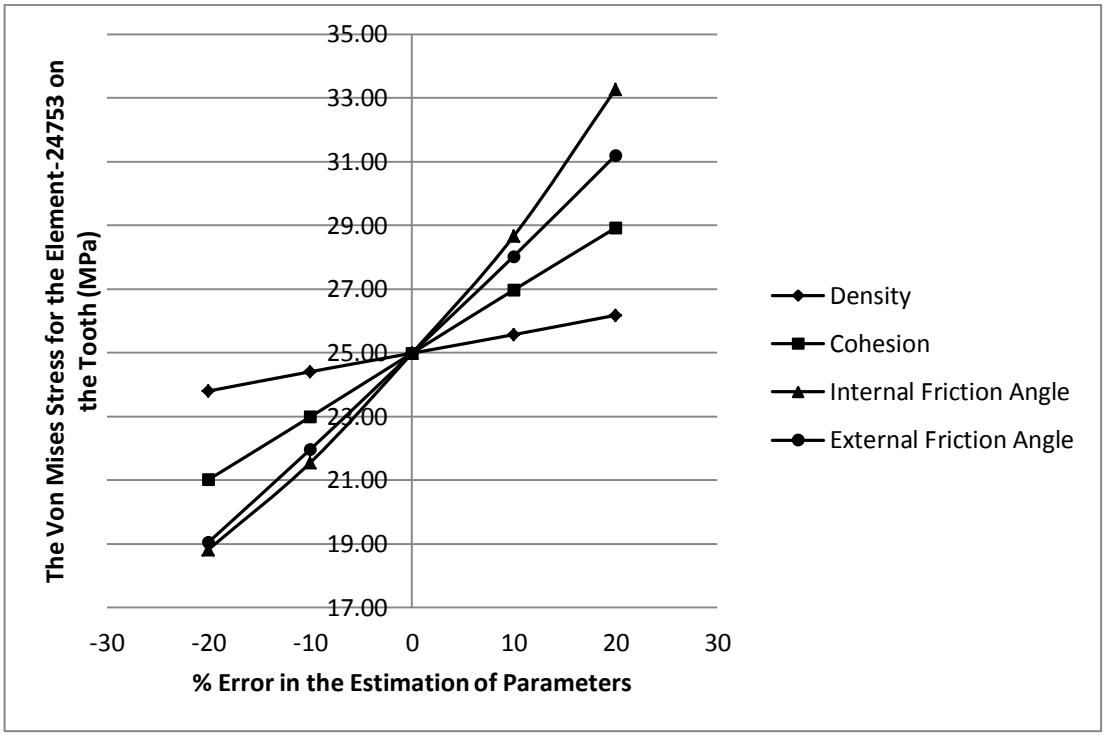

Figure 5.16 Sensitivity Analysis Curves

As seen from Figure 5.16, the analysis showed that the stress formation on the element is most sensitive to internal friction angle, which is steepest curve on the graph, and less sensitive to density factors, which is the curve closest to horizontal.

CHAPTER 6

CONCLUSIONS AND RECOMMENDATIONS

6.1 Introduction

In open-cast mines, overburden removal processes are performed by either excavator-truck system or dragline stripping method. Due to the low maintenance and operating costs and high production rate, dragline stripping method is preferable up to 35 m operation height (Köse, 1987). Earthmoving efficiency of a dragline can be determined by the cycle time utilization and the bucket payload amount (Vynne, 2008). In this regard, the fact that the dragline carries maximum volume of overburden in minimum cycle time without any catastrophic or machinery failure, creates most appropriate working condition for a dragline.

Dragline implements the stripping operation with a bucket suspending from the tip sheaves of the boom. Operator controls the bucket actions with a chain-rope system called rigging mechanism. Productivity of this earthmover directly depends on the performances of working parts, especially bucket and rigging mechanism since interaction between the machine and formation takes place via the bucket. Besides the diggibility of a bucket is critical for whole dragline productivity, it is also required to avoid damages on the bucket due to the overloading conditions or improper bucket selection. Since, these types of failures on bucket elements can cause long-term breaks and loss of time and production. Previous research studies about the bucket performance have mainly focused on the topics such as material filling optimization, rigging mechanism arrangements, kinematical testing of bucket and automation. Although these studies are for improving bucket efficiency, there is still a lack of investigation about strain-stress distribution on a working dragline bucket. Accordingly, formation interaction simulation of dragline bucket in virtual

environment is still an emerging research topic on dragline productivity.

Consequently, this research study combines the use of Finite Element Analysis (FEA), Computer-Aided Design (CAD) and analytical literature review to observe the stress distribution on a three-dimensional dragline bucket model. Determination of dragline bucket and rigging mechanism solid models was performed by Solidworks (Solidworks Co., 2009). Only bucket model was transferred to the simulation environment to focus on the stress investigation on the bucket and to eliminate the possible inaccuracies and long simulation time due to curvatures and the interaction areas between solid parts. Abaqus 6.9-2 (Simulia, 2010) was chosen as a finite element executer. Two case studies with different boundary conditions were computed in Abaqus environment, with Static, Riks method. Each simulation was repeated for three different formation specifications as very compact, compact and loose formations, respectively.

6.2 Conclusions

First case study, with ten iterations, aimed to measure the single effect of passive earth pressure magnitude on a fixed bucket. Simulation result showed that lower edge of the bucket lip fails for the very compacted formation analysis and come to critical levels for compacted and loose formation types. Second case, with fifty iterations, allowed investigating stress analysis on a dragline bucket with constant velocity. In this case, drag hitch parts of the bucket and digging teeth were detected as failure zones on the bucket. Besides the simulations, a sensitivity analysis was executed to see the impacts of each formation specification on the stress simulation findings. The analysis indicated that stress amounts on the elements were mostly effected by the change in internal friction angle and least effected by the change in density. Detailed stress analysis on the dragline bucket shows that:

i. Sharp edges on the front of bucket are closest to fail during the operation. These edges are required to be rounded and strengthened by welding or any other metallurgical method.

ii. Drag hitch element of the bucket and the tips of the digging teeth are most sensitive parts on the bucket. Stress accumulation mostly occurs in these sections. A possible overloading dragging condition primarily causes the yields in these parts.

iii. Internal friction is most significant formation factor to determine the resistive forces on the bucket. On the other hand, density is least effective to change the pressure values on the bucket parts.

iv. Defined criteria in the boundary condition and number of the iterations considerably affect the simulation time and simulation results.

v. Material selections for the solid bodies greatly influence the mechanical behavior of the parts under loading conditions.

6.3 Recommendations

The main recommendations related to this study are:

i. Three dimensional simulation of whole dragline could be useful to detect all stress-strain formations on the machine.

ii. Projects which include both industry and university could eliminate the lack of data in the analysis and help to obtain more realistic simulation results.

iii. Performing computational stress investigation together with field measurements in the mine site could validate the simulation model.

iv. Fracture and fatigue analysis on the stress-intensive parts of dragline could be beneficial to investigate the working life of the components. Therefore, more sensitive performance calculations could be made for the dragline.

v. Virtual reality studies for the dragline operator could be useful for the efficient training of the operators in safe conditions.

REFERENCES

Abaqus 6.9 User's Manual. (2009). Elements. *4*.

Abaqus 6.9 User's Manual. (2009). Getting Started with Abaqus.

Abo-Elnor, M., Hamilton, R., & Boyle, J. T. (2004). Simulation of Soil–Blade Interaction for Sandy Soil Using Advanced 3D Finite Element Analysis. *Soil & Tillage Research, 75*, 61–73.

Alekseeva, T. V., Artem'ev, K. A., Bromberg, A. A., Voitsekhovskii, R. I., & Ul'yanov, N. A. (1985). *Machines for Earthmoving Work: Theory and Calculations.* Rotterdam: Balkema.

Aluko, O. B. (2008). Finite Element Aided Brittle Fracture Force Estimation During Two-Dimensional Soil Cutting. *International Agrophysics, 22*, 5-15.

Aluko, O. B., & Chandler, H. W. (2004). A Fracture Strength Parameter for Brittle Agricultural Soils. *Biosystems Engineering, 88*(3), 369-381.

Aluko, O. B., & Seig, D. A. (2000). An Experimental Investigation of the Characteristics of and Conditions for Brittle Fracture in Two-Dimensional Soil Cutting. *Soil and Tillage Research, 57*, 143-157.

Anonymous. (2004). *Dragline Excavator.* Retrieved August 22, 2010, from Wikipedia: http://www.enotes.com/topic/Dragline_excavator

Anonymous. (2008). Retrieved December 2010, from http://www.pbase.com/intermodal/image/99215155/original

Anonymous. (2010, March 31). *Arch Western Resources Annual Report- Form NO:10-K.* Retrieved December 14, 2010, from http://www.faqs.org/sec-filings/100331/ARCH-WESTERN-RESOURCES-LLC_10-K/

Baafi, E. Y., Mirabediny, H., & Whitchurch, K. (1997). Computer Simulation of Complex Dragline Operations. *International Journal of Surface Mining, Reclamation and Environment, 11*(1), 7-13.

Berg, P. v. (1994). *Analysis of Soil Penetration.* Stevinweg: Delft University Press.

Blouin, S., Hemami, A., & Lipsett, M. (2001). Review of Resistive Force Models for Earthmoving Processes. *Journal of Aerospace Engineering*, 102-111.

Bucket and Teeth. (2008, September). Retrieved June 2, 2010, from ESCO Corporation Web Site: http://www.escocorp.com/media/articles/ESCO_and_Rosebud_Mine.pdf

Chi, L., & Kushwaha, R. L. (1989). Finite Element Analysis of Forces on A Plane Soil Blade. *Canadian Agricultural Engineering, 31*(2), 135-140.

Cleary, P. W. (1998). The Filling of Dragline Buckets. *Mathematical Engineering in Industry, 7*(1), 1-24.

Cobcroft, T. (2007). Virtual Reality for Dragline Planners. *Coal Age*, 22-26.

Coetzee, C. J., Basson, A. H., & Vermeer, P. A. (2007). Discrete and Continuum Modelling of Excavator Bucket Filling. *Journal of Terramechanics, 44*, 177–186.

Corke, P., Winstanley, G., Dunbabin, M., & Roberts, J. (2006). Dragline Automation: Experimental Evaluation through Productivity Trial. *The International Conference on Field and Service Robotics*, (pp. 459-468).

Craig, R. F. (1997). *Soil Mechanics.* London: Taylor & Francis Group.

Davis, M. (2010, June). *Photograph of Bucyrus Erie 2550-W Walking Dragline.* Retrieved December 2010, from http://www.flickr.com/photos/perspectivephotography/5055431041/

Davoudi, S., Alimardani, R., Keyhani, A., & Atarnejad, R. (2008). A Two Dimensional Finite Element Analysis of a Plane Tillage Tool in Soil Using a Non-linear Elasto-Plastic Model. *American-Eurasian Journal of Agricultural & Environmental Sc, 3*(3), 498-505.

Dayawansa, P., Chitty, G., Kerezsi, B., Bartosiewicz, H., & Price, J. W. (2003). The Cracking of Clusters in Mining Dragline Booms: Causes and Responses. *Proceedings of International Conference on Failure Analysis and Maintenance Technologies.*

Demirel, N. (2009). Çekme-Kepçe Performansını Etkileyen Operasyonel Faktörler.

Türkiye 2. Maden Makinaları Sempozyumu Bildiriler Kitabı, (pp. 267-276). Zonguldak.

Demirel, N. E. (2007). Dynamic Dragline Modeling and Boom Stress Analysis for Efficient Excavation. *PHD Thesis*.

Dragline Excavator. (n.d.). Retrieved May 15, 2010, from Wikipedia Online Encyclopedia: http://en.wikipedia.org/wiki/Dragline_excavator

Dragline Methods. (n.d.). Retrieved May 3, 2010, from United States Environmental Protection Agency Web Site: epa.gov/region3/mtntop/pdf/appendices/h/mrt-symposium/fugpres1.pdf

Erdem, B., Çelebi, N., & Paşamehmetoğlu, A. G. (1998). İkili Dragline Sistemlerinde Dragline Eşzamanlanmasına Yönelik Bir Yaklaşım. *Türkiye 11. Kömür Kongresi Bildiriler Kitabı*, (pp. 145-154). Amasra.

Erdem, B., Duran, Z., & Çelebi, N. (2004). A Model for Direct Dragline Casting in a Dipping Coal-Seam. *The Journal of The South African Institute of Mining and Metallurgy*, 9-16.

Erdem, B., Neş'e, Ç., & Paşamehmetoğlu, A. G. (2005). Dragline Yığın Kümesi Tasarımı İçin Bilgisayar Destekli Bir Yaklaşım. *Türkiye 19. Uluslararası Madencilik Kongresi ve Fuarı*, (pp. 113-123). İzmir.

Erdem, B., Şahin, S., & Duran, Z. (2005). Dragline Yığın Kümesi Tasarımı İçin Bilgisayar Destekli Bir Yaklaşım. *Türkiye 19. Uluslararası Madencilik Kongresi ve Fuarı Bildiriler Kitabı*, (pp. 113-123). İzmir.

Ericsson, A., & Slattengren, J. (2000). A Model for Predicting Digging Forces When Working in Gravel or Other Granulated Material. (pp. 1-9). Rome: 15th ADAMS European Users Conferance Proceedings.

Esco Dragline Buckets. (2010). *ESCO ProFill™ Dragline Bucket.* Retrieved December 2010, from Esco Corporation Official Website: http://www.escocorp.com/markets/mining/dragline_buckets.html

Fielke, J. M. (1999). Finite Element Modelling of the Interaction of the Cutting Edge of Tillage Implements with Soil. *Journal of Agricultural Engineering*

Research, 74, 91-101.

Genç, M. (2002). Computer aided Modeling Of Dragline Operation In Open Pits And Investigation of Dragline Applications in Western Anatolia. *D.E.Ü Mining Engineering Department Msc Thesis.*

Gilewicz, P. (1999, August). U.S. Dragline Census . *Coal Age, 104*(8).

Gilewicz, P. (2000). International Dragline Population Matures. *Coal Age, 105*(6), 30-32.

Gill, W. R., & Vanden Berg, G. E. (1968). *Soil Dynamics in Tillage and Traction.* Washington, U.S.A.: Agricultural Research Service.

Gurgenci, H., & Guan, Z. (2001). Mobile Plant Maintenance and the Dutymeter Concept. *Journal of Quality in Maintenance Engineering, 7*, 275-285.

Hartman, H. L. (Ed.). (1992). *SME Mining Engineering Handbook* (2nd Edition ed., Vol. 1). Society for Mining, Metallurgy, and Exploration, Inc.

Hartman, H. L., & Mutmansky, J. M. (2002). *Introductory Mining Engineering* (2nd Edition ed.). John Wiley and Sons, Inc.

Hemami, A., Goulet, S., & Aubertin, M. (1994). Resistance of Particulate Media to Excavation: Application to Bucket Loading. *International Journal of Surface Mining, Reclamation and Environment , 8*, 125-129.

Hettiaratchi, D., & Reece, A. (1974). The Calculation of Passive Soil Resistance. *Geotechnique, 24*(3), 289-310.

Hofstetter, K. (2002). Analytic Method to Predict the Dynamic Interaction of Dozer Blade with Earthen Material. *Proceedings of the 14th International Conference of the ISTVS.* Vicksburg.

Kannan, G., Schmitz, L., & Larsen, C. (2000). An Industry Perspective On The Role Of Equipment Based Earthmoving Simulation. *Proceedings of Simulation Conference, 2*, pp. 1945-1952.

Kavetsky, A. (1999). *Modeling Dragline Bucket Dynamics and Digging (including Bucket Filling Animations CD).* Report No: C3048, Australian Coal

Association Research Program (ACARP).

Kennedy, B. A. (1990). *Surface Mining* (2nd Edition ed.). Society for Mining, Metallurgy, and Exploration, Inc .

Köse, H., & Yalçın, C. (1985). *Örtü Kazı Yöntemlerinin Ekonomik Açıdan Değerlendirilmesi.* İzmir: DEÜ Maden Mühendisliği Bölümü.

Legg, T., Dymond, G., & Eeden, J. v. (2008). *Taper VS. Conventional Bucket.* VR Steel.

Lever, P. (2003, April). *Open Cut Automation Scoping Study*. Retrieved from Australian Coal Association Research Program (ACARP) Web Site: http://www.acarp.com.au/abstracts.aspx?repId=C11054

Maciejewski, J., & Jarzebowski, A. (2002). Laboratory Optimization of the Soil Digging Process. *39*, 161-179.

Matt, W., Blair, J., & McGovern, P. (1997). *Determining the Functionality ofa Dragline Training Simulator.* Retrieved from http://www.findtoyou.com/ebook/dragline+method.html

McKyes, E. (1985). *Soil Cutting and Tillage.* Retrieved from McGill Bioresource Engineering Website: http://www.mcgill.ca/files/bioeng/BREE512_part1.pdf

Meyers, T., & Leslie, B. (2001, August). *Optimised Bucket for Parallel/Universal Rig*. Retrieved August 2010, from Australian Coal Association Research Program (ACARP) Web Site: http://www.acarp.com.au/abstracts.aspx?repId=C10034

Mirabediny, H., & Baafi, E. Y. (1998). Dragline Digging Methods in Australian Strip Mines - A Survey. *Coal Operators' Conference* , (pp. 313-324). Wollongong.

Mootaz, A. E., Hamilton, R., & Boyle, J. T. (2003). 3D Dynamic Analysis of Soil–Tool Interaction Using the Finite Element Method. *Journal of Terramechanics, 40*, 51-62.

Mouazen, A. M., & Nemenyi, M. (1999, July). Finite Element Analysis of Subsoiler Cutting in Non-Homogeneous. *Soil and Tillage Research, 51*, 1-15.

Nedoredzov, I. (1992). Forces Prediction of Underwater Soil Cutting by Excavating Robots. *9th International Symposium on Automation and Construction.* Tokyo.

O'Beirne, T., & Lumley, G. (1997, July). *Improved Dragline Productivity Through Rigging Design.* Retrieved June 2010, from Australian Coal Association Research Program (ACARP) Web Site: http://www.acarp.com.au/abstracts.aspx?repId=C4003

Offei, K. A., & Frimpong, S. (2009). Formation Excavation Resistance Modelling for Shovel Dippers. *International Journal of Mining and Mineral Engineering, 1*(2), 127-146.

Osman, M. S. (1964). The Mechanics of Soil Cutting Blades. *Journal of Agricultural Engineering Research, 9*(4), 313-328.

Owen, D., Feng, R. J., Neto, T., Cottrell, E. A., Wang, M., Pires, F. M., et al. (2002). The modeling of Multi-Fracturing Solids and Particulate Media. *Proceedings of the 5th World Congress on Computational Mechanics.* Vienna.

Özdoğan, M. (1984). Çekmekepçe (Dragline) Örtükazı Yöntemleri ve Tunçbilek Uygulaması. *Madencilik, 23*(2), 25-42.

Özdoğan, M. (2003). Dragline Yerkazarlarda Kepçe Saplanış Mekanizması ve Kuvveti. *Madencilik, 42*(1), 17-26.

Parlak, T. (1985). Açık Kömür İşletmeciliğinde Yerinde Dragline İncelenen Dragline Uygulamaları. *Madencilik, 24*(2), 5-34.

Raper, R. L., & Erbach, D. C. (1990). Prediction of Soil Stresses Using the Finite Element Method. *Transactions of the ASAE, 33*(3), 725-730.

Ridley, P., & Algra, R. (2004). Dragline Bucket and Rigging Dynamics. *Mechanism and Machine Theory, 39*, 999-1016.

Rowlands, J. (2000, March). *Dragline Rigging and Control System for Universal Dig & Dump*. Retrieved August 20, 2010, from Australian Coal Association Research Program (ACARP) Web Site: http://www.acarp.com.au/abstracts.aspx?repId=C9039

Ryerson, R. (1980). *Patent No. 4233761.* United States of America.

Singh, S. (1997). The State of the Art in Automation of Earthmoving. *Journal of Aerospace Engineering, 10*(4), 1-29.

Srour, J. (1999, March). *evelopment of Tools and Methods for Rigging Data Specification for use in Dragline Bucket Simulation*. Retrieved August 2010, from Australian Coal Association Research Program (ACARP) Web Site: http://www.acarp.com.au/abstracts.aspx?repId=C6010

Swick, W. C., & Perumpral, J. V. (1988). A Model for Predicting Soil-Tool Interaction. *Journal of Terramechanics, 25*(1), 43-56.

Townson, P., Murthy, P., Guan, Z., & Gurgenci, H. (2001, January). *Optimisation of Design Load Levels for Dragline Buckets*. Retrieved June 2010, from Australian Coal Association Research Program (ACARP) Web Site: http://www.acarp.com.au/abstracts.aspx?repId=C7003

Vynne, J. F. (2008, May). *Innovative Dragline Monitoring Systems and Technologies.* Retrieved August 25, 2010, from http://tbirdpac.com/support/pdf/innovativedraglinevynne.pdf

WCI Energy Excellence Programme Case Study. (2008, 11). Retrieved May 6, 2010, from World Coal Institute Official Website: http://www.worldcoal.org/resources/case-studies/energy-excellence-programme/

Weber, R. P. (n.d.). *Earth Pressure and Retaining Wall Basics for Non-Geotechnical Engineers.* Retrieved June 6, 2010, from PDH Online Courses c155 Lecture Notes: http://www.pdhonline.org/courses/c155/c155content.pdf

Wilkinson, A., & DeGennaro, A. (2007). Digging and Pushing Lunar Regolith: Classical Soil Mechanics and the Forces Needed for Excavation and Traction. *Journal of Terramechanics, 44*, 133–152.

Worley, M. D., & Saponara, V. L. (2008, May 9). A Simplified Dyanamic Model for Front-End Loader Design. *Journal of Mechanical Engineering Science, 222*, 2231-2249.

Young, R., & Hanna, A. (1977, September). Finite Element Analysis of Plane Soil Cutting. *Journal of Terramechanics, 14*(3), 103-125.

Yu, H. S., & Mitchell, J. K. (1998, February). *Analysis of Cone Resistance: Review of Methods.* Retrieved September 15, 2010, from http://www.scribd.com/doc/22892133/analysis-of-cone-resistance-review-of-methods

Zelenin, A. N., Balovnev, V. I., & Kerov, L. P. (1986). *Machines for Moving the Earth.* Rotterdam: Balkema.

APPENDIX A

N-FACTORS IN THE UNIVERSAL EARTHMOVING EQUATION

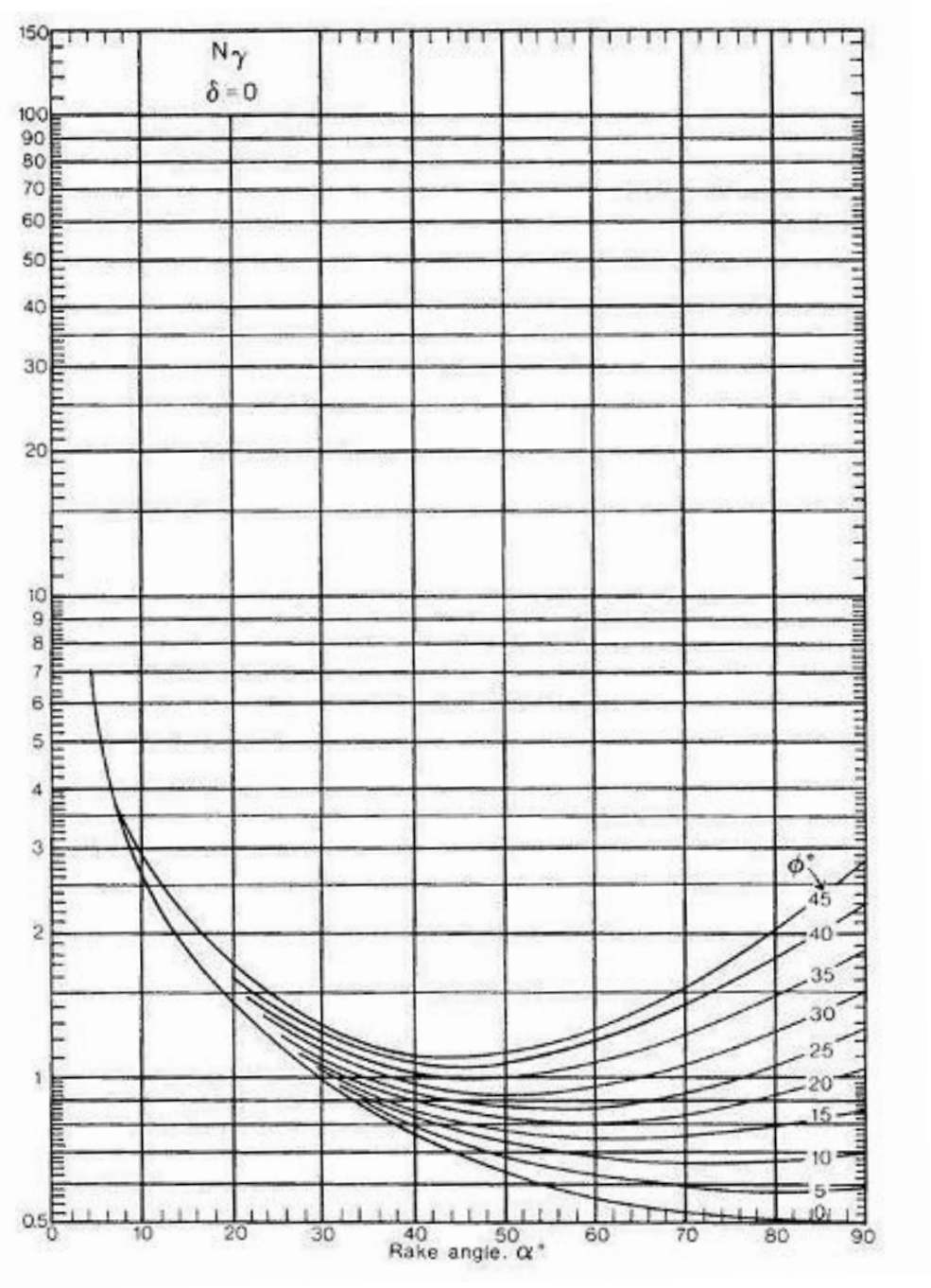

Figure A.1 Chart of Nγ for δ=0 (Hettiaratchi,1974)

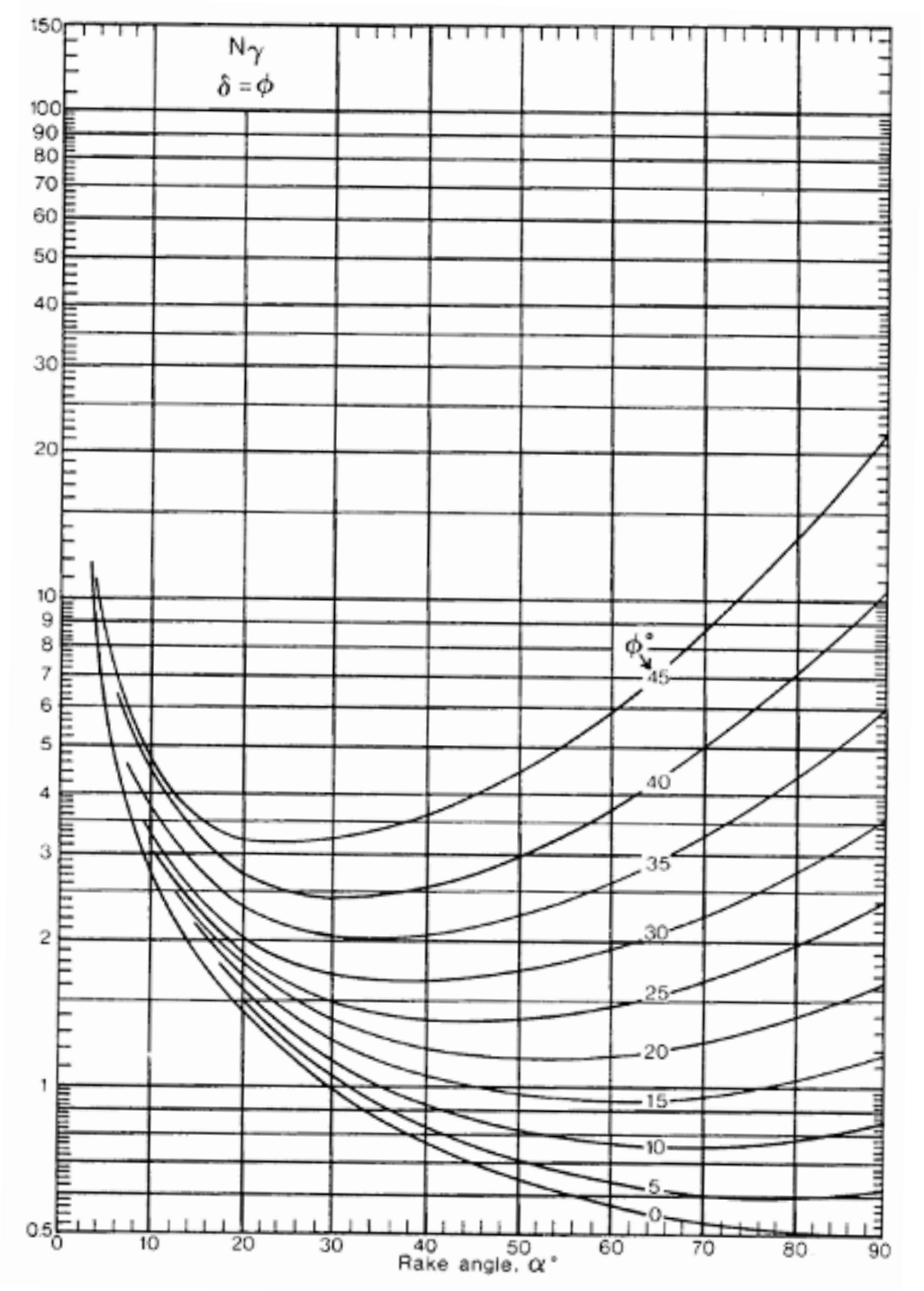

Figure A.2 Chart of Nγ for δ=ϕ (Hettiaratchi,1974)

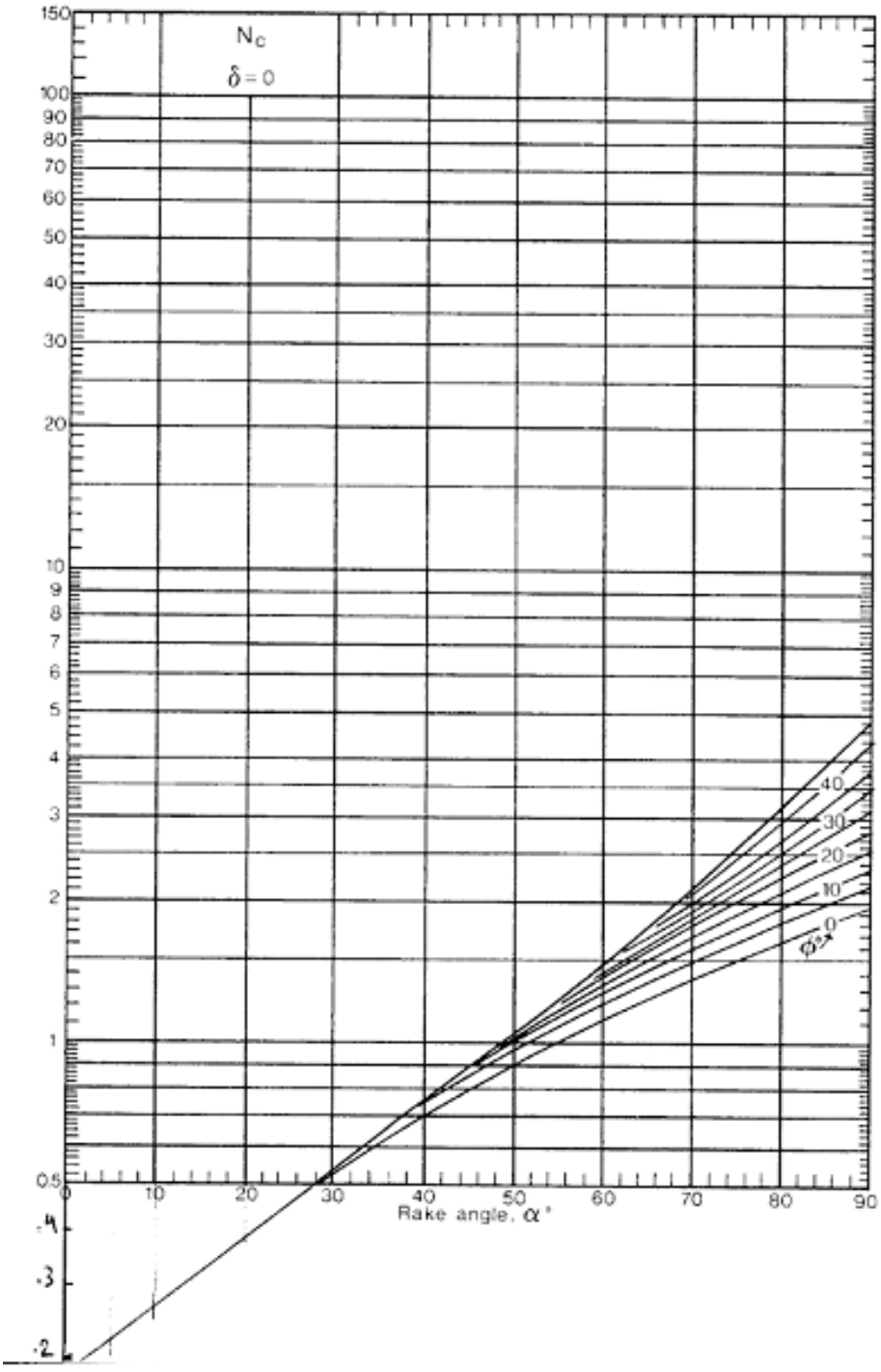

Figure A.3 Chart of N_c for δ=0 (Hettiaratchi,1974)

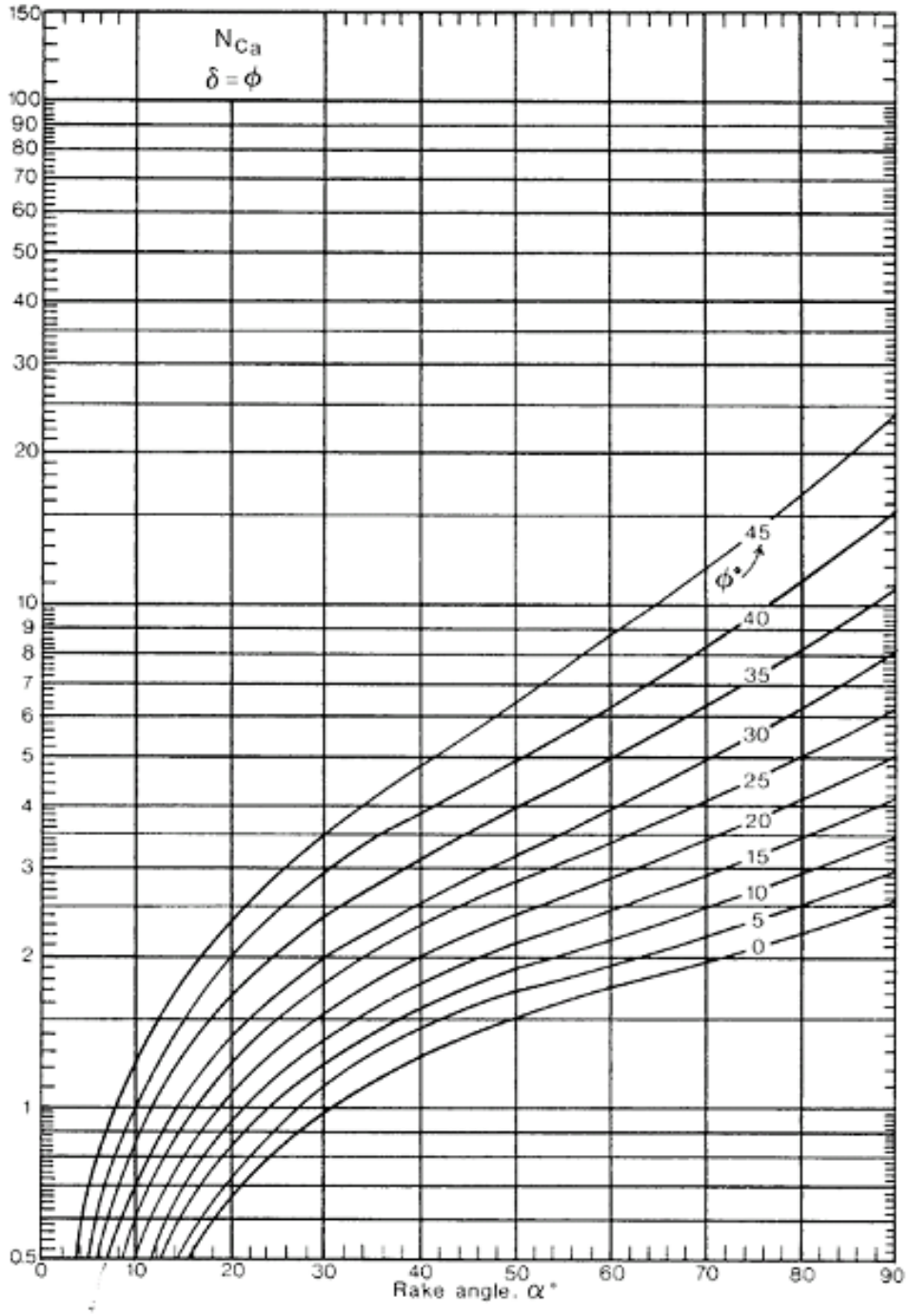

Figure A.4 Chart of N_c for $\delta=\phi$ (Hettiaratchi,1974)

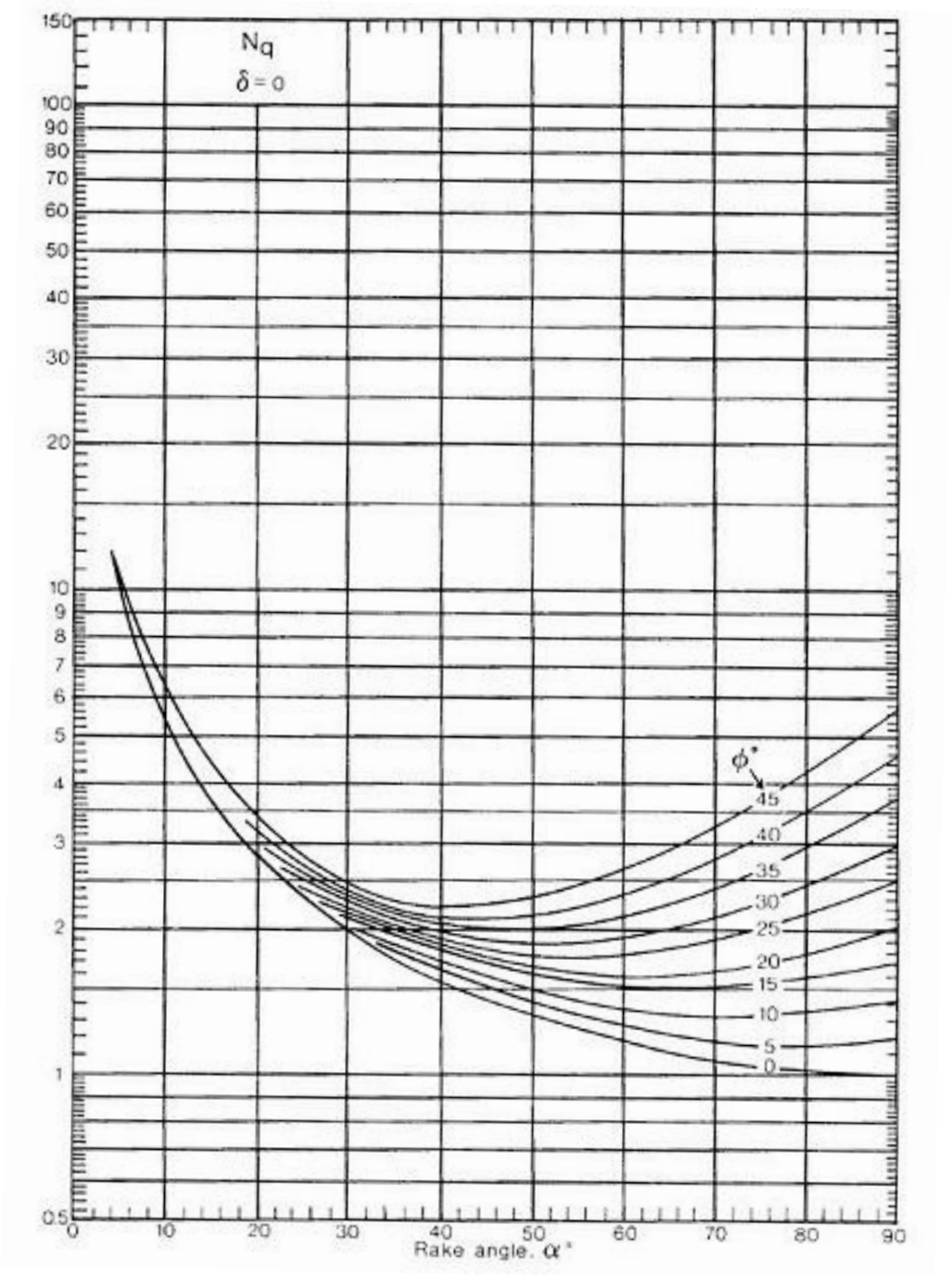

Figure A.5 Chart of N_q for δ=0 (Hettiaratchi,1974)

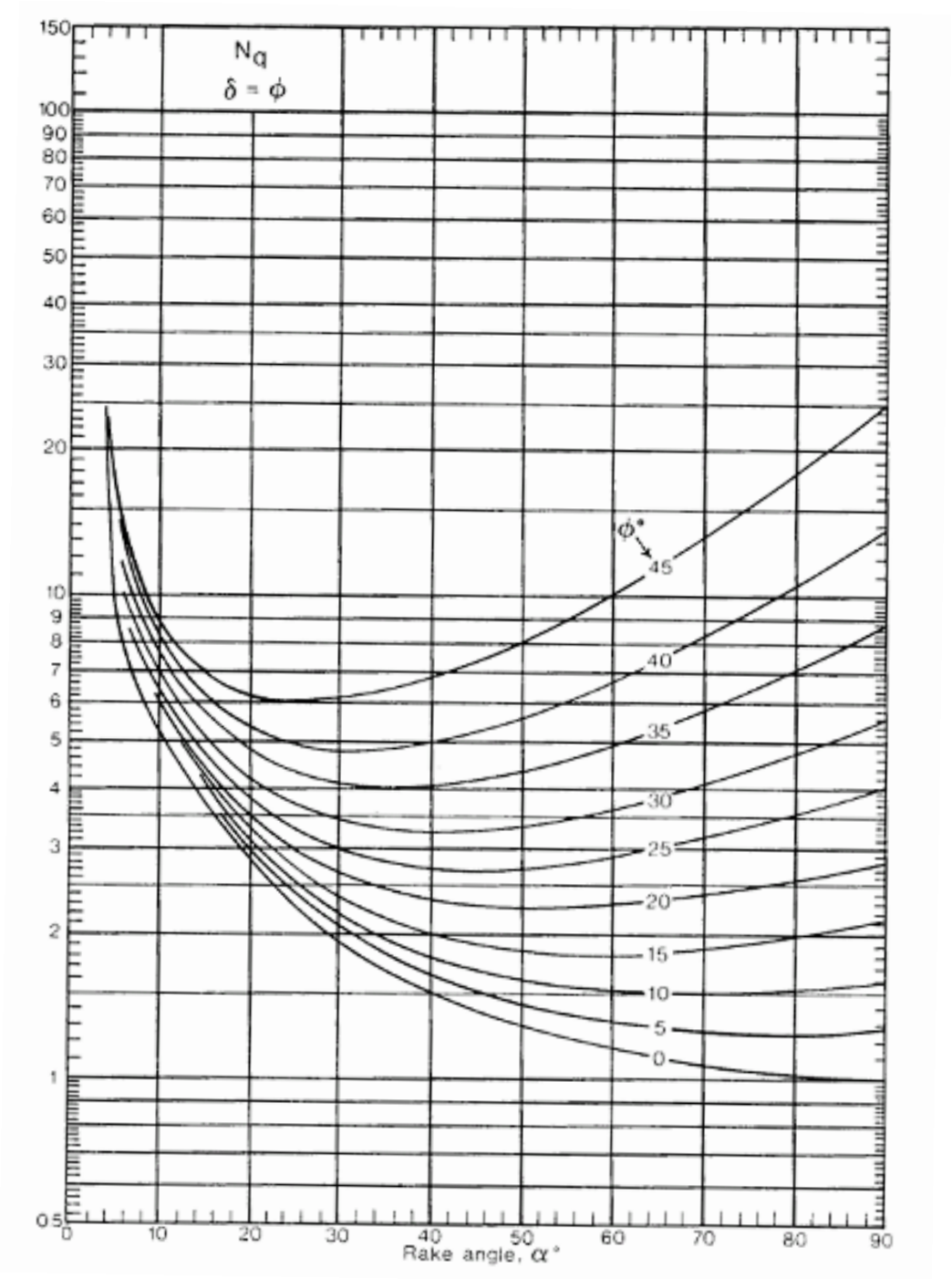

Figure A.6 Chart of N_q for $\delta=\phi$ (Hettiaratchi,1974)

APPENDIX B

NORMAL PRESSURE CALCULATIONS FOR THE SENSITIVITY ANALYSIS

Table B.1 Change of Normal Pressure According to the Density

		Density Change				
		-20%	-10%	0%	10%	20%
Cutting Width (m)	w	4.295	4.295	4.295	4.295	4.295
Depth of Work (m)	d	0.512	0.512	0.512	0.512	0.512
Formation Density (t/mm^3)	γ	**1.472**	**1.656**	**1.840**	**2.024**	**2.208**
Gravitational Acceleration (m/s^2)	g	9.810	9.810	9.810	9.810	9.810
Formation Cohesion Strength (KPa)	c	20.400	20.400	20.400	20.400	20.400
Internal Friction Angle (Deg)	Φ	34.000	34.000	34.000	34.000	34.000
External Friction Angle (Deg)	δ	25.000	25.000	25.000	25.000	25.000
Inclination (Deg)		43.780	43.780	43.780	43.780	43.780
Weight Factor	N_γ	1.733	1.733	1.733	1.733	1.733
Cohesion Factor	N_c	2.652	2.652	2.652	2.652	2.652
TOTAL CUTTING FORCE (KPa)	T	147.117	150.638	154.159	157.680	161.202
Attack Angle to Horizontal (Deg)		21.220	21.220	21.220	21.220	21.220
Number of Teeth		6.000	6.000	6.000	6.000	6.000
Total Cutting Force per Tooth (KPa)		24.519	25.106	25.693	26.280	26.867
Contact Area of a Tooth		210000	210000	210000	210000	210000
TOTAL PRESSURE ON TOOTH (MPa)	P	0.117	0.120	0.122	0.125	0.128
External Friction Angle (Radian)	δ	0.436	0.436	0.436	0.436	0.436
NORMAL PRESSURE ON TOOTH (MPa)	P_n	0.1058	0.1084	0.1109	0.1134	0.1160

Table B.2 Change of Normal Pressure According to the Cohesion

		Cohesion Change				
		-20%	-10%	0%	10%	20%
Cutting Width (m)	w	4.295	4.295	4.295	4.295	4.295
Depth of Work (m)	d	0.512	0.512	0.512	0.512	0.512
Formation Density (t/mm^3)	γ	1.840	1.840	1.840	1.840	1.840
Gravitational Acceleration	g	9.810	9.810	9.810	9.810	9.810
Formation Cohesion Strength (KPa)	c	**16.320**	**18.360**	**20.400**	**22.440**	**24.480**
Internal Friction Angle (Deg)	Φ	34.000	34.000	34.000	34.000	34.000
External Friction Angle (Deg)	δ	25.000	25.000	25.000	25.000	25.000
Inclination (Deg)		43.780	43.780	43.780	43.780	43.780
Weight Factor	N_γ	1.733	1.733	1.733	1.733	1.733
Cohesion Factor	N_c	2.652	2.652	2.652	2.652	2.652
TOTAL CUTTING FORCE (KPa)	T	130.370	142.264	154.159	166.054	177.949
Attack Angle to Horizontal (Deg)		21.220	21.220	21.220	21.220	21.220
Number of Teeth		6.000	6.000	6.000	6.000	6.000
Total Cutting Force per Tooth (KPa)		21.728	23.711	25.693	27.676	29.658
Contact Area of a Tooth		210000	210000	210000	210000	210000
TOTAL PRESSURE ON TOOTH (MPa)	P	0.103	0.113	0.122	0.132	0.141
External Friction Angle (Radian)	δ	0.436	0.436	0.436	0.436	0.436
NORMAL PRESSURE ON TOOTH (MPa)	P_n	0.0938	0.1023	0.1109	0.1194	0.1280

Table B.3 Change of Normal Pressure According to the Internal Friction Angle

		Internal Friction Angle Change				
		-20%	-10%	0%	10%	20%
Cutting Width (m)	w	4.295	4.295	4.295	4.295	4.295
Depth of Work (m)	d	0.512	0.512	0.512	0.512	0.512
Formation Density (t/mm^3)	γ	1.840	1.840	1.840	1.840	1.840
Gravitational Acceleration	g	9.810	9.810	9.810	9.810	9.810
Formation Cohesion Strength (KPa)	c	16.320	18.360	20.400	22.440	24.480
Internal Friction Angle (Deg)	Φ	**27.200**	**30.600**	**34.000**	**37.400**	**40.800**
External Friction Angle (Deg)	δ	25.000	25.000	25.000	25.000	25.000
Inclination (Deg)		43.780	43.780	43.780	43.780	43.780
Weight Factor	N_γ	**1.426**	**1.561**	**1.733**	**1.912**	**2.168**
Cohesion Factor	N_c	**2.459**	**2.525**	**2.652**	**2.789**	**2.964**
TOTAL CUTTING FORCE (KPa)	T	117.220	133.670	154.159	176.485	203.620
Attack Angle to Horizontal (Deg)		21.220	21.220	21.220	21.220	21.220
Number of Teeth		6.000	6.000	6.000	6.000	6.000
Total Cutting Force per Tooth (KPa)		19.537	22.278	25.693	29.414	33.937
Contact Area of a Tooth		210000	210000	210000	210000	210000
TOTAL PRESSURE ON TOOTH (MPa)	P	0.093	0.106	0.122	0.140	0.162
External Friction Angle (Radian)	δ	0.436	0.436	0.436	0.436	0.436
NORMAL PRESSURE ON TOOTH (MPa)	P_n	0.0843	0.0961	0.1109	0.1269	0.1465

Table B.4 Change of Normal Pressure According to the External Friction Angle

		External Friction Angle Change				
		-20%	-10%	0%	10%	20%
Cutting Width (m)	w	4.295	4.295	4.295	4.295	4.295
Depth of Work (m)	d	0.512	0.512	0.512	0.512	0.512
Formation Density (t/mm^3)	γ	1.840	1.840	1.840	1.840	1.840
Gravitational Acceleration	g	9.810	9.810	9.810	9.810	9.810
Formation Cohesion Strength (KPa)	c	16.320	18.360	20.400	22.440	24.480
Internal Friction Angle (Deg)	Φ	34.000	34.000	34.000	34.000	34.000
External Friction Angle (Deg)	δ	**20.000**	**22.500**	**25.000**	**27.500**	**30.000**
Inclination (Deg)		43.780	43.780	43.780	43.780	43.780
Weight Factor	N_γ	**1.584**	**1.658**	**1.733**	**1.807**	**1.881**
Cohesion Factor	N_c	**2.291**	**2.471**	**2.652**	**2.832**	**3.012**
TOTAL CUTTING FORCE (KPa)	T	114.412	133.461	154.159	176.473	200.371
Attack Angle to Horizontal (Deg)		26.220	23.720	21.220	18.720	16.220
Number of Teeth		6.000	6.000	6.000	6.000	6.000
Total Cutting Force per Tooth (KPa)		19.069	22.243	25.693	29.412	33.395
Contact Area of a Tooth		210000	210000	210000	210000	210000
TOTAL PRESSURE ON TOOTH (MPa)	P	0.091	0.106	0.122	0.140	0.159
External Friction Angle (Radian)	δ	**0.349**	**0.393**	**0.436**	**0.480**	**0.524**
NORMAL PRESSURE ON TOOTH (MPa)	P_n	0.0853	0.0979	0.1109	0.1242	0.1377